In-vitro selection, characterization and application of a silver-specific DNAzyme

by

Runjhun Saran Narayan

A thesis

presented to the University of Waterloo

in fulfilment of the

thesis requirement for the degree of

Doctor of Philosophy

in

Chemistry

Waterloo, Ontario, Canada, 2018

Examining Committee Membership

The following served on the Examining Committee for this thesis. The decision of the Examining Committee is by majority vote.

External Examiner	**Dr. Philip Johnson,** Associate professor, Department of Chemistry, York University, Toronto, Canada.
Supervisor	**Dr. Juewen Liu,** Associate professor, Department of Chemistry, University of Waterloo, Waterloo, Canada.
Internal Member	**Dr. John Honek,** Professor, Department of Chemistry, University of Waterloo, Waterloo, Canada.
Internal Member	**Dr. Thorsten Dieckmann** Associate professor, Department of Chemistry, University of Waterloo, Waterloo, Canada.
Internal Member	**Dr. Richard Manderville,** Associate professor, Department of Chemistry, University of Guelph, Guelph, Canada.
Internal–External Member	**Dr. Moira Glerum** Associate professor, Department of Biology, University of Waterloo, Waterloo, Canada.

Author's Declaration

"This thesis consists of material all of which I authored or co-authored: see Statement of Contributions included in the thesis. This is a true copy of the thesis, including any required final revisions, as accepted by my examiners.

I understand that my thesis may be made electronically available to the public."

Statement of Contributions

The work presented in this thesis is the result of work performed by the author and several scientific collaborations. Contributions from each scientist and the resulting publications are listed in detail below.

The work in Chapter 2 has been published as: Saran R.; Liu, J. A Silver DNAzyme. *Anal. Chem.* 2016, 88, 4014-4020. All the work in this chapter was performed by the author.

The work in Chapter 3 has been published as: 1) Saran R.; Kleinke K.; Zhou W.; Yu T.; Liu J. A Silver-Specific DNAzyme with a New Silver Aptamer and Salt-Promoted Activity. *Biochemistry*. 2017, 56, 1955−1962. 2) Saran R.; Yao L.; Hoang P.; Liu J. Folding of the silver aptamer in a DNAzyme probed by 2-aminopurine fluorescence. *Biochimie*. 2018, 145, 145-150. Kim Kleinke and Tianmeng Yu provided assistance on DNAzyme kinetics assays and gel electrophoresis. Lu Yao and Peter Hoang provided assistance on fluorescence spectrometry. Other work presented in this chapter was performed by the author.

The work in Chapter 4 has been published as: Saran R.; Liu J. A Silver DNAzyme. *Anal. Chem.* 2016, 88, 4014-4020. All the work in this chapter was performed by the author.

The work in Appendix A (chapter 6) has been published as: Saran R.; Chen Q.; Liu J. Searching for a DNAzyme Version of the Leadzyme. *J. Mol. Evol.* 2015, 81, 235-244. Qingyun Chen provided assistance on DNAzyme kinetics assays and gel electrophoresis. Other work presented in this appendix was performed by the author.

The work in Appendix B (chapter 7) has been published as: Saran R.; Liu J. A comparison of two classic Pb^{2+}-dependent RNA-cleaving DNAzymes. *Inorg. Chem. Front.*, 2016, 3, 494-501. All the work in this chapter was performed by the author.

Abstract

Evolution of novel DNA-based catalysts (DNAzymes) through *in-vitro* selection has expedited the research by manifolds, in both fundamental and analytical aspects of bio-nanotechnology. DNAzymes are attractive for their high stability, high catalytic efficiency and ease of modification. Among the known DNAzymes, those cleaving RNA have attracted most attention. Many of the known RNA-cleaving DNAzymes recruit multivalent metal ions for successful catalysis, while the catalytic involvement of monovalent metal ions yet remains underexplored. Before this thesis work, only a few Na^+-dependent DNAzymes are known, and I was interested in exploring monovalent transition metals, such as silver. In this thesis, an Ag^+-dependent selection experiment and its outcomes are described. In Chapter 1, relevant background information on DNA and DNAzymes is introduced, and the current state-of-the-art of the field was reviewed.

In chapter 2, a new RNA-cleaving DNAzyme named Ag10c with a well-defined bulged hairpin structure was isolated after six rounds of *in-vitro* selection. The selection was performed using Ag^+ as the intended target metal, and Na^+ was present in the selection buffer to maintain the ionic strength of the buffer. This DNAzyme shows remarkable selectivity for Ag^+, and attains a maximum speed of 0.41 min^{-1} in the presence of 10 μM Ag^+ in buffer 50 mM MOPS (pH 7.5) and 200 mM $NaNO_3$. This discovery expands the repertoire of metal-dependent RNA-cleaving DNAzymes and also draws much needed attention to the role of monovalent ions in DNAzyme catalysis.

In chapter 3, the DNAzyme Ag10c was studied in extensive detail. The study revealed that most of the nucleotides in the catalytic loop are significant for activity. This study

confirmed that Ag10c bears a well-defined silver aptamer in its catalytic loop, and it can fold into a compact structure by binding Ag^+. Most nucleotides in the catalytic loop are highly conserved and mutations to them often dropped the activity by over 1000-fold. Using salt-dependent catalytic activity measurement, it was found that Ag10c was more active in buffers with higher NaCl concentration. However, other tested DNAzymes were inhibited by such salt. In addition, phosphorothioate modifications were made at the scissile phosphate. Based on these biochemical data, it was established that this Ag10c DNAzyme needs two metals for catalysis: one Na^+ (or other group 1A metals or Mg^{2+}) binds to the pro-R_p oxygen of the scissile phosphate, and two Ag^+ ions bind cooperatively to Ag10c aptamer loop. It was also reported that Ag10c undergoes a single deprotonation step during catalysis. The investigation of Ag10c-Ag^+ binding has been further characterized with fluorescence-based folding studies using 2-aminopurine as a probe. This study provides a new aptamer for Ag^+ which is completely different from the well-known C-Ag^+-C structure, and floats a new theme of DNAzyme catalysis that may be used by soft metals to escape interaction with the scissile phosphate and yet confer effective catalysis.

In chapter 4, the DNAzyme Ag10c was used to develop a highly sensitive analytical probe for silver. This study reports a FRET-based system with the DNAzyme Ag10c for sensing low concentrations of Ag^+ ions, with the limit of detection being 24.9 nM, which is far below the permissible limit of silver in water by WHO. The study exhibits that amongst the metals tested i.e. upto 100 mM, 10 mM and 100 μM of most of the group 1A metals, few of group 2A metals and many of the divalent transition metal ions respectively, the sensor is exceptionally selective for Ag^+ ions. This study also demonstrates the robustness of the sensor in real world samples i.e. in Lake Huron water. This study puts forth a rare example of DNAzyme beacons

being used for sensing of monovalent ions, and highlights the possibility of using DNAzyme beacons for sensing transition metal ions up to low nanomolar concentrations.

In addition to the work pertaining to the silver DNAzyme, *in-vitro* selection was also performed on another toxic heavy metal, lead. A very short DNAzyme PbE22 was obtained. This DNAzyme consists of only 5 nucleotides in its catalytic loop and shows excellent selectivity for Pb^{2+}. This part of information is presented in the Appendix A (chapter 6) of the thesis. Previously known Pb^{2+}-specific DNAzymes, 17E and GR5, have also been characterized. By performing systematic mutations in their catalytic cores, and side-by-side comparison of both, four highly conserved nucleotides in both DNAzymes playing similar roles were identified and it was deciphered that they share the same activity pattern. This part of information is presented in the Appendix B (chapter 7) of the thesis.

In summary, *in-vitro* selection is a powerful tool to obtain interesting metal-specific DNA sequences. This work has expanded the previous work to a monovalent heavy metal, silver. By studying Ag10c, a new mechanism of DNAzyme catalysis was revealed.

Acknowledgements

First and foremost I want to profusely thank my supervisor Prof. Juewen Liu for being my mentor and advisor for the last 4 years. It has indeed been an honor to work under his tutelage. He has taught me both consciously and unconsciously, how good research is done. I thank him for all his time, ideas and funding to make my PhD experience productive and stimulating. Dr. Liu has guided me through tough times and made me learn things pragmatically. He has set an example of ‘patience’, ‘perseverance’ and ‘commitment’. I take these as keywords of success not only for academic research but life in general. I express my sincere and deepest gratitude to him for being a wonderful supervisor.

I would like to thank my committee members Dr. John Honek, Dr. Thorsten Dieckmann, and Dr. Richard Manderville for agreeing to be on my PhD advisory committee, the directions provided by them in this work and their valuable time spent in evaluating my PhD research. I would like to thank my external examiner Dr. Philip Johnson, and my internal-external examiner Dr. Moira Glerum, for taking out their precious time to attend my examination. A special thanks goes to Cathy van Esch who has always promptly and patiently made her best effort in advising me throughout my PhD. I also thank Marguerite Greavette and Kim Rawson for their support and help.

I would also like to thank members of the Liu lab Dr. Jimmy Hoang, Dr. Feng Wang, Dr. Biwu Liu, Dr. Wenhu Zhou, Zijie Zhang, Yibo Liu, Lingzi Ma, Tianmeng Yu, Anand Lopez, Zhicheng Hoang, Ziyi Sun, Mahsa Vazin, Howard Tsai, Michael Hoang, Qingyun Chen. and other research students who worked with me during my PhD. I also take this opportunity to thank undergraduate volunteers and co-op researchers who worked with me: Kim Kleinke,

Lu Yao, Peter Hoang, and Gu Lide. It was a wonderful journey with all you guys! This group has been a source of good friendship as well as good advice and collaborations.

Financial support from the University of Waterloo, the Natural Sciences and Engineering Research Council (NSERC) of Canada, and Canadian Institutes of Health Research (CIHR) are greatly appreciated. I would use this opportunity to show my gratitude towards the University of Waterloo and its Department of Chemistry for financial support and for providing access to research facilities.

In the end, I thank my parents Late Mrs. Kiran Saran & Dr. Rajat Saran for all the laborious days and sleepless nights spent in grooming me to be worthy enough of pursuing a PhD degree. I owe every bit of my success to them in all spheres of life. I thank my parents in law Mrs. Neera Bhatnagar & Mr. Anurag Bhatnagar for being pillars of support and encouragement throughout my PhD. I thank my sister Mrs. Nupur Saran Saboo and brother in law Mr. Abhijeet Saboo who have always firmly stood by me, and taken good care of my parents while I was busy in my research. I can't find words that are thankful enough to acknowledge the unconditional love and unshakable strength and support my better half Dr. Apurva Narayan has showered me with. Last but not the least, I express a huge thanks to my 9 months old daughter Nyaari Narayan who was born in the last year of my doctoral studies as a lucky charm. Her purest love and charming personality have constantly motivated me during the hard times of thesis writing.

Dedication

To Most Revered Prof. Prem Saran Satsangi Sahab for

His boundless blessings, incessant support and unparalleled guidance in all spheres of life!

Table of Contents

List of figures

List of Tables

List of Abbreviations

A	adenine
2-AP	2- amino purine
AgNP	silver nanoparticle
AuNP	gold nanoparticle
ATP	adenosine triphosphate
bp	base pairs
C	cytosine
cDNA	complementary DNA
CTP	cytosine triphosphate
CCP	cationic conjugated polymers
D	1-deazaadenine
DNA	deoxyribonucleic acid
dPAGE	denaturing polyacrylamide gel electrophoresis
dsDNA	double-stranded DNA
dNTP	deoxyribonucleotide triphosphate
EPA	Environmental Protection Agency
EB	ethidium bromide
εA	1, N^6-ethenoadenine
FAM	fluorescein amidite
FRET	fluorescence resonance energy transfer
G	guanine

G-quartet	guanine quartet
GTP	guanosine triphosphate
GTPγS	guanosine 5'-O-[gamma-thio]triphosphate)
HEPES	4-(2-Hydroxyethyl)piperazine-l-ethanesulfonic acid
HIV-1	human immunodeficiency virus – 1
HX	hypoxanthine
ICP-MS	inductively coupled plasma-mass spectroscopy
I	inosine
Im	imidazole
K_{cat}	turnover number
K_d	dissociation constant
K_a	acid dissociation constant
K.	Michaelis constant
Ln^{3+}	lanthanides ions
MCL	maximum contaminant level
MES	2-(N-morpholio)ethanesulfonic acid
µL	micro-liter
µM	micro-molar
µmol	micro-mole
pm	micrometer
ml	milli-liter
mM	milli-molar
mmol	milli-mole

M^{n+}	metal ion with valency '+n'
pm	pico-mole
pM	pico-molar
pmol	pico-mole
pC	pyrrolo - cytosine
MOPS	3-(N-morpholino)propanesulfonic acid
nm	nano-meter
nM	nano-molar
nmol	nano-mole
NMR	nuclear magnetic resonance
NA	nucleic acids
PAGE	polyacrylamide gel electrophoresis
PO	phosphodiester
PG	picogreen
ppb	parts-per-billion
ppm	parts-per-million
ppt	parts-per-trillion
PS	phosphorothioate
Q	fluorescence quencher
QCM	quartz crystal microbalance
RFU	relative fluorescence units
rA	ribo-adenosine
Ref	Reference

RNA	ribonucleic acid
RT-PCR	real-time polymerase chain reaction
RLS	resonance light scattering
SELEX	systematic evolution of ligands by exponential enrichment
SPR	surface plasmon resonance spectroscopy
SERS	surface enhanced raman spectroscopy
SG-I	SYBR Green - I
ssDNA	single-stranded DNA
Tris	tris(hydroxymethyl)aminomethane
PCR	polymerase chain reaction
T	thymine
T_m	melting temperature
tRNA	transfer RNA
TTP	thymine triphosphate
U	uracil
VS	varkud satellite
WHO	World Health Organization

1. Chapter 1 – Introduction to functional nucleic acids

1.1 Nucleic acids and their interaction with metal ions

1.1.1 Introduction to nucleic acids

Polymeric biomolecules constitute a large part of the living organisms. These biopolymers contain monomeric units which are covalently bonded to each other. Biological systems are mainly made up of three classes of biopolymers: (a) polynucleotides (ribonucleic acids (RNA) and deoxyribonucleic acids (DNA)), which are composed of nucleotide monomers, (b) polypeptides, polymers of monomeric amino acids, and (c) polysaccharides, which are polymeric carbohydrate structures. Apart from these, the fourth major constituent of biological systems is a non-polymeric macromolecule called lipid. All these constituents work synergistically to successfully carry out the intricate functionality of all living systems, by storing energy and information, carrying out signaling and regulatory processes, and contributing as structural components. The polynucleotides DNA and RNA, have long been known to preserve, store and transfer genetic information in living cells and thus, hold an indispensable role in the propagation of life. However, the functional potential of nucleic acids outside living systems, has been underestimated and had not attracted much interest. Recently, owing to their interesting chemical structures, small size, and useful chemical and physical properties, nucleic acids have been discovered to bear multiple novel functions e.g. catalysis, molecular recognition, etc. Therefore, in today's date, DNA is not only known as a genetic material, but it is now also acknowledged as a generic nanomaterial.

1.1.2 Chemical structure of nucleic acids

As mentioned above, nucleic acids are vital biological molecules and can be classified into RNA and DNA, which are both linear biopolymers made from monomers called nucleotides. Each of these monomeric nucleotide possess three constituents: a) a five-membered pentose sugar ring, b) a nitrogenous base and c) a phosphate group.

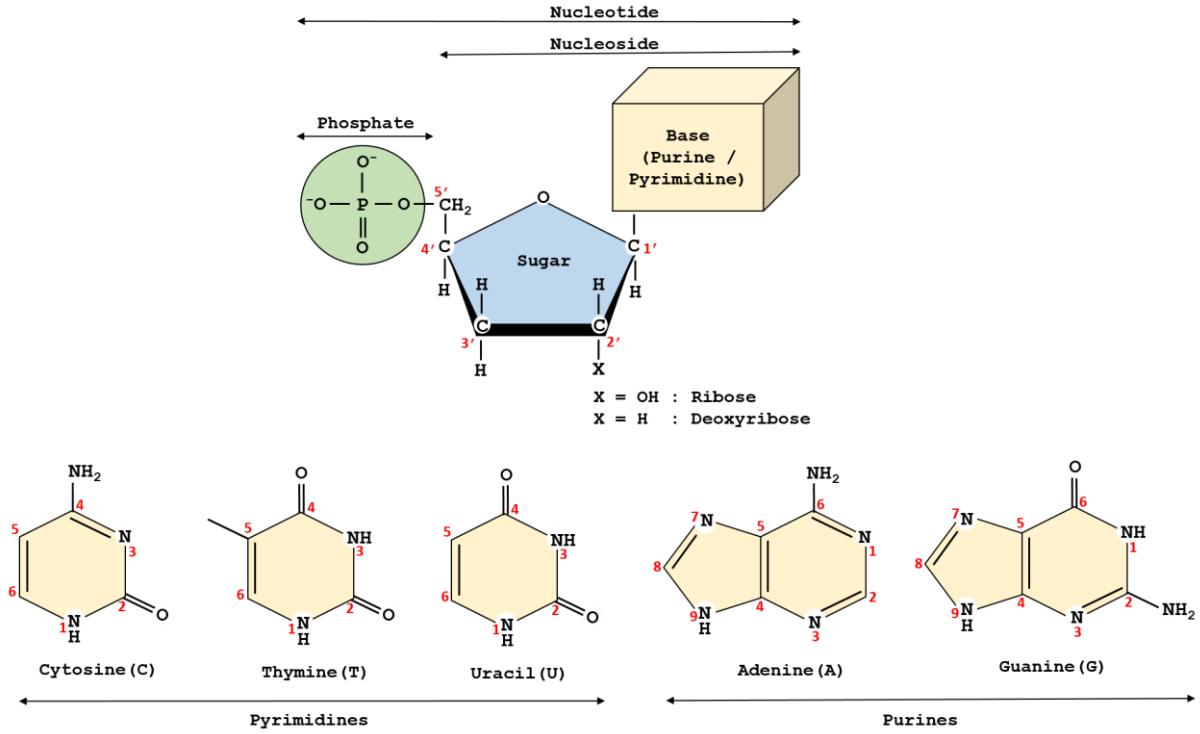

Figure 1.1 Representation of the chemical structure of nucleobases, nucleosides and nucleotides.

The sugar ring. The sugars in both DNA and RNA are pentoses (Figure 1.1). There is a small but crucial structural difference between the ribose and deoxyribose sugar ring in RNA and DNA respectively. DNA has a hydrogen instead of a hydroxyl at the 2′-position of the pentose. ***The nitrogenous base***. The nitrogenous bases are aromatic planar heterocyclic systems, and are classified into (i) pyrimidines: *Cytosine* (C), *Thymine* (T), *and Uracil* (U), and (ii) purines:

Adenine (A), *and Guanine* (G) (Figure 1.1). Within each nucleotide, one of these organic nitrogenous bases is attached to the 1′-carbon of the sugar ring via a *N*-glycosidic bond. This molecule (sugar covalently bonded to the base) without any phosphate group is called a nucleoside. The nucleotides in RNA consist of C, G, A, and U, while those in DNA are made up of C, G, A, and T.

The phosphate group. When a phosphate group is covalently bonded to the 5′-carbon of the sugar ring in a nucleoside, the entire molecule is called a nucleotide. Within a polynucleotide, the nucleotide monomers are bonded together linearly by coupling of the 3′-hydroxyl group (in the sugar) of one nucleotide to the 5′-phosphate group of the successive nucleotide (Figure 1.2). This bond is usually referred as the phosphodiester linkage, and in a polynucleotide this chain of hydrophilic phosphates serves as a backbone for its structure. At physiological pH ~ 7.0, the backbone phosphates are completely ionized (pK_a ~ 1.0), and are thus negatively charged. In DNA, the lack of the 2′-hydroxyl group in the pentose sugar ring (as compared to RNA) results in a ~ 100-fold more stable phosphate backbone that is lesser susceptible to hydrolysis.

Base pairing. At the physiological pH ~ 7.0, all the nitrogen present in the aromatic bases are well protonated. Typically, within both DNA and RNA, guanine (G) is known to form 3 hydrogen bonds with cytosine (C), while adenine (A) forms 2 hydrogen bonds with uracil (U) or Thymine (T) in RNA or DNA respectively. These base interactions are referred as Watson-Crick base pairing (Figure 1.3 A and B). The base pairs contribute significantly to the structural stability of nucleic acids, making them exist as duplexes. In polynucleotides, the base stacking forces between the aromatic base rings of consecutive nucleotides, aid in stabilizing their structure.

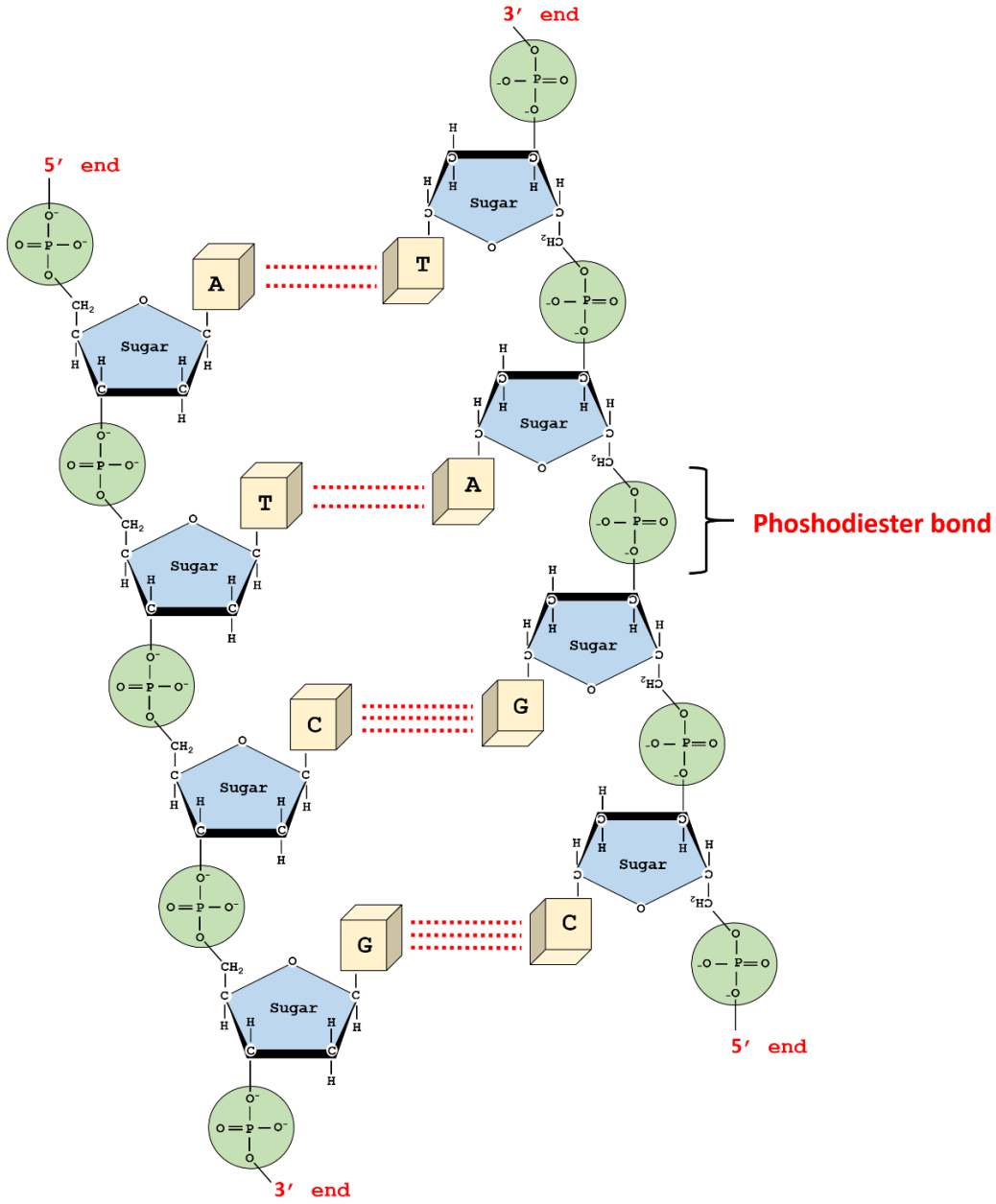

Figure 1.2 A general schematic of the nucleotides bonded together linearly (through a phosphodiester bond) by coupling of the 3′-hydroxyl group (in the sugar) of one nucleotide to the 5′-phosphate group of the successive nucleotide.

Apart from the canonical Watson-Crick base pairs, few other forms of base pairing also exist which differ in the pairing nucleotides, angle between the two glycosidic bonds, carbon - carbon

distances between the two sugar rings, etc. Figure 1.3 C, D and E shows the most studied Hoogsteen (found in triple helices and G-quadraplexes) and wobble (more common in RNA) base pairing.

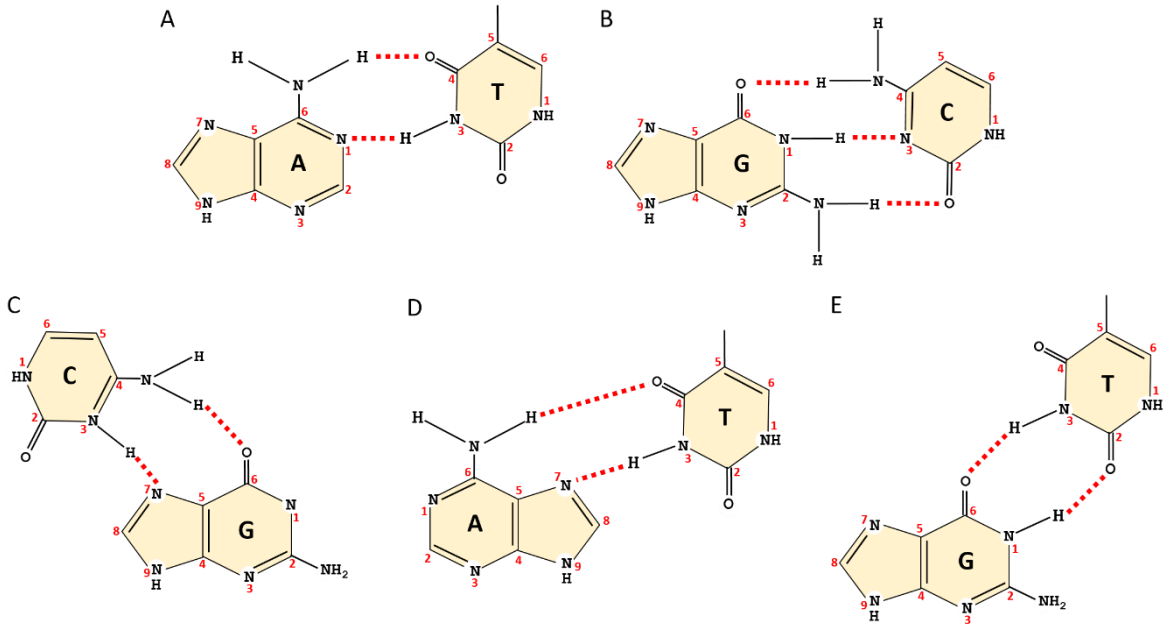

Figure 1.3 Representation of the chemical structure of Watson-Crick base pair of (A) adenine with thymine, and (B) guanine with cytosine. Representation of the Hoogsteen base pair of (C) cytosine with guanine, (D) adenine with thymine, and (E) guanine with thymine. The hydrogen bonds are shown as red dashed lines.

1.1.3 Interaction of metals with nucleic acids

Metal ions occupy an indispensable role in maintaining the structural and functional stability of many biological molecules. Coordination of metal ions with nucleic acids has been a topic of aggressive and significant research.[1–3] DNA is a polyanion as the hydrophilic backbone phosphates have a pK_a value near 1, making them completely ionized and negatively charged at pH ~ 7.0. The negative charges encourage electrostatic attraction of metal ions. Interaction

of metal ions with the phosphate backbone also facilitates the formation of a stable DNA duplex by screening the electrostatic repulsion between phosphate groups and increasing its melting temperature, T_m. DNA phosphates prefer to bind hard/borderline metals with high charge density, for e.g. group 1A and 2A metals. The nucleobases are also capable of coordinating with various metal ions with different affinities.[2–6] The deprotonated forms of N1 ($pK_a \sim 3.5$) and N3 of adenine, N3 of cytosine ($pK_a \sim 4.2$), N3 of thymine ($pK_a \sim 9.9$), and N3 and N7 ($pK_a \sim 2.1$) of guanine are potent sites for metal binding in the nucleobases. Although the N3 in thymine is protonated and unavailable for metal binding at neutral pH, Hg^{2+} is known to displace its hydrogen at neutral or even slightly acidic pH.[7] The O6 of guanine and O2 of cytosine are also known to coordinate with metal ions. Interestingly, it has been deciphered that the affinities of metal ions are quite weak for the individual sites, but the presence of multiple binding sites or a chelation effect increases the stability of metal interaction with nucleobases.[3] Some metals are known to bind with both the phosphates and the bases, e.g. the first row transition metals, Cd^{2+}, Pb^{2+}, and trivalent lanthanides. In general, soft metals mainly coordinate with DNA bases (e.g. Ag^{+} and Hg^{2+}),[1] and a few metals are capable of strong and nearly irreversibly (under ambient conditions) interaction with the nucleobases, e.g. platinum and chromium, due to extremely slow ligand exchange rates of these metals.[8] As far as the deoxyribose sugar ring is concerned, it contributes little to metal coordination but in some instances, the ribose ring in RNA is known to bind metal complexes, e.g. Os^{4+}.[9,10] Metal ions have multiple properties that contribute towards coordination with DNA. Firstly, the size of metal ions is a very useful property. The size of hydrated metal ions is more pertinent because in aqueous solutions metal ions are hydrated with a water shell. The size of metal ions plays a crucial role in determining its charge density and both these properties are critical for inner-

sphere (direct binding) and outer-sphere (water mediated binding) co-ordination. Secondly, charge is an important fundamental property. Because DNA is a polyanion, the number of charges on metal ions is pivotal for DNA binding. This is emphasized well by the fact that group 1A metals are effective above 10 mM, group 2A metals at ~1 mM, while trivalent lanthanide ions at ~10 μM. Thirdly, the pK_a of metal bound water is an important property. At room temperature (25 °C), water has a pK_a of 14, but when a water molecule binds with a metal ion, it often becomes more acidic and can hydrolyze to release a proton and become a metal bound hydroxyl group. This has important consequences like decrease in metal charge, metal hydrolysis into anions (e.g. MnO^{4-}) which repel DNA, and formation of metal hydroxides or oxides (e.g. group 3A and 4A metals) that decrease their interaction with DNA. The metal bound hydroxyl (after deprotonation) can also act as a general base, and this property plays an important role in the catalytic activity of RNA-cleaving DNAzymes. Fourthly, since metal ions are electron deficient, they can generally accept electron pairs from ligands and thus act as Lewis acids. Therefore, hard metals (e.g. Mg^{2+}) interact favorably with the phosphates (hard Lewis bases) in DNA. Fifthly, the coordination preference of metal ions plays a decisive role in DNA binding. For instance, Hg^{2+} prefers linear coordination and therefore in the B-form DNA, Hg^{2+} can mediate a with a thymine − thymine mismatch with high affinity and selectivity.[11] Lastly, the ligand exchange rate of metal ions can be deterministic for its strength of DNA binding. Most common metal ions have relatively fast ligand exchange rates in water (>1 s^{-1}).[12] However, a few metals e.g. Pt^{2+} (<10^{-3} s^{-1}),[8,13] Ir^{3+} (<10^{-9} s^{-1}), Rh^{3+} (<10^{-8} s^{-1}), Cr^{3+} (<10^{-5} s^{-1}), and Ru^{3+} (<10^{-5} s^{-1}) have very slow ligand exchange rates resulting in nearly irreversible DNA binding.[12]

1.2 Aptamers for metal ions

1.2.1 Introduction

Aptamers are nucleic acid sequences or peptides that are capable of binding to a specific target molecule. My interest lies in oligonucleotide aptamers. Aptamers are generally evolved and isolated through a method called '*Systematic Evolution of Ligands by Exponential Enrichment*' or SELEX (Figure 1.4).[14,15]

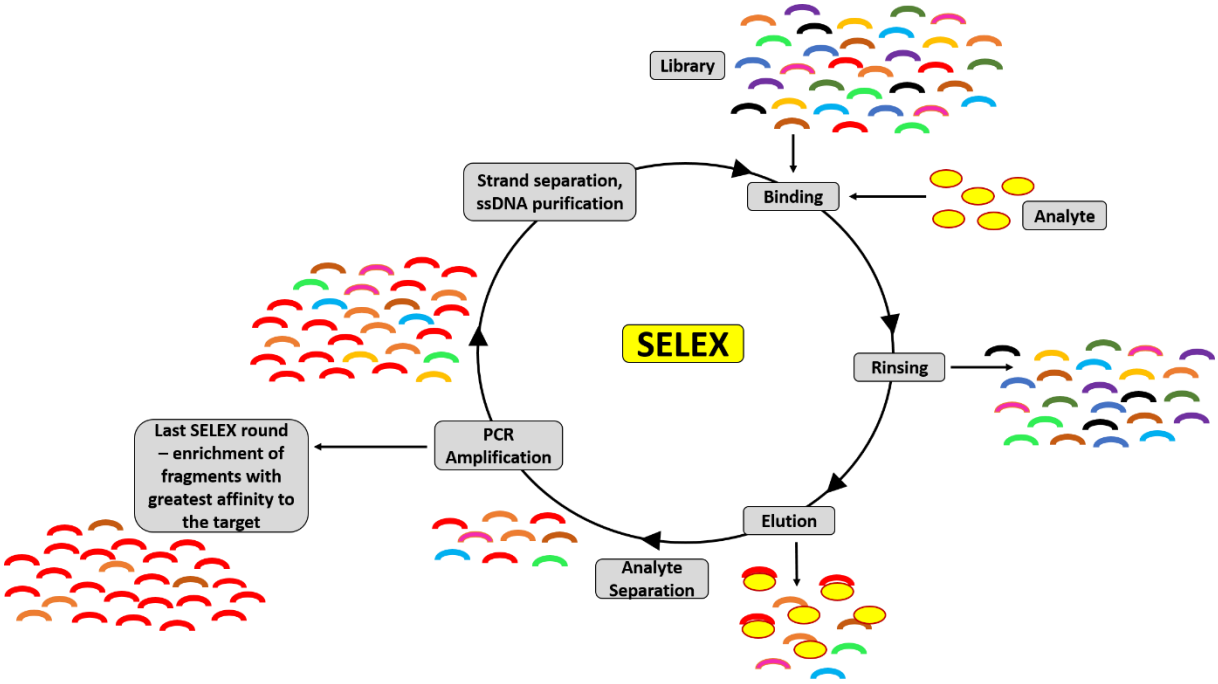

Figure 1.4 General schematic of Systematic Evolution of Ligands by Exponential Enrichment (SELEX).

This combinatorial selection begins with a huge library constituted by 10^{13} to 10^{16} random sequences. Typically, the library is incubated with the target molecule under stringent conditions of temperature, pH, salt, time, etc. The sequences binding to the target are collected and amplified. The library is reconstituted from the amplified sequences for the next round.

This process is iterated until the desired aptamer (with high selectivity and affinity for the target molecule) is obtained. Metals are very small molecules and difficult targets for aptamer discovery. Multiple alterations and improvements have been reported in the experimental design of SELEX to make it favorable for small sized metal ions.[16–20] Rational design of aptamers has also been explored. This is possible for metal ions which have specific nucleotide binding properties or have data available regarding their interaction with DNA. Multiple attempts have been made by all these methods to discover aptamers that bind selectively to metal ions and a gist of the same is presented in section 1.2.2.

1.2.2 Metal-aptamer interactions

Metal induced folding of nucleic acids. Metals are known to bind and fold nucleic acid sequences into specific 3-dimentional structures. The most extensively studied example of this phenomenon is the G-4 DNA. The G-4 nucleic acid structures are constituted by stacks of guanine tetrads which are assembled by Hoogsteen hydrogen bonding. These could be unimolecular, dimolecular, and even tetramolecular structures, and can exist in parallel or antiparallel orientation. The G-4 DNA are known to be stabilized by some monovalent ions Na^+,[21] K^+, Li^+,[22,23], Tl^+,[24–26] Rb^+,[27] NH_4^+,[28] and a few divalent ions Sr^{2+}, Ba^{2+} and Pb^{2+}.[29–34] Each of these metal ions is located differently within the G-4 structure, and stabilize the G-4 structure with different efficiency.[22] For example, a schematic representation of the PS2.M DNA folding into a G-4 structure in presence of Tl^+ is shown in Figure 1.5 A.

Isolated through SELEX. Some of the aptamers have been found for transition metal ions through SELEX. A few Zn^{2+} binding RNA sequences with K_d ~ 100-400 μM (e.g. Zn^{2+} binding motif in HIV-1 Tat aptamer),[35–37] and DNA aptamers (e.g. Zn-6m2),[16,17] are known. An RNA

aptamer for Ni^{2+} (K_d = 1μM) has been reported.[38] Cd^{2+} is known to tightly coordinate with the nucleobases,[3,39,40] and multiple Cd^{2+} binding DNA aptamers (e.g. Cd-4 and Cd-2-2) have been isolated.[18,19] The lanthanide ions have high affinity to both the DNA phosphates and the bases.[41] Amongst the lanthanides, an aptamer for Gd^{3+} (K_d ~ 330 nM) has been discovered. For example, the secondary structure of Cd^{2+} binding Cd-2-2 aptamer and Zn^{2+} binding Zn-6m2 aptamer is shown in figure 1.5 B and C respectively.

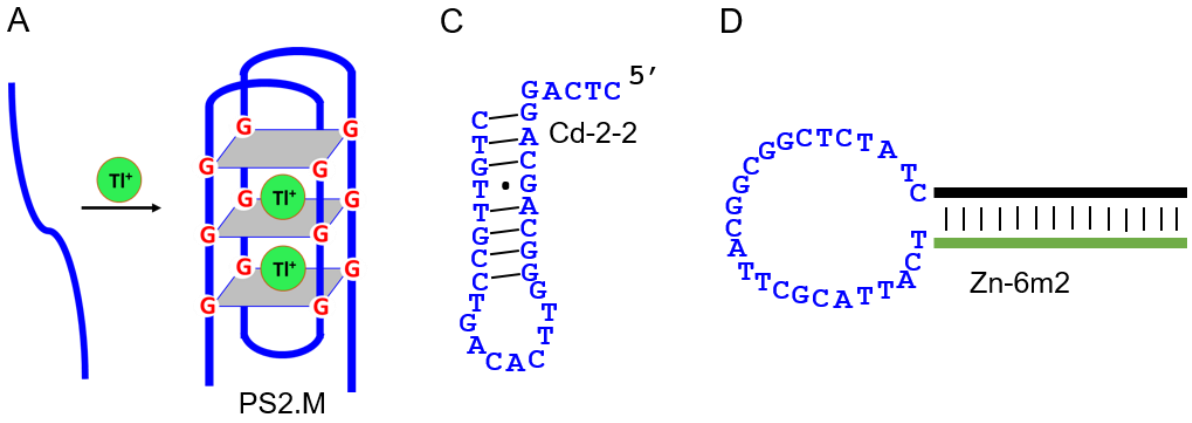

Figure 1.5 (A) A schematic representation of the PS2.M DNA folding into a G-4 structure in presence of Tl^+ (figure adapted and modified with permission from ref 43. Copyright 2016, American Chemical Society).[42,43] Secondary structure of the (B) Cd^{2+} binding aptamer Cd-2-2,[18,42] (figure adapted and modified with permission from ref 18, Copyright (2016), Elsevier) and the (C) Zn^{2+} binding aptamer Zn-6m2 (figure adapted and modified with permission from ref 17, Copyright 2007, Springer Science Business Media new York).[17,42]

Developed through rational design. Rational design of aptamers is possible for certain metal ions which possess some specific DNA binding properties. The property of the formation of metal assisted base pairs by Ag^+ (Cytosine-Ag^+-Cytosine) (Figure 1.13 A and 1.14 A),[44] and Hg^{2+} (Thymine-Hg^{2+}-Thymine)[45] has been utilized to do so. Here, the aptamer sequence is designed to be either C-rich or T-rich for Ag^+ and Hg^{2+} respectively. The design is such that in

the absence of the metal ions, the sequence is free from any specific structure but binding of the metal ions folds the DNA upon itself into a hairpin.[46] These aptamers turned out to be extremely metal specific and provided a platform for developing rapid and easy metal sensing strategies.

1.3 Metal-dependent catalysis of nucleic acids

1.3.1 Catalytic RNAs

Enzymes are vital macromolecules that execute biological catalysis with remarkable speed and accuracy, and work in synchrony with all other cellular components to make life possible. The traditional viewpoint of proteins alone being considered as biocatalysts, was shaken with the discovery of RNA-based enzymes or Ribozymes.[47] In today's date, several naturally occurring and artificially developed ribozymes are known. The naturally occurring ribozymes can be categorized into: a) Small self-cleaving ribozymes- These are 50-150 nucleotides long nucleolytic ribozymes. These include the hepatitis delta virus (HDV),[48,49] hammerhead ribozyme,[50] GlmS ribozyme/riboswitch,[51] hairpin ribozyme,[52,53] and Varkud Satellite (VS) ribozyme.[54,55] They mostly catalyze sequence-specific intramolecular cleavage of RNA and their activity is supported by metal ion cofactors, and the specific 3-dimentional arrangement of the nucleobases in their active sites. b) Large ribozymes- These are large RNAs of several hundred nucleotides. These include the group I,[47,56] and group II introns,[57,58] which catalyze two different phosphoryl transfer reactions in mRNA splicing. While group I introns need Mg^{2+} or other divalent cations for activity, the group II introns often require protein cofactors. The RNA subdomain of RNase P also belongs to this category. It catalyzes the cleavage of a specific

phosphodiester bond during the 5′-maturation of tRNA.[59,60] The RNase P RNA relies upon the presence of divalent cations for catalysis.[61,62] Apart from these, a number of artificial ribozymes bearing different properties have been discovered. Some examples of these include RNA-dependent RNA polymerase,[63] a ribozyme catalyzing ribozyme synthesis,[64] a Cu^{2+}-dependent ribozyme that catalyzes phosphate transfer from GTP or thiophosphate transfer from GTPγS,[65] Diels-Alderase ribozyme which catalyzes carbon-carbon bond formation,[66] etc.

1.3.2 Introduction to catalytic DNAs

DNA based catalysts are referred to as DNAzymes. They can be considered as DNA counterparts of Ribozymes. However, while ribozymes exist in nature, DNAzymes are evolved in test tubes using a specific methodology, called *in-vitro* selection (Figure 1.7 A).

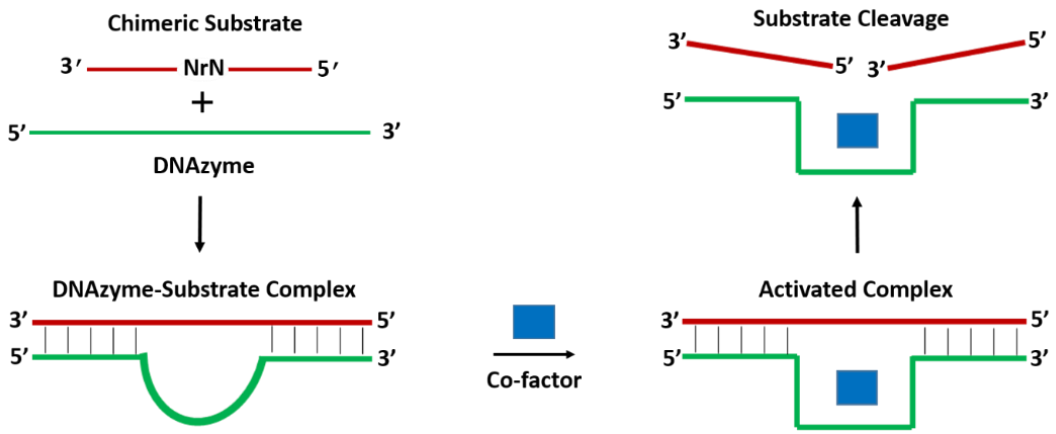

Figure 1.6 The general schematic of a typical RNA-cleaving DNAzyme.

In 1994, the first DNAzyme 'GR5' (RNA-cleaving DNAzyme) was discovered through *in-vitro* selection.[67] In today's date multiple DNA-catalyzed reactions have been discovered, including RNA hydrolysis, RNA ligation (of native 3′-5′ and non-native 2′-5′ phosphodiester

linkages),[68–70] RNA branching,[71–73] RNA lariat formation,[74] DNA depurination,[75,76] oxidative DNA cleavage,[77–79] DNA ligation via 3′ or 5′ activation,[80,81] DNA branching,[82] DNA coupling (by phosphorothioester linkage),[83,84] DNA phosphorylation,[85–87] DNA adenylation,[88] phosphoramidite cleavage,[89] porphyrin metallation,[90] peroxidation,[91,92] thymine dimer cleavage,[93] formation of nucleopeptide linkages,[94] and formation of carbon-carbon bonds.[95] However, DNAzymes that catalyze the cleavage of RNA are the largest class of catalytic DNA molecules.[96] The general schematic of a typical RNA-cleaving DNAzyme is shown in Figure 1.6. It consists of a DNA substrate strand which has enzyme binding sequences on both ends and one RNA nucleotide embedded in the center as the cleavage site. The second component is the DNA enzyme strand which consists of the catalytic core in the center and sequences at both the 5′ and 3′ ends which base pair with the substrate. Both these strands hybridize together and form an inactive DNAzyme complex. Upon interaction with a specific cofactor, the enzyme-substrate complex gets activated and confers the RNA bond cleavage in the chimeric substrate strand.

1.3.3 Metal-dependent RNA-cleaving DNAzymes

In-vitro selection. *In-vitro* selection is an innovative methodology for the discovery of novel functional nucleic acids. Within this process, a large random pool of nucleic acids (e.g. 10^{14} unique sequences) undergoes directed evolution to isolate molecules bearing certain desired properties. It comprises of iterative series of selection, amplification and mutagenesis (optional). The general schematic for isolating metal-dependent RNA-cleaving DNAzymes is shown in Figure 1.7 A. One of the most important components of this method is the initial library.

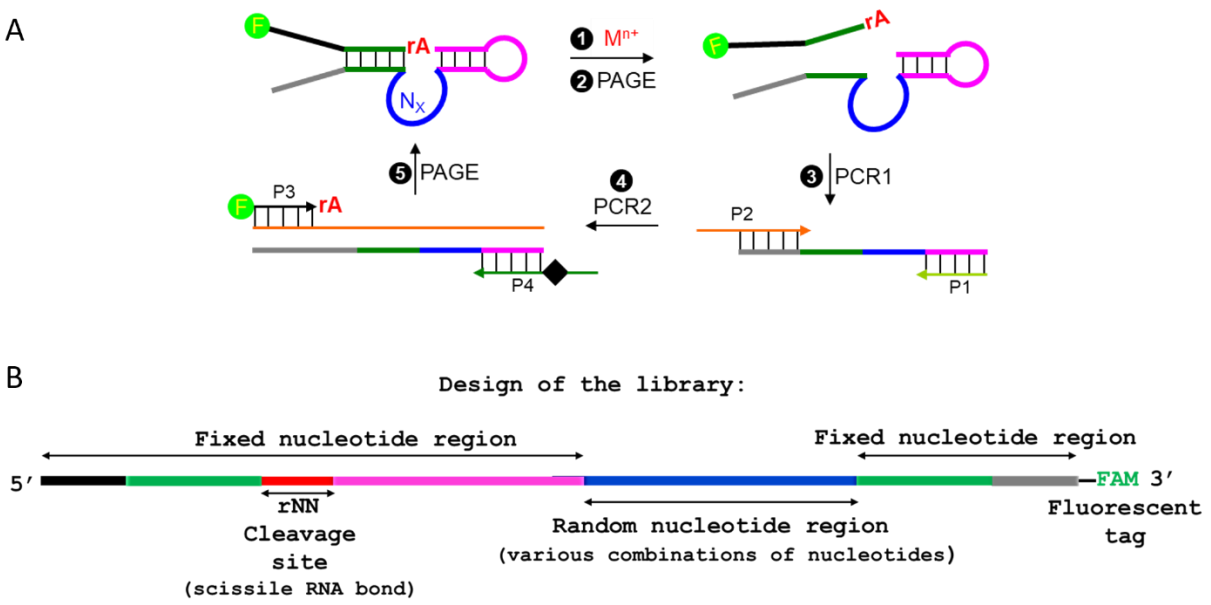

Figure 1.7 General schematic of the (A) *in-vitro* selection for isolating metal-dependent RNA-cleaving DNAzymes (figure adapted with permission from ref 101. Copyright 2014, American Chemical Society).[42,101] The protocol has five main steps. 1: metal induced cleavage, 2: PAGE-based separation and extraction of the cleaved strands, 3: polymerase chain reaction of the extracted pool (PCR1) to produce the full-length library, 4: PCR2 to introduce the FAM-label and the rA base in the reconstituted library, and 5: PAGE-based purification to isolate the positive strand (the one bearing the cleavage site) from the duplex PCR2 product. (B) General schematic of the library for the selection of RNA-cleaving DNAzymes.

It consists of two parts, one of them is the randomized region (labeled as 'random nucleotide region' in Figure 1.7 B) which consists of the putative enzymes. Flanking the random region on both the 3′ and 5′ side is the fixed region of the library, which usually contains a single RNA linkage as the embedded cleavage site. The general schematic of the library used for the selection of RNA-cleaving DNAzymes is shown in Figure 1.7 B. The sequence of the fixed region is designed such that the library folds upon itself bringing the random region in proximity with the cleavage site. The library is incubated with a fixed concentration of a target metal ion under specific and stringent conditions, and a small library fraction may cleave the RNA

linkage. The cleaved sequences would be shorter, would migrate faster in denaturing PAGE (Poly Acrylamide Gel Electrophoresis), and can thus be collected and amplified by PCR. Usually, two PCR reactions are carried out to amplify the cleaved sequences, reconstitute library's full length and to incorporate the RNA base (cleavage site) as well as a fluorophore. This new library is subjected to another round of selection and this entire process is iteratively performed to obtain the desired DNAzyme. To increase the selectivity of the library for the target metal, the non-specific sequences can be removed by carrying out negative selections where the uncleaved library is sequestered and amplified.[97–100]

General role of metal ions in RNA-cleaving DNAzyme catalysis. The role of metal ions in DNAzyme catalysis can range from general charge shielding of the polyanioinc DNA to specific coordination at particular sites for structural and functional stability. In the catalysis of RNA-cleaving DNAzymes, the substrate cleavage dinucleotide comprises of a chimeric dinucleotide junction of one RNA and one DNA base. Generally, the cleavage takes place at the 3′ side of the RNA base.

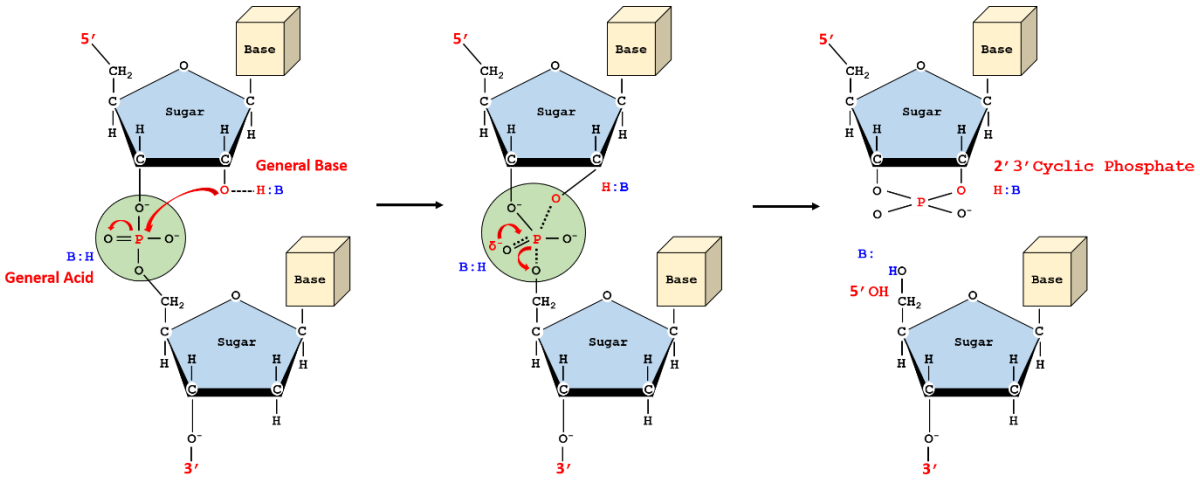

Figure 1.8 A general schematic of the RNA cleavage hydrolysis reaction (figure adapted and modified with permission from ref 102. Copyright 2014, American Chemical Society).[102]

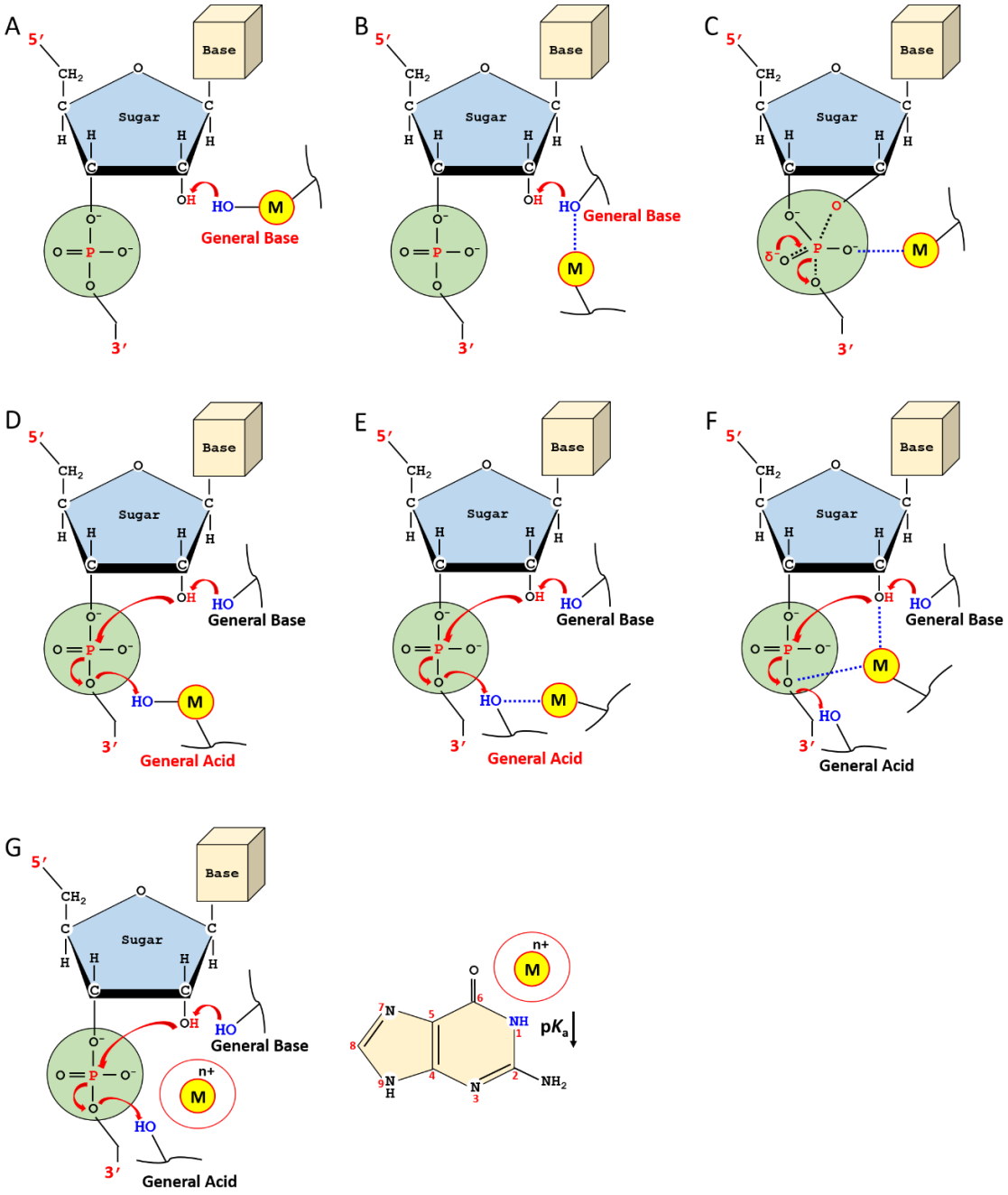

Figure 1.9 The possible roles of metal ions (M or M^{n+}) in DNAzyme mediated RNA cleavage reaction (figure adapted and modified with permission from ref 102. Copyright 2014, American Chemical Society). Metal ion (A) acting as a general base or proton acceptor, (B) coordinating a general base near the cleavage site, (C) coordinating with the phosphate oxygen in the pentavalent phosphorene transition state intermediate, (D) acting as a general acid or proton donor, (E) coordinating a general acid near the cleavage site, (F) coordinating with the 2′-OH group / the leaving group to assist the proton transfer steps, or (G) influencing the catalysis electrostatically.[102]

Usually, the RNA cleavage hydrolysis reaction is initiated by a nucleophilic attack on the phosphodiester bond between the cleavage site dinucleotide, proceeds through a phosphorane intermediate and finally results into intramolecular phosphoryl transfer leading to the breakage of the RNA bond (Figure 1.8). More than often, the activated oxygen of the 2′-OH of the RNA nucleotide is known to act as the nucleophile. Metal ions play a key role in the success of this catalysis.[102] Potential roles of metal ions are: i) Metal hydroxides can act as general bases (proton acceptors) to deprotonate the 2′-OH of the cleavage site RNA and activate its oxygen making it a more potent nucleophile (Figure 1.9 A). ii) Inner sphere coordination of the metal with the cleavage site phosphate oxygen can help in stabilizing the accumulated negative charge on the pentavalent phosphorane transition state intermediate (Figure 1.9 C). iii) Metal hydroxides can act as general acids (proton donors) to donate protons to the leaving group for the final cleavage of the phosphodiester bond (Figure 1.9 D). iv) Metals can directly coordinate to the 2′-OH group / the leaving group to assist the proton transfer steps (Figure 1.9 F). v) Metals can help through outer sphere interactions by organizing a water molecule or by coordinating with a proton donor / acceptor in proximity to the cleavage site for general acid-base catalysis (Figure 1.9 B and E). vi) Metal ions juxtaposed to the active site can have electrostatic influence on catalysis. For e.g. by stabilization of the highly anionic transition states, or by alteration of the pK_a of the catalytically significant functional groups present in nucleobases (Figure 1.9 G).

Monovalent metal ion specific RNA-cleaving DNAzymes. The catalytic potential of monovalent cations has long been underestimated, but the recent discoveries of Na^+-dependent RNA-cleaving DNAzymes have drawn attention to the catalytic abilities of group 1A metal ions. *NaA43* (Figure 1.10 B) works selectively in the presence of Na^+ with the reasonably high

rate of 0.1 min^{-1} in presence of 400 mM Na^{+}.[104] Another Na^{+} specific DNAzyme *EtNa* (Figure 1.10 A), is highly selective with a rate of 0.06 min^{-1}, and possess a unique property of catalyzing substrate cleavage in organic solvents.[105]

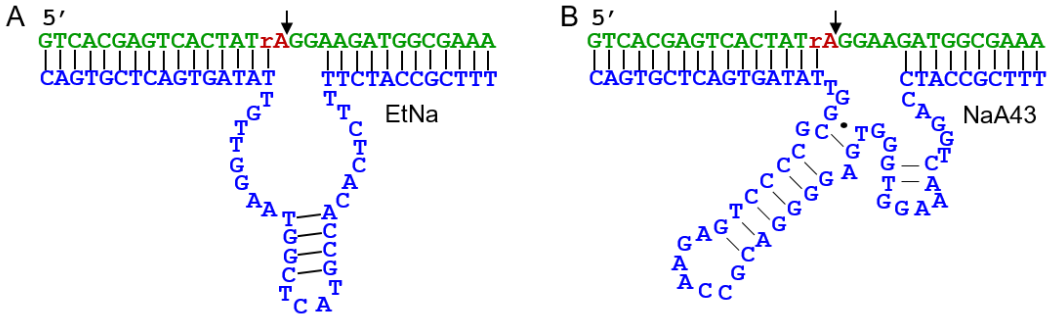

Figure 1.10 Secondary structure of the monovalent ion-dependent RNA-cleaving DNAzymes (A) EtNa (figure adapted and modified with permission from ref 103, Copyright 2015, John Wiley and Sons),[103] and (B) NaA43 (figure adapted and modified with permission from ref 104).[104]

Divalent metal ion specific RNA-cleaving DNAzymes. This represents the largest class as most of the RNA-cleaving DNAzymes use divalent cations as cofactors. The first RNA-cleaving DNAzyme discovered through *in-vitro* selection in 1994 was *GR5* (Figure 1.11 A), a highly selective and active (rate ~ >10 min^{-1}) Pb^{2+}-dependent enzyme.[67] Another DNAzyme *17E* (Figure 1.11 B) initially discovered in a Zn^{2+} selection, is now known to be highly active with Pb^{2+} (rate $>10^{-1}$).[112,113] However, the17E is less selective and apart from Zn^{2+} it has reoccurred as a result of Cd^{2+}, Ca^{2+} and Mg^{2+} selections.[112,114–118] As GR5 and 17E share the same critical nucleotides for catalysis, I have performed a detailed comparative study of the two DNAzymes which suggests that they both may have similar Pb^{2+} binding mechanism (See Appendix A – Chapter 6, for detailed experimentation).[106] Leadzyme is a very small Pb^{2+}-dependent ribozyme containing only 6 residues in its catalytic loop. Inspired by this, I had undertaken a Pb^{2+}

selection to see if a very small Pb^{2+}-dependent RNA-cleaving DNAzyme exists. As a result, I reported the discovery of *PbE22* (Figure 1.11 C) which was highly selective for Pb^{2+} and consists of only 5 nucleotides in its catalytic loop (See Appendix B – Chapter 7, for detailed experimentation).[108]

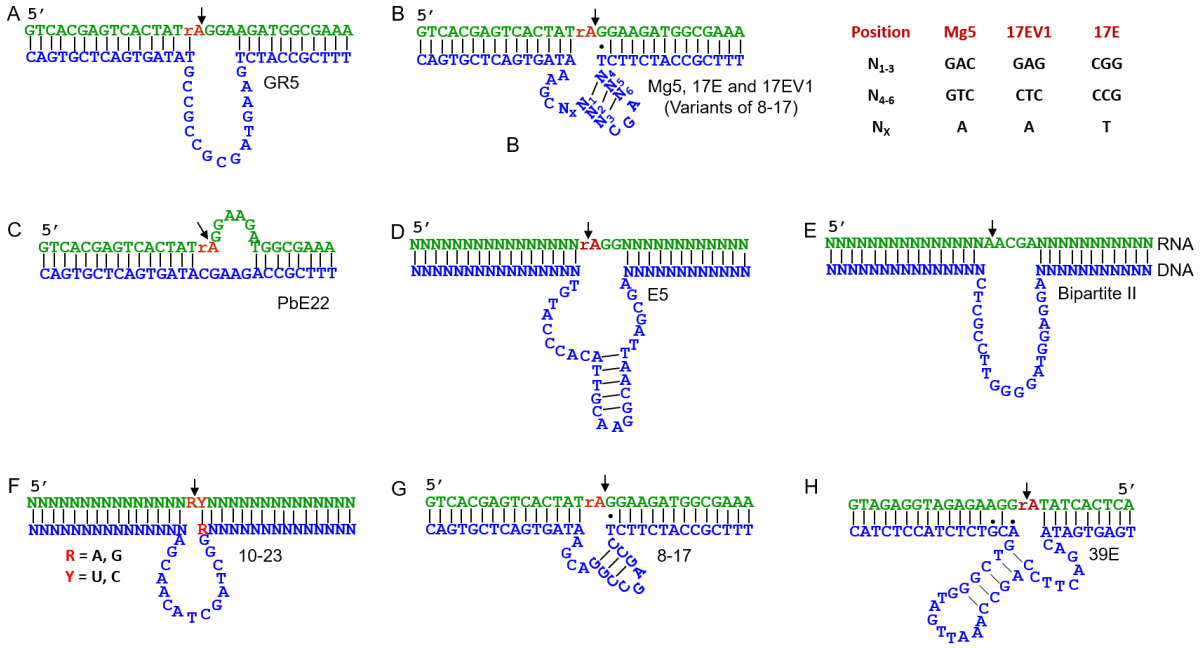

Figure 1.11 Secondary structure of the divalent ion-dependent RNA-cleaving DNAzymes (A) GR5 (figure adapted and modified with permission from ref 67, Copyright (1994), Elsevier),[67] (B) Mg5, 17E and 17EV1 (variants of 8-17 DNAzyme) (figure adapted and modified with permission from ref 107. Copyright 2016, American Chemical Society),[107] (C) PbE22 (figure adapted and modified with permission from ref 108, Copyright 2015, Springer Science Business Media new York),[108] (D) E5 (figure adapted and modified with permission from ref 109, Copyright (1995), Elsevier),[109] (E) Bipartite II (figure adapted and modified with permission from ref 110, Copyright (2001), Elsevier),[110] (F) 10-23 (figure adapted and modified with permission from ref 111, Copyright (1997) National Academy of Sciences, U.S.A),[111] (G) 8-17 (figure adapted and modified with permission from ref 111, Copyright (1997) National Academy of Sciences, U.S.A) ,[111] and (G) 39E (figure adapted and modified with permission from ref 97, Copyright (2007) National Academy of Sciences, U.S.A).[97]

Being a physiologically significant metal ion, Mg^{2+} has been used to carry out multiple selections leading to the discovery of *E5* (also shows activity with Cd^{2+} and Pb^{2+}) (Figure 1.11 D),[109] *BipartiteI* (also shows activity with Ca^{2+}, Mn^{2+}, Zn^{2+}, and Co^{2+}),[110] *BipartiteII* (Figure 1.11 E),[110] *10-23 (Figure 1.11 F)*,[111] *8-17* (much more active with Pb^{2+} and Zn^{2+}) (Figure 1.11 G),[111] and *Mg5* DNAzyme (shows 10-fold more activity with Ca^{2+}) (Figure 1.11 B).[115,119] Another Ca^{2+}/Mg^{2+}-dependent DNAzyme *17EV1* was discovered as a result of a selection in undiluted serum (Figure 1.11 B).[107] The DNAzyme *EtNa*, initially known to work with Na^{+} in organic solvents, is now also known to catalyze with Ca^{2+} and Mg^{2+} in aqueous solutions (Figure 1.11 A).[120] Amongst the actinides, UO^{2+} is utilized as the cofactor by the RNA-cleaving DNAzyme *39E,* in which uranyl is known to bind specific nucleotides in the bulge-loop, stem-loop and the substrate strand (Figure 1.11 H).[97] In the transition metals, Cu^{2+} and Cd^{2+} have been used for *in-vitro* selection with a library containing a PS modification at the cleavage site, resulting into the DNAzymes *PsCu10,*[99] and *Cd16* respectively **.**[98] A Hg^{2+}-dependent DNAzyme has also been reported with a library consisting of two modified DNA bases.[121]

Trivalent metal ion specific RNA-cleaving DNAzyme. Owing to their high charge density and affinity for the phosphates and nucleobases in DNA, the trivalent lanthanides (Ln^{3+}) have been efficiently utilized as cofactors by multiple RNA-cleaving DNAzymes. Many Ln^{3+} specific selections have been undertaken. One of the most interesting RNA-cleaving DNAzymes *Ce13d* (Figure 1.12 A) was selected for Ce^{4+}, and turned out to be active in presence of all trivalent Ln^{3+} but not for Ce^{4+}.[101,124] Another DNAzyme *Lu12* (Figure 1.12 B), initially selected for Lu^{3+} works with lighter lanthanides and exhibits decreased activity with heavier Ln^{3+}.[122] A Tm^{3+} specific selection has resulted into the DNAzyme *Tm7* (Figure 1.12 C).[123] Dy^{3+} has also been used for selection which finally evolved into the DNAzyme *Dy10a* (Figure 1.12 D).[125]

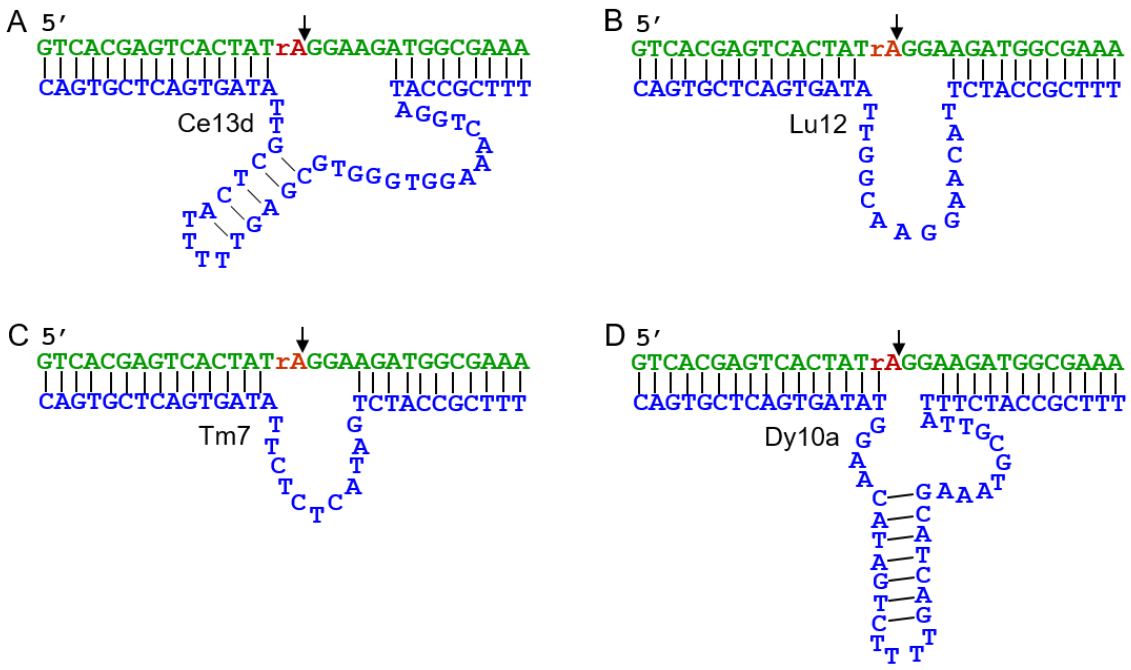

Figure 1.12 Secondary structures of the trivalent ion-dependent RNA-cleaving DNAzymes (A) Ce13d (figure adapted and modified with permission from ref 101. Copyright 2014, American Chemical Society),[101] (B) Lu12 (figure adapted and modified with permission from ref 122. Copyright 2014, American Chemical Society),[122] (C) Tm7 (figure adapted and modified with permission from ref 123. Copyright 2014, Oxford university Press),[123] and (D) Dy10a (figure adapted and modified with permission from ref 125. Copyright 2016, American Chemical Society).[125]

Aptazymes. Aptazymes are DNAzymes which contain a specific aptamer sequence and whose catalytic activity is modulated by aptamer binding. Target-aptamer binding changes the structural fold of the aptazyme such that it gets activated for catalysis. Aptazymes have an edge over both DNAzymes and aptamers, in terms of enhancement of signal amplification and reduction of nonspecific signals respectively. Multiple strategies have been adopted to club a known aptamer with a known DNAzyme in order to make the catalytic activity dependent on target binding. The incorporation of aptamer in the hairpin of the catalytic loop,[126] as well as in substrate binding strand,[127] has been reported. Within these, catalysis is modulated by the

unfolded/ folded state of the DNAzyme in the absence/ presence of the target respectively. Apart from these rationally designed examples, some reports of *in-vitro* selection of aptazymes also exist. For instance, Co^{2+} binding aptazymes have been selected by Breaker and co-workers.[128] The unintentional discovery of aptazyme Ce13d is worth mentioning in this regard. Ce13d bears an aptamer for Na^{+} within its catalytic loop (Figure 1.12 A). Ce13d-Na^{+} binding brings in conformational changes and activates the enzyme, while a lanthanide ion interacts with the cleavage dinucleotide to carry out the catalysis.[101,129,130]

Concerted action of multiple metal ions. While all the known DNAzymes require one specific type of metal ion for activity, it is worth noting that Ce13d can be categorized under a new section of DNAzymes which require two metal ions which are different in their identity. Ce13d is a unique DNAzyme which requires the concerted action of two dissimilar metal ions acting at two distinct sites for successful catalysis to take place.[129]

1.4 Nucleic acid based metal sensing

1.4.1 Need for metal biosensors

Extensive use of metals in all domains of civilization ranging from large scale industrial applications to everyday household utilities, and their consequent disposal into natural resources, makes metal sensing indispensable for environmental monitoring. While traditional analytical methods such as inductively coupled plasma - mass spectroscopy (ICP-MS) are available, rapid and on-site measurement of metal ions in various types of environmental samples is an urgent need. Biosensors have the potential to attain excellent sensitivity and selectivity owing to the possibility of excellent target binding affinity and signal amplification.

With the advent of DNA based beacons, information regarding metal speciation can be quickly obtained e.g. Fe^{2+}/Fe^{3+} or Cu^{2+}/Cu^{+}, while most of the instrumentation methods can report total metal concentration and not the oxidation state. Apart from environmental samples, it is also important to measure metal concentration in intracellular samples and biological fluids. DNA based technology has made this possible in temporal and spatial resolution, which has expedited the development of diagnostic applications. Taken together, the advent of molecular sensors may have revolutionary effects on the society in multiples spheres of life.

1.4.2 DNA based molecular beacons

In the past decade there has been aggressive research to develop various platforms for detecting metal ions in water samples. With the high programmability and stability of nucleic acids, multiple types of DNA based sensing methods have developed over the years for aqueous metal ions. One of the most selective sensors are the catalytic beacons, which consist of mostly the RNA-cleaving DNAzymes. Typically, for such sensors, the substrate and enzyme strand is labelled with a fluorophore and quencher respectively. In the absence of the metal ion, the enzyme-substrate duplex is formed enabling the measurement of baseline fluorescence due to FRET between fluorophore-quencher pair. The sequence of the duplex is designed such that in the presence of the metal ion, the cleavage of the substrate causes the T_m between enzyme-substrate to go below room temperature leading to dissociation of the fluorophore labeled substrate. This dissociation decreases FRET and the metal concentration-dependent rise in fluorescence can be calibrated and used as a sensitive metal ion sensor. Many variations in the sensor design to improve sensor performance have been explored e.g. position of labeling,[131] number of quenchers,[132] asymmetric design of DNAzyme complex,[133] etc. An extensive

category of sensors are aptamer beacons**.** Usually, upon binding to its target, the aptamer undergoes a specific 3-dimensional change in its conformation.[134] Whether it be a local or a global change, it can be detected and utilized to indicate target-aptamer binding. Various different designs and signaling strategies have been used for this purpose. For e.g. calibrated changes in fluorescence (FRET, pyrrolo-cytosine, 2- amino purine, etc.),[46,135,144,145,136–143] and color,[146] is a popular detection method. In some cases, electrochemistry,[147,148] Rayleigh scattering,[149] SERS,[150] Resonance Light scattering (RLS),[151] and quantifiable digital signals,[152] have also been used in this regard. Apart from these methods which require covalent conjugation of signaling labels with the DNA, many label free and cost-effective options are also developed for both DNAzyme and aptamer beacons. These include dyes which can bind / intercalate into DNA or stain abasic sites,[153,154] e.g. SYBR Green I (SGI),[155] ethidium bromide (EB),[156] picogreen (PG),[157] fluorescent cationic conjugated polymers (CCP),[158] etc. AuNPs are known to aggregate in the presence of folded aptamers while remain protected against aggregation with unfolded aptamers. This change in color of AuNPs upon aggregation due to metal-aptamer binding is an interesting label free signaling method. Similarly, change in dielectric constant (i.e. SPR signals),[159] or mass (i.e. QCM signals),[160] of aptamer functionalized gold surfaces upon metal binding has also been harnessed. Lately, lateral flow devices are also being explored and developed for metal detection.[161–163]

1.5 Ag^+ - DNA interaction

1.5.1 Properties of Ag^+

In terms of metal ions, their properties like size, pK_a of metal bound water, Lewis acidity, charge, coordination preference, ligand exchange rate, etc. play an important role in determining their interaction with nucleic acids. Silver (Ag) is a chemical element that falls under the category of transition metals with an atomic number of 47 and a standard atomic weight of 107.8682. When solubilized, silver loses a $5s^1$ electron to form Ag^+ and +1 is its most common oxidation state, while rare occurrence of -2, -1, +2, and +3 oxidation states has also been reported.[164–166] The number of charges on metal ions is of great relevance for DNA binding, mainly because DNA is a polyanion. Usually, the effect of monovalent ions (mostly the group 1A metals) has been seen above 10 mM. In solution Ag^+ exists in form of aqua complexes. Ag^+ exhibits coordination numbers of 2, 3, 4, 6 with linear, trigonal planar, tetrahedral and octahedral stereo-chemistries respectively.[167] The empirical atomic radius of silver is 144 pm, while the 6-coordinated Ag^+ ionic radius is reported to be 129 pm.[168] With respect to DNA binding, the size of hydrated metal ion is more significant, and the $Ag(H_2O)_4^+$ ion radius is reported to be 0.98 + 1.2 Å.[169] The charge density of the 6-coordinated Ag^+ ion is reported as 15 (C mm^{-3}).[170] Metal ions are electron deficient species, due to this they can accept electron pairs from ligands and thus act as Lewis acids. Similarly, the aqua coordinated Ag^+ draws electron density from the O-H bond in water present in its coordination sphere. The subsequent release of aqueous proton makes Ag^+ behave like a weak acid. The first pK_a of Ag^+ is around 10.0.[171] These solution properties of metal ions majorly influence their interaction with DNA in a decisive manner.

1.5.2 Known Ag^+ - DNA interactions

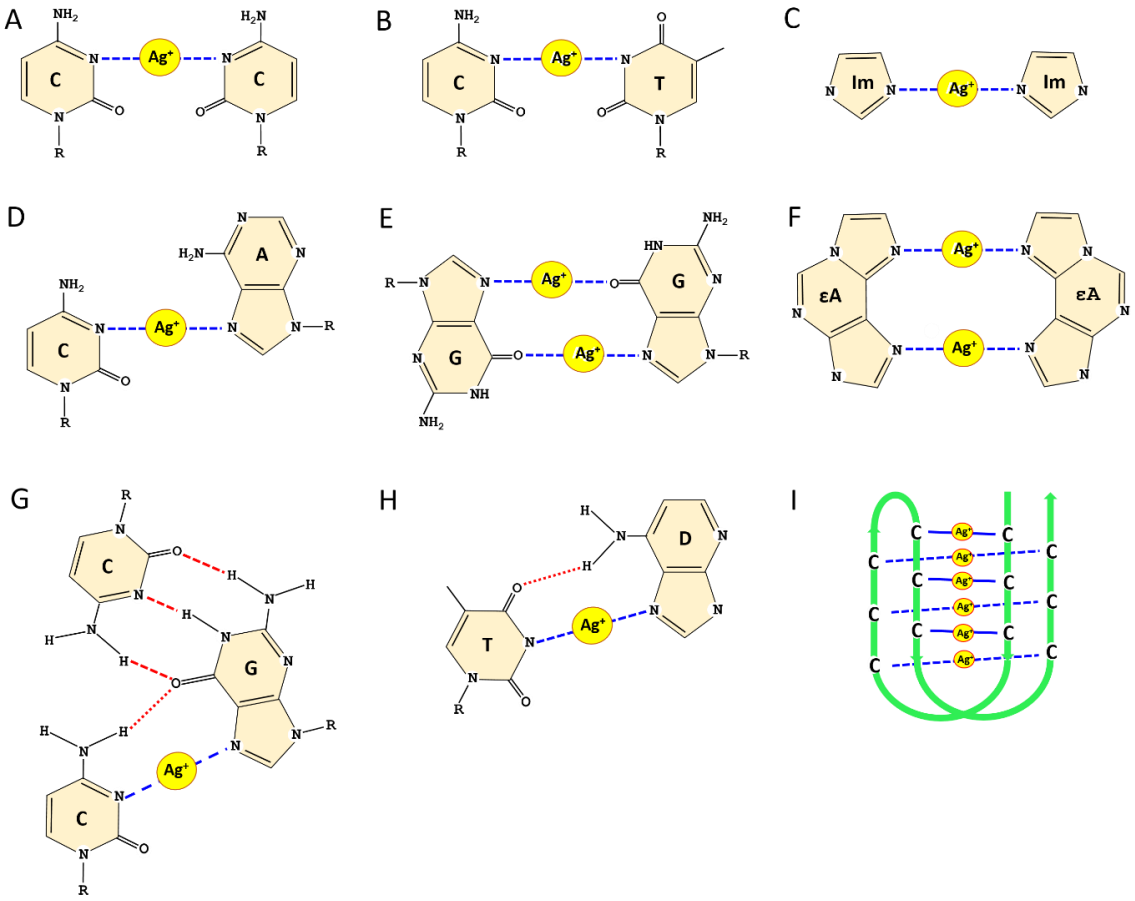

Figure 1.13 Representation of the chemical structure of the Ag^+ assisted base pairs between (A) two cytosines (figure adapted and modified with permission from ref 173. Copyright 2008, Royal Society of Chemistry),[173] (B) cytosine and thymine (figure adapted and modified with permission from ref 183. Copyright 2007, John Wiley and Sons),[183] (C) 2 imidazole rings (figure adapted and modified with permission from ref 189. Copyright 2010, Springer Nature) ,[189] (D) cytosine and adenine thymine (figure adapted and modified with permission from ref 181. Copyright 1999, Springer Nature),[181] (E) two guanines thymine (figure adapted and modification with permission from ref 176. Copyright 2010, American Chemical Society),[176] (F) two1, N^6-ethenoadenines (figure adapted and modified with permission from ref 186 under Creative Commons Attribution License),[186] (G) cytosine and guanine in a CG.CAg^+ base triplet (figure adapted and modified with permission from ref 179. Copyright 2009, American Chemical Society),[179] and (H) thymine and 1-deazaadenine (figure adapted and modified with permission from ref 180. Copyright 2011, Elsevier).[180] (I) A schematic of a Ag^+ mediated i-motif (figure adapted and modified with permission from ref 175. Copyright 2013, American Chemical Society).[175] The hydrogen bonds are shown as red dashed lines, and the Ag^+ assisted bonds are shown as blue dashed lines.

As mentioned above, co-ordination of metal cations with nucleic acid is of high appeal because of their indispensable implication in biology and nano-biotechnology. Amongst the metal ions, the Ag^+ cation has attracted noteworthy attention. Many interactions of Ag^+ with nucleic acids or with nucleobases have been summarized below:

C-Ag$^+$-C base pair. Ag^+ is known to co-ordinate with cytosine residue at its N3 position and selectively bring together two cytosines to form a stable C-Ag^+-C metal assisted base pair (Figure 1.13 A). This binding has been testified by UV melting, ITC and ESI-MS, CD spectroscopy and NMR. Ag^+ was found to be in a 1:1 ratio with the C:C mismatched base pair in the duplex with a binding constant of 10^6 M^{-1} , which is remarkably higher than other known nonspecific DNA-metal interactions.[172,173]

I-motif. It has been validated in 1993 through NMR structural studies that, at acidic pH hemi-protonated cytosine$^+$-cytosine base pairs form between oligomers containing tracts of cytosine residues to make a four stranded secondary structure called i-motif.[174] It consists of two parallel duplexes hydrogen bonded together in an antiparallel orientation by intercalated cytosine$^+$-cytosine base pairs. In 2013 it was reported that owing to its ability to form C-Ag^+-C base pairs, Ag^+ can mediate the formation of i-motif (Figure 1.13 I) at neutral pH.[175]

Ag$^+$- Guanosine co-ordination. It is well established that silver can strongly chelate to the N7 and O6 position in guanosine and GMP, and combines with them in a 1:1 ratio at neutral pH. pH-dependent Ag^+ titrations, UV, IR and CD spectroscopy as well as ITC studies have confirmed that Ag^+ uniquely form stable dimers of guanine (Figure 1.13 E) and can assemble and aggregate GMP with the same kind of co-ordination.[1,176,177] Ag^+ can also assist in pairing of guanine homo-base strands by bridging two guanines together, with a stronger stability than the Watson-crick guanine-cytosine pairing.[178]

C-Ag$^+$-G Hoogsteen-type base pair. It has been experimentally shown that Ag^+ can displace the N3 proton of cytosine in Hoogsteen base pairing to mediate the formation of a CG.CAg^+ base triplet in a triple helix (Figure 1.13 G).[179,180]

C-Ag$^+$-A base pairs. Interestingly, the Klenow fragment DNA polymerase is known to misincorporate adenine into the site opposite to cytosine in the template strand in the presence of Ag^+. It is reasoned that this is due to the formation of the Ag^+ mediated base pair C-Ag^+-A. However, it has been demonstrated that the C-C mismatch duplex bears higher stability than the C-A mismatch containing base pair in the presence of Ag^+.[172] Based on ab initio studies of the C-Ag^+-A base pair and the X-ray crystallography data available for the [(1-MeC)Ag(9-MeA)(H2O)]$^+$ complex, it is predicted that a single Ag^+ forms coordinative bonds with N3 of cytosine and N7 of adenine (Figure 1.13 D).[181,182]

C-Ag$^+$-T base pair. Silver (I) ion is capable of deprotonating thymine in oligonucleotides and is known to bind the N3 atom of deprotonated thymine to form an Ag^+–thymine complex which does not bear any charge.[183] This Ag^+–thymine complex has affinity towards aromatic tertiary nitrogen atom and is able to co-ordinate to the N3 position in cytosine in oligodeoxynucleotides (Figure 1.13 B). The T-Ag^+-C base pair is stabilized by 1 equivalent of Ag^+ ions and has approximately comparable thermal stability to that of C-Ag^+-C base pair.[184]

Ag$^+$ interaction with non-canonical bases. Ag^+ is proved to co-ordinate with some modified or non-natural bases. Ag^+ can co-ordinate with the N7 position of base 1-deazaadenine (D) and the formation of Ag^+ assisted Hoogsteen-type base pair between Thymine and 1-deazaadenine T-Ag^+-D (stabilized by H-bonding as well as metal ion binding), has been experimentally demonstrated (Figure 1.13 H).[180,183] It has been shown that in the presence of Ag^+, 1, N^6-ethenoadenine (εA) forms a stable homo base pair εA-$(Ag^+)_2$-εA (Figure 1.13 F) in both parallel

and antiparallel stranded DNA. It can also form εA-$(Ag^+)_2$-T base pair in double helical DNA, as well as εA-(Ag^+)-C and εA-$(Ag^+)_2$-C base pairs depending on the relative orientation of the oligonucleotide strands.[185–187] Ag^+ can co-ordinate to N3 position of 5-methylisocytosine (m^5iC) and can thus aid the formation of m^5iC-Ag^+-C and m^5iC-Ag^+-T base pairs in oligonucleotides.[184] Another cytosine analogue that Ag^+ can co-ordinate with is pyrollo-deoxycytosine (PdC), via its N3 position and the formation of PdC-Ag^+-C base pair in duplex DNA has been demonstrated.[145] Ag^+ has been investigated to bring together two imidazole (Im) bases into Im-Ag^+-Im base pair.[188] Formation of Im-Ag^+-Im base pair in B-type DNA duplex has been demonstrated by solution NMR structure (Figure 1.13 C).[189] A single Im-Ag^+-Im base pair is around one order of magnitude more stable than the C-Ag^+-C base pair. Contiguous Im-Ag^+-Im base pairs have been found to form in a co-operative manner through ITC, UV and CD spectroscopy.[190] Detection of complexes of Ag^+ with bases *Inosine* as well as *Caffeine* have also been detected using electrospray ionization mass spectrometry.[191]

DNA templated fluorescent silver nanoclusters. Since 2004, it is known that because of the high affinity between Ag^+ and DNA bases, short oligonucleotide-encapsulated fluorescent Ag nanoclusters can form.[192] Multiple reports regarding the synthesis of DNA-templated fluorescent silver nanoclusters (AgNCs) have been published and most commonly C-rich DNA can be used as a template.[193–196] It has also been proposed that poly-C templated AgNCs can form a dimer upon addition of free Ag^+ ion.[197] However, instances of poly-G DNA templated AgNCs are also present.[198]

1.5.3 Ag^+ biosensors

Fluorescence based sensing. Formation of Ag^+ assisted C-Ag^+-C base pairs has been well utilized for the purpose of sensing Ag^+ ions (Figure 1.14 A).[199]

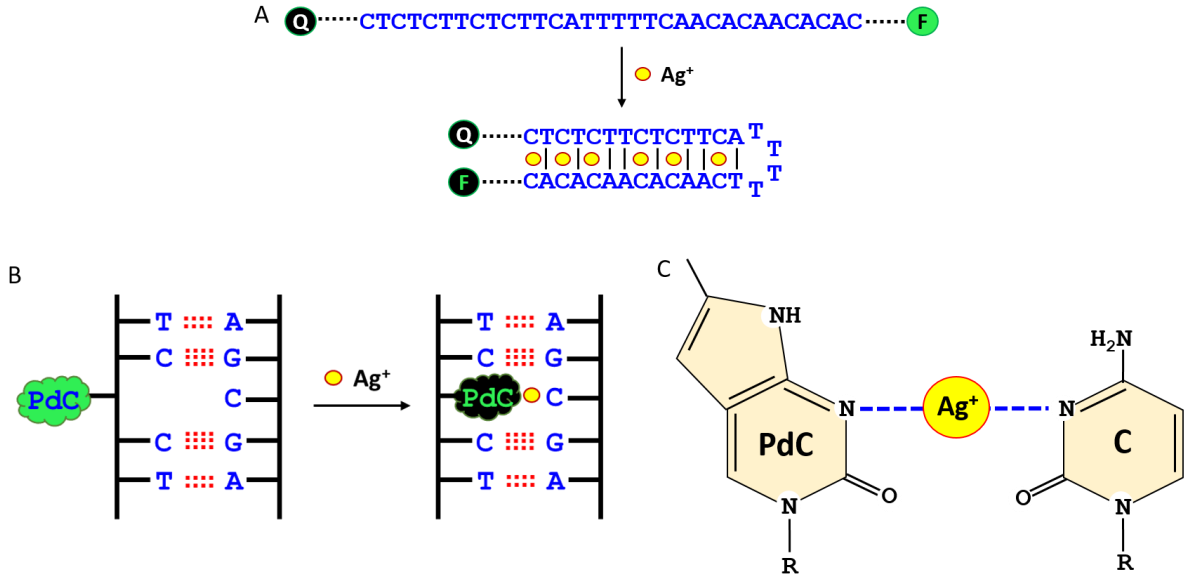

Figure 1.14 Schematic of fluorescence based Ag^+ sensor based on the formation of (A) C-Ag^+-C base pairs (figure adapted and modified with permission from ref 199. Copyright 2008, Royal Society of Chemistry)[199] and (B) PdC-Ag^+-C base pair.[145] (C) Representation of the chemical structure of Ag^+ assisted base pair between pyrrolo-cytosine and cytosine.[145] Figures (B) and (C) adapted and modified with permission from ref 145. Copyright 2012, Royal Society of Chemistry.

Within this design, a C-rich DNA has been labelled with a quencher on one end and a fluorophore on the other. Upon the addition of Ag^+, the sequence folds upon itself into a hairpin structure due to the formation of C-Ag^+-C base pairs. This brings the quencher sufficiently proximal to the fluorophore to diminish its fluorescence via FRET. Since the decrease in fluorescence was [Ag^+]-dependent, this method could be developed into an Ag^+ sensor. Pyrrolo-deoxycytosine (PdC), an analogue of cytosine possesses two interesting properties. Firstly, as mentioned above (section 1.5.2) it exhibits intrinsic fluorescence in the single stranded form

and upon base pairing the fluorescence reduces manifolds. Secondly, similar to cytosine, PdC can form Ag^+ assisted base pairs with cytosine. Both these traits together have proved to be very beneficial in developing a highly sensitive and selective PdC based Ag^+ sensor (Figure 1.14 B and C).[145] For this, PdC was incorporated in the middle of a single stranded oligomer. A complementary oligo was designed which placed cytosine opposite to PdC upon hybridization. In the absence of Ag^+, PdC and cytosine are left unpaired in the duplex, leaving PdC fluorescent. Upon the addition of Ag^+, PdC-Ag^+-C base pairing takes places reducing the fluorescence and indicating the presence of silver. This method could detect Ag^+ down to ~ 9.2 nM.

Label free sensing. Tb^{3+} luminescence has been a useful probe for DNA fold and structures. Tb^{3+} has low emission as a free molecule but when bound to nucleobases its luminescence strengthens significantly. It has been reported that when Ag^+ coordinates to Tb^{3+} bound poly-G/T DNA, it drastically enhances the Tb^{3+} luminescence (Figure 1.15 A). For Ag^+ sensing, a G7 DNA has been used. An Ag^+ concentration-dependent increase was found in the fluorescence of Tb^{3+} bound G7 DNA, and the limit of detection was calculated to be ~ 57 nM.[200] It has been mentioned in section 1.5.2 that Ag^+ can bind to a C-rich sequence to form i-motif structure at neutral pH. This Ag^+-i-motif structure can be disrupted using cysteine. As Ag^+ has strong affinity to cysteine, it can be extracted away by forming a cysteine-Ag^+ complex, leading to the deformation of i-motif. To use this as an Ag^+ sensing system, the fluorescent probe Thiazole orange (TO) was used. TO is not fluorescent as a free unbound molecule, but when incorporated in the i-motif it shows strong fluorescence. Therefore, the presence or absence of Ag^+ can be detected by probing the presence or absence of TO fluorescence respectively (Figure 1.15 B). A detection limit of ~ 17 nM has been achieved using this method.[201]

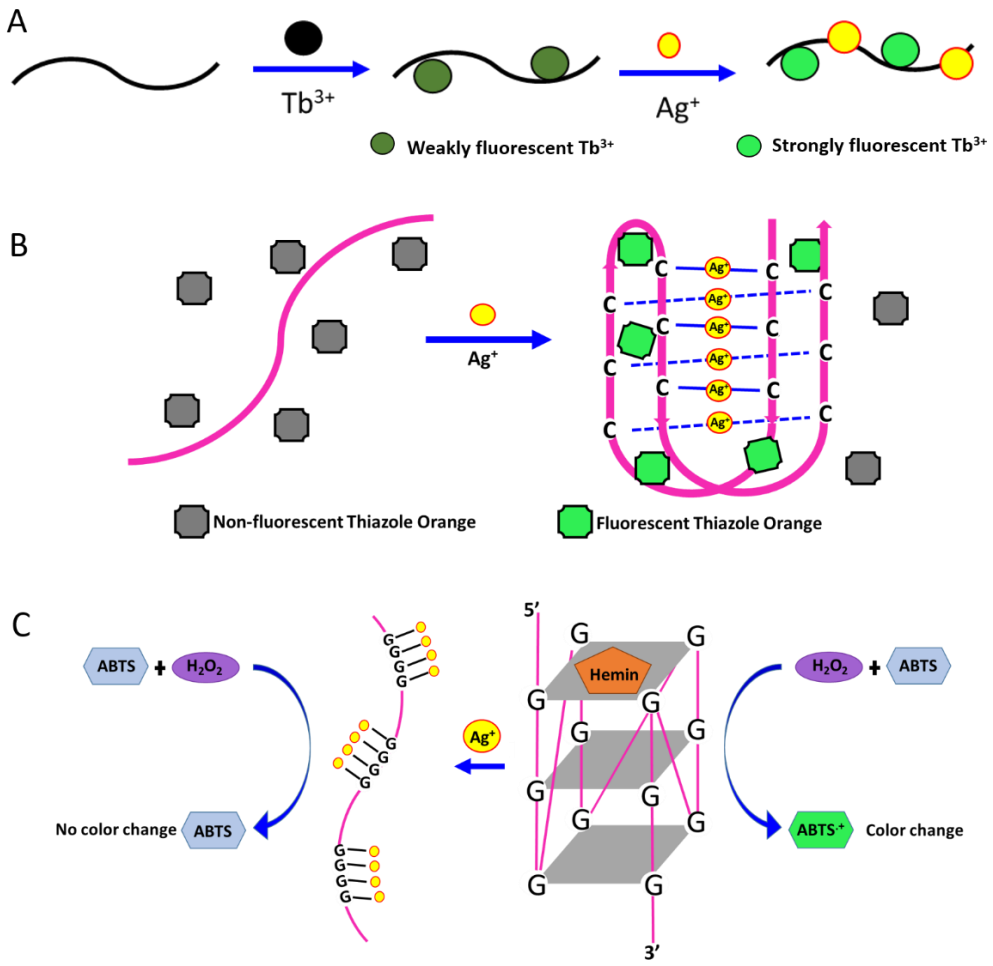

Figure 1.15 Schematic of Ag^+ sensor based on (A) Ag^+ enhanced Tb^{3+} luminescence (figure adapted and modified with permission from ref 200 under the Creative Commons Attribution License),[200] thiazole orange binding to Ag^+ mediated i-motif formation (figure adapted and modified with permission from ref 201. Copyright 2016, Elsevier),[201] and (C) Ag^+ mediated disruption of G-quadruplex hemin DNAzyme activity (figure adapted and modified with permission from ref 202. Copyright 2010, American Chemical Society).[202]

G-quadraplex DNAzymes have also been used to develop sensing systems for Ag^+.[202,203] The binding sites on Guanines needed to form G-quadraplexes are same as those needed to coordinate with Ag^+. Therefore, Ag^+ is capable of disrupting the secondary structure of G-quadraplex-hemin DNAzymes and consequently diminish their peroxidase activity (Figure 1.15

C). The presence or absence of the activity has been correlated with the absence or presence or Ag^+ respectively and a detection limit of 64 nM has been achieved with the same.

Colorimetric Sensing. Formation of DNA templated silver nanoclusters (AgNCs) has been discussed in section 1.5.2. For making an AgNC based Ag^+ sensor, a 12-mer cytosine oligo was used to template the formation of AgNCs which exhibited weak red fluorescence. As Ag^+ was added to the system the fluorescence switched to strong green, due to the dimerization of Cyt_{12}-AgNCs mediated by Ag^+ (Figure 1.16).[197] Low Ag^+ concentrations such as ~ 10 nM have been detected using this system.

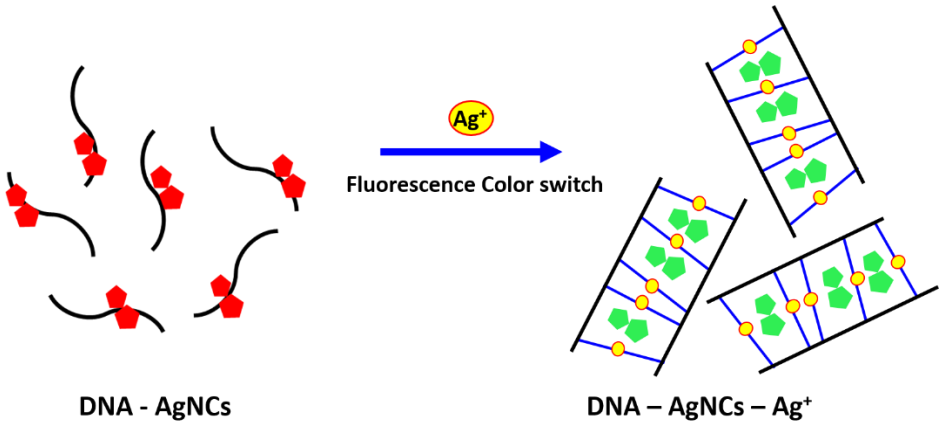

Figure 1.16 Schematic of DNA-AgNCs based colorimetric sensor for Ag^+ (figure adapted and modified with permission from ref 197. Copyright 2015, Elsevier).[197]

Apart from the G-quadraplex peroxidase activity dependent method, the Ag^+ mediated disruption of G4 structures has been used for Ag^+ sensing in an alternative way as well. For this, gold nanoparticles (AuNPs) were capped with G4 structures. In the absence of Ag^+, the AuNPs were found to be mono-dispersed. Addition of Ag^+ induced the disruption of the G4 structures and consequent aggregation of AuNPs. This aggregation brought a change in the

color emitted by AuNPs and this change was used as an indicator of the presence of aqueous silver.[204]

1.6 Research focus

DNA-metal interaction has been a very significant topic of research. Since past two decades, study of DNAzymes and their metal-dependent catalysis has provided crucial insights regarding DNA-metal interactions. There is extensive data available about the catalytic potential of divalent and trivalent lanthanides with respect to DNAzymes. However, not many monovalent ions have been explored in this regard. Although a few Na^+-specific RNA-cleaving DNAzymes have been recently reported, a majority of them still remain untouched. Inspired by the same, the research focus herein is to explore the monovalent metal ion Ag^+ as a cofactor for RNA-cleaving DNAzymes, and to get novel insights into DNA-Ag^+ interactions. So far, most studied interaction of Ag^+ with DNA is of the cytosine-Ag^+ binding and the formation of C-Ag^+-C metal assisted base pairs.[44] Most of the Ag^+ sensing strategies also rely on the same interaction.[173] There are many fundamental challenges of using Ag^+ to activate RNA-cleaving DNAzymes. First, it is a monovalent metal ion, and most DNAzymes require divalent or trivalent metals. Second, it is a very soft metal. Without a sulfur modification, it is challenging to obtain Ag^+-dependent RNA cleavage. On the other hand, Ag^+ can strongly bind to various DNA bases and this gives a platform for new and interesting Ag^+-dependent mechanisms of DNAzyme activation. The main focus of research herein is to expand the repertoire of monovalent ion-dependent RNA-cleaving DNAzymes, as well as to explore novel DNA-Ag^+ interactions. Taking Ag^+ as the target metal ion, *in-vitro* selection experiments focused on discovering novel Ag^+-dependent DNAzymes have been undertaken, and subsequent

development of a sensitive and selective DNAzyme beacon for silver sensing has been done. In addition, systematic biochemical characterization of a selected Ag^{+}-specific DNAzyme has been performed to gain mechanistic insights. Aside from the work on Ag^{+}, another relatively soft metal, Pb^{2+}, was also studied as a cofactor for DNAzyme. To be focused for writing this thesis, the Pb^{2+} related data is presented in Appendix A and B as chapter 6 and 7 respectively.

2. Chapter 2 - *In-vitro* selection of a silver-specific DNAzyme[a]

2.1 Introduction

DNAzymes are DNA-based catalysts (also known as deoxyribozymes and catalytic DNA) isolated using *in-vitro* selection.[205–210] They often recruit metal ions for catalysis, and *in-vitro* selections can be intentionally performed to evolve DNAzymes that work only in the presence of specific metals.[102,211–213] The first DNAzyme was reported in 1994 for RNA cleavage in the presence of Pb^{2+}.[67] Since then many DNAzymes were isolated for specific metals including Zn^{2+},[112] Mg^{2+},[111] Cu^{2+},[78,80] UO_2^{2+},[97] Cd^{2+},[98] Hg^{2+},[121] and recently, important advancements have been made on trivalent metals as well.[122,123,214] The perception of the requirement of multivalent metal ions was relaxed by the recent discovery of DNAzymes that use only monovalent Na^+.[104,215,216] For example, the Lu group reported a DNAzyme with a rate of ~0.1 min^{-1} using Na^+ as the sole metal.[104] To reach such a high rate, however, 400 mM Na^+ is needed. The same Na^+ binding motif was also identified in another lanthanide-dependent DNAzyme.[101,129,130] The Liu group has isolated a Na^+-specific DNAzyme named EtNa, which requires high mM Na^+ in water but low mM Na^+ in ethanol.[103] However, it remains unclear whether it is possible to obtain DNAzymes that can work with nanomolar transition metals. If existing, these DNAzymes will be not only be analytically useful, but can answer fundamental questions in bioinorganic DNA chemistry. The most studied interaction between DNA and silver is the specific binding between the cytosine base and Ag^+.[199,217] This interaction was used to develop Ag^+ biosensors,[218–220] and for making fluorescent silver nanoclusters.[221,222] While DNAzymes have

[a] This chapter is the basis for a published manuscript: Saran R.; Liu, J. A Silver DNAzyme. *Anal. Chem.* **2016**, 88, 4014-4020.

also been used for Ag^+ detection,[220] these sensors still rely on the capturing of Ag^+ by cytosine pairs, and Ag^+ does not participate in catalysis. Herein, the first Ag^+-specific RNA-cleaving DNAzyme named Ag10c, is reported.

2.2 Results and discussions

2.2.1 Selection scheme

As mentioned earlier, *in-vitro* selection refers to the sequestration of a subset of DNA sequences with a desired function from a large library.[205] The aim here was to obtain RNA-cleaving DNAzymes that work specifically with Ag^+. The scheme of selection is shown in Figure 2.1. The initial DNA library is approximated to consist of ~10^{14} unique DNA sequences.

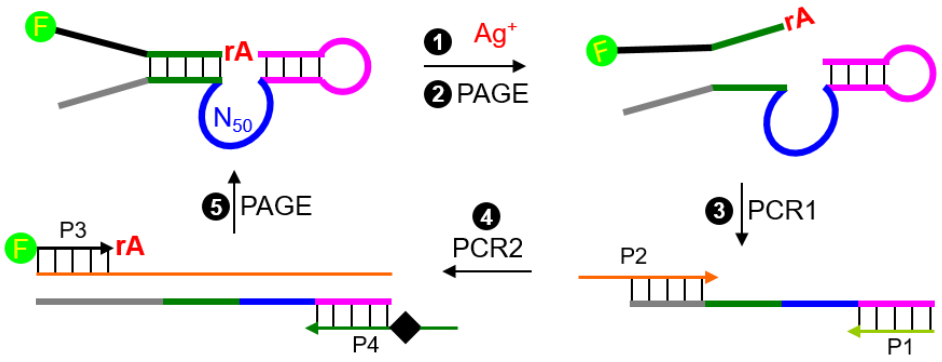

Figure 2.1 The schematic representation of the *in-vitro* selection experiment executed. Ag^+ was used to induce cleavage. Two PCR steps were used to convert the cleaved sequence back to the original full length, and to reintroduce the fluorescent label (denoted by the green circle). The P4 primer has a polymer spacer (denoted by the black diamond) to stop the PCR extension, yielding two strands of unequal lengths. The shorter strand was harvested for the next round of selection.

Each sequence is constituted by 50 random nucleotides (N_{50}) (blue region), flanked by known sets of sequences on both 3′ and 5′ side (pink and green region), and a single RNA linkage (rA, denotes for ribo-adenine). Since RNA is much more susceptible to cleavage,[104] it has been artificially introduced as the cleavage site. The fixed or known sequences which form two short base paired duplexes, guide the folding of the library and thus, proximate the randomised nucleotides with the single RNA cleavage site. The role of metal ions in RNA cleavage has been extensively studied.[104,129] If certain DNA sequences would utilize Ag^+ for the RNA cleavage reaction, a fraction of the library (originally length = 119 nucleotide (nt)) would get cleaved at the RNA junction by Ag^+, and thus become shorter by 28 nt. Therefore, the cleaved fragments (91 nt) were harvested using denaturing gel electrophoresis, and amplified by two rounds of PCR for the next round of selection. The PCR1 brings the library back to the original length, and PCR2 introduces the FAM fluorophore and reconstitutes the cleavage site by introduction of rA.

2.2.2 Ag^+ selection and sequence analysis

In order to narrow down to an Ag^+-dependent RNA-cleaving DNAzyme, the selection scheme explained in section 2.2.1 was used. The sequence of the library used is shown in Figure 2.2 A. Throughout the selection, the Ag^+ concentration was maintained at 10 µM with 1 h incubation time. The FAM label allowed the quantification of the cleavage yield at each round, and a gradual increase was observed (Figure 2.2 B). However, this increase was quite slow. At round 6, only ~8 % of the library was cleaved. This indicates that Ag^+-dependent sequences did not

dominate the library, and non-specific cleavage was competing. The gradually increased cleavage however still suggested a small population that might depend on Ag^+. To identify this population at round 6, instead of the conventional cloning method, deep sequencing was resorted to. A total of 54,961 sequences were obtained. Upon aligning the sequences, 874 families were obtained. The most populated first 200 families, accounting for 88.8 % of all the sequences, were examined for their secondary structures using Mfold.[41] Interestingly, a few families accounting to 1.5 % of the analyzed sequences belong to the Ce13d DNAzyme or its variants, which was previously selected in the Liu lab.[101,124] About 91 % of the analyzed sequences contained a motif of TTCTCACA, which is a signature of another DNAzyme discovered in the Liu lab, named EtNa.[103] Only 7.5 % of the analyzed sequences appeared novel, from which nineteen different trans-cleaving DNAzymes were engineered Figure 2.3 A. The enzyme strand binds the substrate using the two duplex regions, and the middle part is the catalytic core.

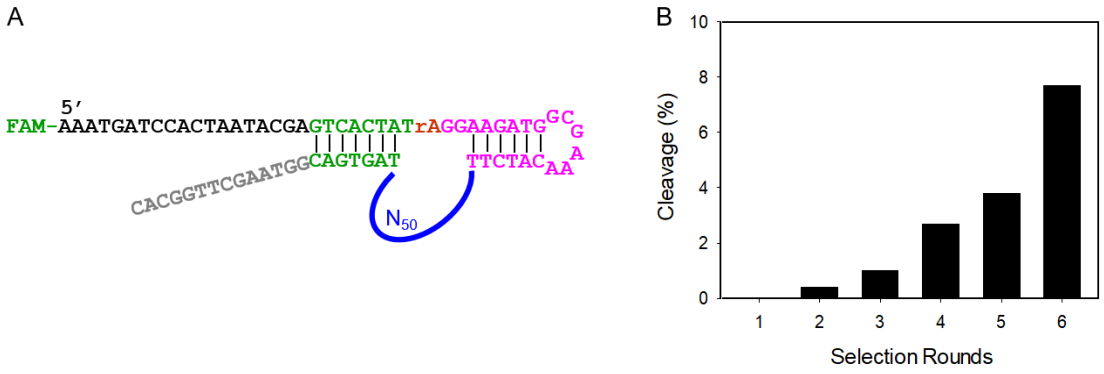

Figure 2.2 (A) The sequence of the library used for *in-vitro* selection with 50 random nucleotides (N_{50}). The cleavage site is at the rAG junction (3′ side of rA). (B) Progress of the selection. At each round, 10 µM Ag^+ was used with 1 h incubation in 50 mM MES, pH 6.0, 25 mM $NaNO_3$ (Buffer A).

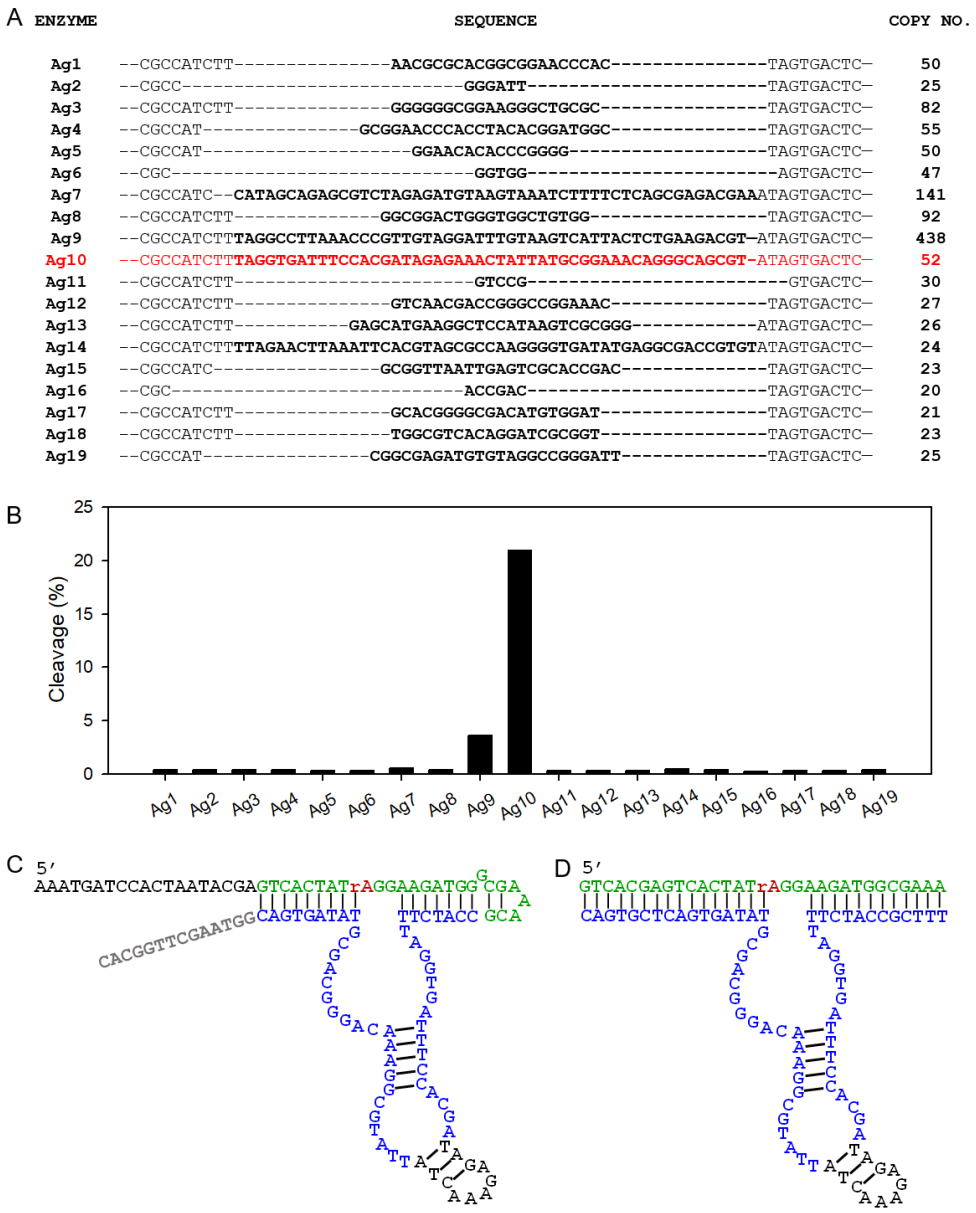

Figure 2.3 (A) The sequences of the 19 potential Ag^{+}-dependent trans-cleaving DNAzymes from 5′ to 3′ with the hypothetic catalytic loop regions in bold. The catalytic loops are connected to the substrate binding arms. The copy number of each sequence is also shown. The Ag10 sequence is in red. (B) Cleavage yield of the above sequences in buffer A with 10 μM Ag^{+} for 1 h. The secondary structures of (C) cis-Ag10 predicted by Mfold right after sequencing, and (D) the Ag10 trans-cleaving DNAzyme. The substrate strand is in green and the enzymes in blue/ black.

The postulated catalytic cores are in boldface, and the rest of the sequences are the substrate binding arms (see Table 2.1 under section 2.4.1 for complete DNA sequences). Each of these sequences was hybridized with the FAM-labeled substrate and individually tested for activity in 10 μM Ag^+ (Figure 2.3 B). Significant cleavage after 1 h was observed for only two sequences Ag9 and Ag10. Ag10 produced the highest cleavage and was studied further. The secondary structure (predicted by Mfold) of the full-length cis-cleaving Ag10 DNAzyme which was obtained from the library, and of its designed trans-cleaving version is shown in Figure 2.3 C and D respectively.

2.2.3 Ag10c DNAzyme

Based on the secondary structure of Ag10, the nucleotides in black which appear redundant (Figure 2.3 D) were truncated. This truncated DNAzyme is named Ag10c. The secondary structure of the Ag10c DNAzyme is shown in Figure 2.4 A. Ag10c retained a similar activity as the original Ag10 DNAzyme (Figure 2.4 B). To identify an optimal condition for catalysis, preliminary characterizations on Ag10c were performed. First, the effect of pH was studied (Figure 2.4 C). The cleavage yields at two time points (5 and 60 min) were measured, and higher pH produced higher cleavage yields up to pH 8. Therefore, high pH is more favorable for the reaction, which might be related to the deprotonation of the 2′-OH of the cleavage site RNA base, making it a better nucleophile.[223] The solubility limit of Ag^+ is about 1 mM at pH 9.[224] Therefore, the Ag^+ concentration used in the above experiments, was far below this limit, and Ag^+ precipitation was not a concern here.

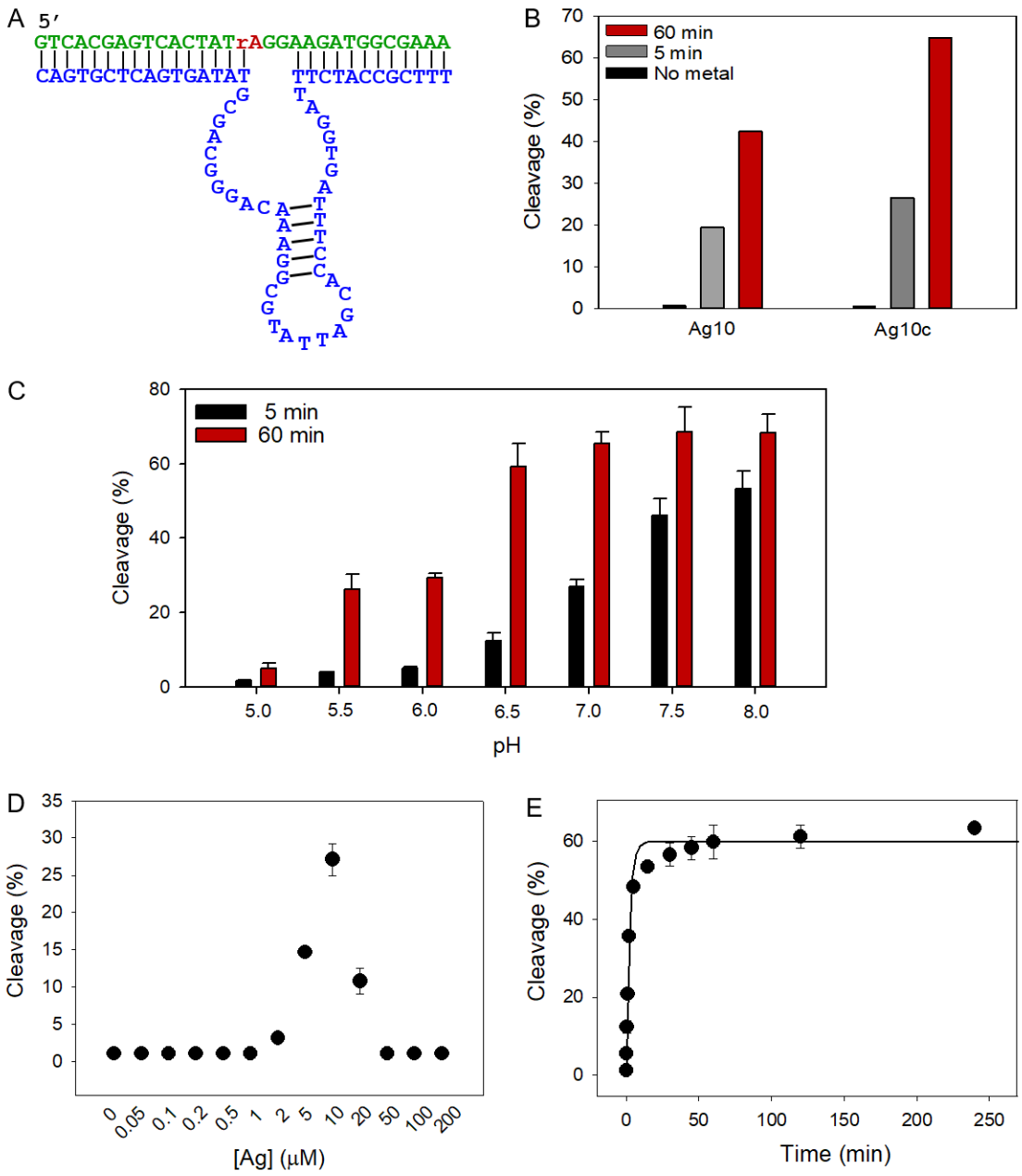

Figure 2.4 (A) Secondary structure of the DNAzyme Ag10c. (B) The cleavage yields of Ag10 and Ag10c DNAzymes with 10 μM Ag^+ at a few time points measured in 50 mM MOPS, pH 7.0, 25 mM $NaNO_3$. The cleavage yield of the Ag10c DNAzyme at (A) different pH with 25 mM $NaNO_3$, (B) pH 7.0, 50 mM MOPS and 25 mM $NaNO_3$ at various Ag^+ concentrations in 5 min. (C) Kinetics of Ag10c cleavage with 10 μM Ag^+ at pH 7.5 with 200 mM $NaNO_3$, yielding a rate of 0.41 min^{-1}.

Next, various concentrations of Ag^+ were tested at pH 7.0 in 25 mM $NaNO_3$ by measuring the cleavage yield after a short reaction time of 5 min. Initially, the yield was low below 1 µM Ag^+, and then it rapidly increased. The most optimal concentration was 10 µM Ag^+ (Figure 2.4 D). At even higher Ag^+ concentrations, inhibition was observed which might be attributable to Ag^+ binding to DNA bases non-specifically, and inducing denaturation or misfolding of the DNAzyme. Under an optimal condition of pH 7.5 with 200 mM $NaNO_3$ and 10 µM Ag^+, the cleavage kinetics of Ag10c was measured (Figure 2.4 E). The kinetic profile was fitted to a first-order reaction with a rate constant of 0.41 min^{-1}. This is a very fast rate considering Ag^+ is a monovalent metal ion and no divalent metals were added. For comparison, the Liu lab recently reported Na^+-specific DNAzyme, which has a rate of 0.11 min^{-1} with 400 mM Na^+. So far, no DNAzymes with Na^+ alone can achieve such a high rate.[103,104,216]

2.2.4 Secondary structure analysis

Ag10c has a hairpin, and two long unpaired bulges connecting this hairpin to the two substrate binding arms. Such a structure is typical of RNA-cleaving DNAzymes,[97,101,103,104] and the hairpins usually play only a structural role. Its substrate strand has a single RNA linkage (rA, ribo-adenine) that serves as the cleavage site. The enzyme strand binds the substrate via two base paired regions. In the presence of Ag^+, the substrate is cleaved into two pieces. To confirm this secondary structure, a mutation study was executed. To confirm the hairpin structure in the catalytic core, a series of mutations were designed which are represented as (a) to (f) in Figure 2.5 C and their cleavage rates are shown in Figure 2.5 B. The wild-type Ag10c has a rate of

0.42 min^{-1} with 10 µM Ag^{+} at pH 7.5. A complete deletion of the hairpin (mutant a) drops the rate by over 1000-fold. On the other hand, upon changing the base sequence of the stem (mutant b), the size and base composition of the loop (mutant c and d), and the length of the stem (mutant e and f), the activity remains unchanged. Therefore, this hairpin needs to be there for the proper folding of the DNAzyme, but it does not directly participate in metal binding or catalysis.

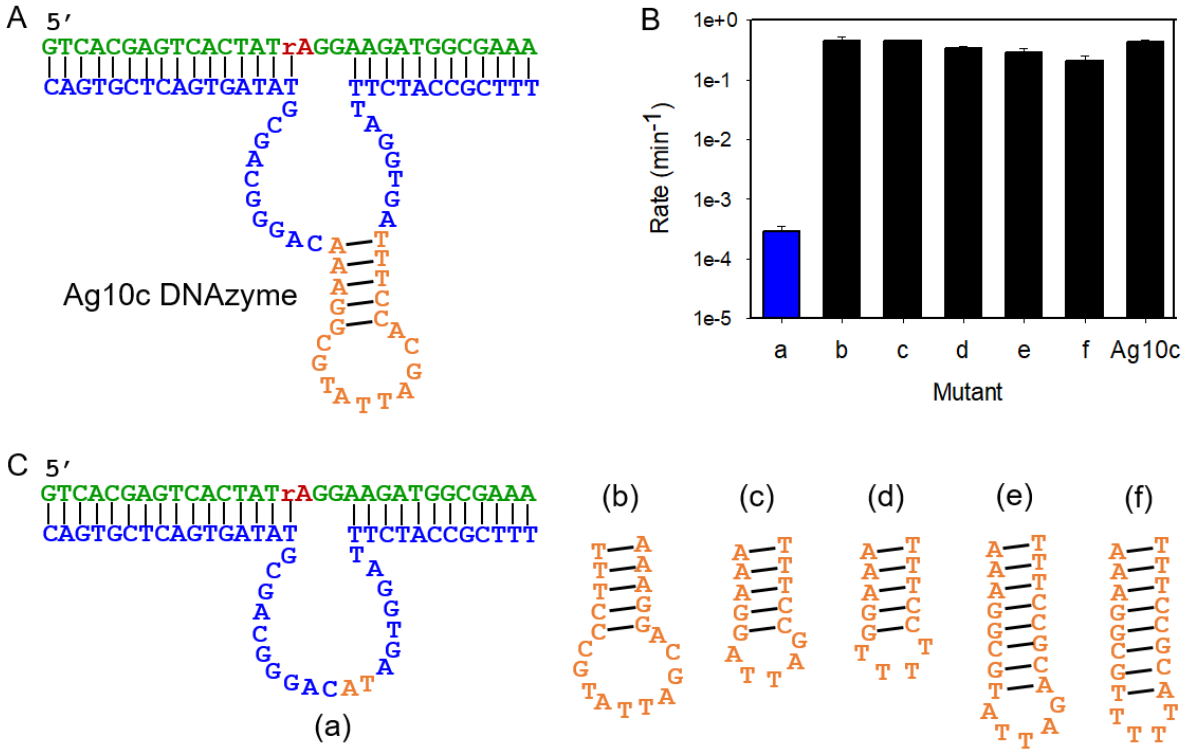

Figure 2.5 (A) Secondary structure of Ag10c with the hairpin region highlighted in brown. (B) Cleavage activity of the mutants with modifications to the hairpin region. The rates were determined in 50 mM MOPS, pH 7.5, 200 mM $NaNO_3$ and 10 µM Ag^{+}. The ~ 1000 fold drop in the activity of the mutant (a) is color coded to be in 'blue'. (C) Secondary structure of the modifications made to the hairpin.

2.2.5 Chloride inhibition to prove the requirement of Ag^+

As this is the first case of DNAzyme catalysis using a monovalent transition metal ion, the following experiment was performed to confirm its Ag^+ requirement. The cleavage yield of Ag10c was measured at pH 7.0 for 1 h in the presence of increasing concentrations of $NaNO_3$ or NaCl (Figure 2.6).

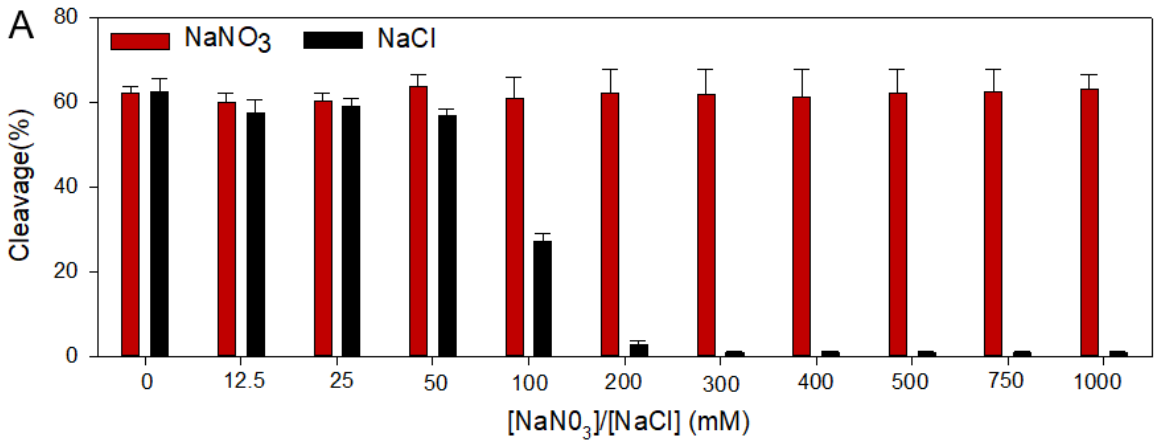

Figure 2.6 The cleavage yield of Ag10c in the presence of 10 μM Ag^+ and various concentrations of NaCl or $NaNO_3$. All the reactions were performed in 50 mM MOPS, pH 7.0 for 1 h.

With $NaNO_3$, the cleavage reached a similar value for all the conditions (red bars), while a strong inhibition effect of NaCl was observed when the Cl^- was greater than 50 mM (black bars). The cleavage went to the background level with more than 100 mM NaCl. The solubility product (k_{sp}) of AgCl is 1.8×10^{-10}. Therefore, with 100 mM Cl^-, the free Ag^+ concentration is only ~18 nM. As will be seen later, the DNAzyme cannot detect Ag^+ beyond this level. Since

$NaNO_3$ did not decrease the cleavage yield, the inhibition by NaCl cannot be attributed to the change in ionic strength. Taken together, the inhibition effect of NaCl is attributable to complex formation with Ag^+ or forming AgCl precipitation. This experiment provides a strong evidence that Ag^+ is critical for the activity of the DNAzyme.

2.2.6. Metal selectivity

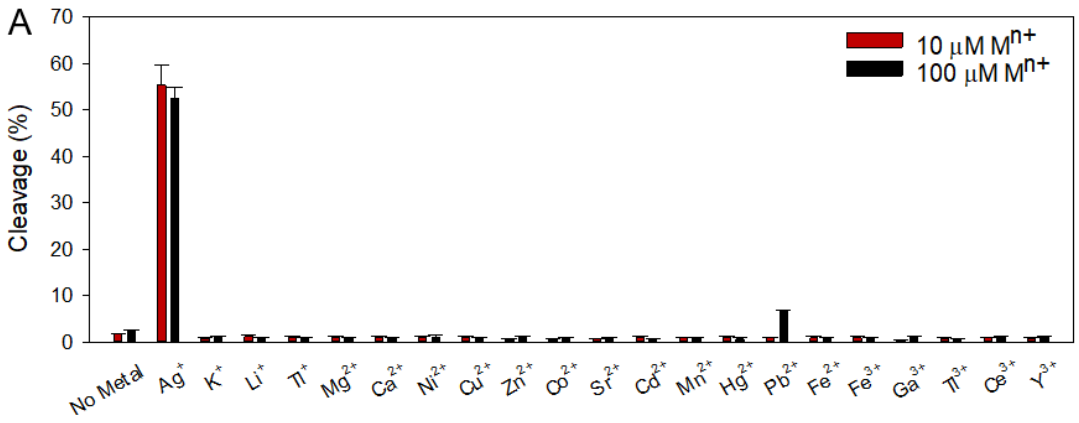

Figure 2.7 Cleavage yield with Ag^+ as compared to 10 µM and 100 µM of 20 other metals. All the reactions were performed in 50 mM MOPS, pH 7.0 for 1 h. While 100 µM Pb^{2+} showed a modest cleavage, its rate is >3000-fold slower compared to the same concentration of Ag^+.

The *in-vitro* selection was carried out with Ag^+ and no negative selections were performed. From the purview of Ag^+ sensing, metal specificity is also very important. Next, Ag10c was tested in the presence of 10 µM and 100 µM of 20 different metal ions (Figure 2.7). Indeed, Ag10c is highly specific for Ag^+ and it has negligible or no activity in the presence of any other metal. Only 100 µM Pb^{2+} produced a very moderate cleavage of ~8 % after 1 h. The interference

by Pb^{2+} is commonly seen in the DNAzyme field,[101,113] possibly due to the close to neutral pK_a value of the Pb^{2+} bound water,[225] making it ideal for activating the 2′-OH nucleophile. Even for Pb^{2+}, the rate of cleavage (~ 0.0013 min^{-1} with 100 μM Pb^{2+}) under the same metal concentration is still >3000-fold slower compared to that for Ag^+ (0.41 min^{-1} with 10 μM Ag^+). For the other metals, the selectivity of Ag10c for Ag^+ is even higher, making it potentially an excellent probe for Ag^+ sensing.

2.3 Summary

In this chapter, *in-vitro* selection of an Ag^+-dependent RNA-cleaving DNAzyme Ag10c, is described. A number of significant observations were reported. Firstly, the very first occurrence of the isolation of a monovalent transition metal ion-dependent RNA-cleaving DNAzyme has been demonstrated. Secondly, the possibility of selecting DNAzymes for soft thiophilic metals using just the natural RNA dinucleotide cleavage junction was floated. So far, only a few modified DNAzymes have been reported for thiophilic metals, such as the Hg^{2+}-specific DNAzyme from the Perrin lab involving a few modified nucleotides.[121] A PS modification has been introduced at the scissile phosphate to obtain DNAzymes for Cd^{2+} and Cu^{2+}.[98,99,226] Ag10c is the first *in-vitro* selected unmodified RNA-cleaving DNAzyme that cleaves efficiently in the presence of a thiophilic metal. Thirdly, the novel DNAzyme Ag10c is shown to achieve a catalytic rate of 0.41 min^{-1} with just 10 μM Ag^+, which is the highest reported till now in the category of monovalent ion-dependent RNA-cleaving DNAzymes. Fourthly, the DNAzyme Ag10c has been testified to exhibit remarkable selectivity for silver ions, amongst all the other

metal ions tested. This work expands the repertoire of RNA-cleaving DNAzymes and throws the much needed spotlight on the role of monovalent ions in DNAzyme catalysis. It also provides a strong platform for the development of DNAzyme based silver biosensor which is very relevant for environmental and water quality surveillance.

2.4 Materials and methods

2.4.1 Chemicals

The DNA library for *in-vitro* selection, related primers, and fluorophore/quencher modified DNAs were purchased from Integrated DNA Technologies (IDT, Coralville, IA). The sequences of DNA used in this selection are listed in Table 2.1. The trans-cleaving enzyme strands and their mutants were from Eurofins (Huntsville, AL). Metal ions that were used for analysis include silver(I) nitrate, potassium(I) chloride, lithium(I) chloride, thallium(I) chloride, lead(II) acetate, magnesium(II) sulfate, manganese(II) chloride tetrahydrate, iron(II) chloride tetrahydrate, cobalt(II) chloride hexahydrate, copper(II) chloride dehydrate, zinc(II) chloride, calcium(II) chloride, nickel(II) chloride, strontium(II) chloride, cadmium(II) chloride, mercury(II) perchlorate, yttrium(III) chloride hexahydrate, gallium(III) chloride, cerium(III) chloride, iron(III) chloride hexahydrate. All these salts were purchased from Sigma-Aldrich except the iron and silver salts were purchased from Alfa Aesar. The purity of the metals used is 99.99 %. Their solutions were made by directly dissolving their salts in Milli-Q water. Tris (Hydroxymethyl) aminomethane (Tris), 2-(N-morpholino) ethanesulfonic acid (MES) free acid

monohydrate, 4-(2-Hydroxyethyl)piperazine-l-ethanesulfonic acid (HEPES), 3-(*N*-morpholino) propanesulfonic acid (MOPS), EDTA disodium salt dehydrate, sodium chloride, sodium bromide, sodium iodide and ammonium acetate were purchased from Mandel Scientific Inc. (Guelph, Ontario, Canada). Acrylamide/bisacrylamide 40 % solution (29:1), urea, and 10 X TBE solution were purchased from Bio Basic Inc. SsoFast EvaGreen supermix was purchased from Bio-Rad for real-time PCR analysis. T4-DNA ligase, deoxynucleotide (dNTP) solution mix, Taq DNA polymerase with ThermoPol buffer, and low molecular weight DNA ladder were purchased from New England Biolabs. All metal ions, buffer and gel stock solutions were prepared with Milli-Q water. The pH of the buffers was measured with Denver Instrument UltraBasic pH meter.

Table 2.1 List of DNA sequences used in chapter 2.

DNA	**Sequence (5′ – 3′)**
Lib-FAM-N_{50}	GGCGAAACATCTTNNNNNNNNNNNNNNNNNNNNNNNNNNNNNNNNNNNNNNNNNTAGTGACGGTAAGCTTGGCAC -FAM
Lib-rA	AATACGAGTCACTATrAGGAAGAT
Splint DNA	AAGATGTTTCGCCATCTTCCTATAGTCCACCACCA
Primer P1	CTGCAGAATTCTAATACGAGTCACTATAGGAAGATGGCGAAACA
Primer P2	GTGCCAAGCTTACCG
Primer P3	FAM- AAATGATCCACTAATACGAGTCACTATrAGG
Primer P4	AACAACAACAAC-S-GTGCCAAGCTTACCG
Primer P701	CAAGCAGAAGACGGCATACGAGATTCGCCTTAGTGACTGGAGTTCAGACGTGTGCTCTTCCGATCTCTGCAGAATTCTAATACGAGTCAC
Primer P501	AATGATACGGCGACCACCGAGATCTACACTAGATCGCACACTCTTTCCCTACACGACGCTCTTCCGATCTGTGCCAAGCTTACCG

Substrate	GTCACGAGTCACTATrAGGAAGATGGCGAAA-FAM
Ag1	TTTCGCCATCTTAACGCGCACGGCGGAACCCACTAGTGACTCGTGAC
Ag2	TTTCGCCGGGATTTAGTGACTCGTGAC
Ag3	TTTCGCCATCTTGGGGGGCGGAAGGGCTGCGCTAGTGACTCGTGAC
Ag4	TTTCGCCATGCGGAACCCACCTACACGGATGGCTAGTGACTCGTGAC
Ag5	TTTCGCCATGGAACACACCCGGGGTAGTGACTCGTGAC
Ag6	TTTCGCGGTGGAGTGACTCGTGAC
Ag7	CGCCATCCATAGCAGAGCGTCTAGAGATGTAAGTAAATCTTTTCTCAG CGAGACGAAATAGTGACTC
Ag8	TTTCGCCATCTTGGCGGACTGGGTGGCTGTGGTAGTGACTCGTGAC
Ag9	CGCCATCTTTAGGCCTTAAACCCGTTGTAGGATTTGTAAGTCATTACT CTGAAGACGTATAGTGACTC
Ag10	CGCCATCTTTAGGTGATTTCCACGATAGAGAAACTATTATGCGGAAA CAGGGCAGCGTATAGTGACTC
Ag11	TTTCGCCATCTTGTCCGGTGACTCGTGAC
Ag12	TTTCGCCATCTTGTCAACGACCGGGCCGGAAACTAGTGACTCGTGAC
Ag13	TTTCGCCATCTTGAGCATGAAGGCTCCATAAGTCGCGGGATAGTGACT CGTGAC
Ag14	CGCCATCTTTTAGAACTTAAATTCACGTAGCGCCAAGGGGTGATATG AGGCGACCGTGTATAGTGACTC
Ag15	TTTCGCCATCGCGGTTAATTGAGTCGCACCGACTAGTGACTCGTGAC
Ag16	TTTCGCACCGACTAGTGACTCGTGAC
Ag17	TTTCGCCATCTTGCACGGGGCGACATGTGGATTAGTGACTCGTGAC
Ag18	TTTCGCCATCTTTGGCGTCACAGGATCGCGGTTAGTGACTCGTGAC
Ag19	TTTCGCCATCGGCGAGATGTGTAGGCCGGGATTTAGTGACTCGTGAC
Ag10c	CGCCATCTTTAGGTGATTTCCACGATTATGCGGAAACAGGGCAGCGT ATAGTGACTCG

2.4.2 *In-vitro* Selection

For this *in-vitro* selection experiment, the initial DNA library was prepared by ligating two pieces of DNA (Lib-FAM-N_{50} and Lib-rA) with a splint DNA (See Table 2.1). Lib-FAM DNA (200 pmol) and Lib-rA DNA (300 pmol) were mixed with splint DNA (300 pmol) first in buffer A (50 mM pH 7.5 Tris-HCl, pH 7.5, 10 mM $MgCl_2$). The three strands of DNA were annealed at 95 °C for 1 min followed by slow cooling to room temperature. The T4 ligation protocol provided by New England Biolabs was followed for the ligation reaction. The ligated DNA product was purified with 10 % denaturing polyacrylamide gel (dPAGE) at 650 V for 80 min and the DNA was extracted from the gel with buffer B (1 mM EDTA, 10 mM Tris-HCl, pH 7.0). The extracted DNA library was further concentrated via ethanol precipitation and re-suspended in 60 μL of buffer C (50 mM MES, pH 6.0, 25 mM $NaNO_3$), which was the selection buffer. This DNA was used directly as the DNA library for the first round of selection. For each of the subsequent round, the library was generated from PCR. For the *In-vitro* selection experiment, the random DNA pool was incubated with final concentration of 10 μM freshly prepared $AgNO_3$ metal ion for 60 min. After incubation, the reaction was quenched with 8 M urea and was purified in 10 % dPAGE. A fraction of the selected DNA was extracted from the gel and further purified with a Sep-Pak C18 column (Waters). The purified selected DNA was then dried in an Eppendorf Vacufuge at 30 °C overnight. The dried DNA was re-suspended in 60 μL of 5 mM HEPES buffer (pH 7.5). A small fraction of this DNA was amplified by two rounds of PCR (PCR1 and PCR2) using thermo-cycling conditions described in section 2.4.3.

2.4.3 Polymerase Chain Reaction (PCR)

Throughout the *in-vitro* selection experiment, each round required three PCR reactions. After the library cleavage reaction in the presence of Ag^{+}, the cleaved DNA that was extracted from the gel and a Real-Time PCR (RT-PCR) was carried out to quantify the amount of extracted DNA and optimize the number of cycles needed to amplify extracted DNA (through PCR1) for the next round. The 20 μL RT-PCR reaction mixture contains 1μL of purified DNA template, 400 nM primer P1 and P2 (see Table 2.1), and 10 μL of SsoFast EvaGreen Supermix (Bio-Rad). The following thermocycling steps followed: 95 °C for 30 s, 95 °C for 5 s, and 55 °C for 5 s. During the PCR1 the full length library is regenerated. For this, a 50 μL PCR reaction mixture contained the following: 1 μL DNA template, 200 nM of each of P1 and P2, 200 μM dNTP mixture, 1× Taq buffer, and 1.25 units of Taq DNA polymerase. The reaction was carried out for the number of cycles optimized in RT-PCR. The DNA was amplified using the following cycling steps: 94 °C for 5 min; 94°C for 30 s, 55 °C for 30 s, and 72 °C 30 s. A gel/PCR DNA fragment extraction kit (IBI Scientific) was used to purify the PCR1 product. The purified product was used as template for PCR2. One-tenth of the purified 50 μL product was further amplified for 12 cycles using P3 and P4 as the primers (see Table 2.1). A 200 μL PCR reaction mixture contained 4 μL of 1:10 diluted template from PCR1, 250 nM each of P3 and P4, 200 μM dNTP mixture, 1× Taq buffer, and 5 units of Taq DNA polymerase. The thermocycling steps mentioned for PCR1 were also used here. The final PCR2 product was purified using 10 % dPAGE and the single-stranded FAM-labeled DNA was excised from the gel, ethanol precipitated and used as the library pool for the subsequent round of selection.

2.4.4 Deep Sequencing

To prepare sample for deep sequencing, the round 6 library was subjected to PCR1 as explained above in section 2.4.3. The full-length library generated from this step was subjected to another PCR reaction so that the Illumina sequencing technology can be used. The forward primer (P701) and the reverse primer (P501), each containing a unique index sequence were used (see Table 2.1 for complete sequences). The PCR product was purified with 2 % agarose gel and extracted using a gel extraction kit (IBI Scientific). The extracted DNA was eluted in 25 µL Milli-Q water and the concentration was quantified using a NanoDrop spectrophotometer. The sequencing was performed at McMaster Genomics Facility, Mc Master University, Hamilton, Ontario, Canada.

2.4.5 Activity assays

For a typical gel-based activity assay, the DNAzyme complex were prepared by annealing the FAM-labeled substrate (10 µM) and enzyme (30 µM) in buffer 50 mM MES (pH 6.0, 25 mM $NaNO_3$) by heating at 85 °C for 1 min and then slowly cooled at room temperature until ~30 °C. The complex was then frozen at -20 °C for at least 2 hours. To initiate the reaction at room temperature, a final of 0.05 - 200 µM Ag^+ or another metal ion (as required) was incubated with 0.4 µM DNAzyme complex in a total 10 µL reaction mixture in buffer 50 mM Na.Acetate (pH 5.0 - 5.5) / 50 mM MES (pH 6.0 - 6.5) / 50 mM MOPS (pH 7.0 – 8.0) with salt concentration varying from 25 - 200 mM $NaNO_3$, for the required time ranging from 10 s – 8 h. The samples

were quenched with 8 M urea at designated time points and run in 15 % dPAGE at 120 V for 80 min. The gel images were taken with Bio-Rad ChemiDoc MP imaging system. For determining the rate of cleavage, the gel band intensities of the cleaved vs. uncleaved substrate were quantified and the data obtained were fitted (using *Sigma Plot 12.0*) according to the first-order rate equation $Y_t = Y_o + a(1-e^{-kx})$, where Y_t and Y_o are the cleavage fractions at a given reaction time '*t*' or '*0*' min, respectively, '*a*' is a constant i.e. the scaling parameter and '*k*' is the observed rate constant.

3. Chapter 3 – Biochemical characterization of the Ag10c DNAzyme for mechanistic insights[b]

3.1 Introduction

In the former chapter, the silver-specific DNAzyme named Ag10c has been introduced and an initial screening of its catalytic activity is shown. Herein, the biochemical characterization of Ag10c is carried out in more detail. It has been shown previously that at pH 7.5, it has a saturated cleavage rate of 0.41 min^{-1}, which makes it faster than most other DNAzymes under the same condition. Its high efficiency is surprising because no divalent metal ions are known to be involved. Ag^{+} is a strongly thiophilic metal, and this is the first report that such thiophilic metals can activate a non-modified DNAzyme.[98,99,121,227] For a greater understanding of its intriguing activity, systematic mutations were performed and studied the effect of variation in the ionic strength and pH. DNAzymes can be classified into two groups based on their origin of metal specificity. The majority of the DNAzymes belong to the first group, where a metal cofactor mainly interacts with the scissile phosphate, and it is difficult to extract a well-defined metal-binding aptamer to explain their metal specificity. The 8-17 DNAzyme is a classic example.[228–230] In such cases, metal binding can be probed by the phosphorothioate

[b] This chapter is the basis for the published manuscripts:

1 Saran R.; Kleinke K.; Zhou W.; Yu T.; Liu J. A Silver-Specific DNAzyme with a New Silver Aptamer and Salt-Promoted Activity. *Biochemistry*. **2017**, 56, 1955−1962.

2 Saran R.; Yao L.; Hoang P.; Liu J. Folding of the silver aptamer in a DNAzyme probed by 2-aminopurine fluorescence. *Biochimie*. **2018,** 145, 145-150.

modification.[123,124,231–233] Interestingly, a few recently discovered DNAzymes contain a metal aptamer responsible for metal specificity and thus, are classified under a second group. For example, the NaA43 and Ce13d DNAzymes,[101,104] both have the same Na^+ binding aptamer.[129,130,234,235] To find out how the metal is interacting in case of Ag10c, phosphorothioate modification was incorporated at the cleavage junction, and DMS footprinting experiments were carried out. Interesting insights were gained into metal binding, and a new Ag^+ aptamer was identified as being responsible for Ag^+ specificity, which is independent of the well-known C-Ag^+- C base pair. The Ag10c is the first DNAzyme in which a transition metal aptamer could be isolated through DNAzyme selection. Many ribozymes require a metal-dependent conformational change before cleavage can occur.[236,237] Similarly, metal-dependent folding of multiple DNAzymes has been studied.[213,229,234,238–242] This folding facet is extremely interesting and studying such dynamics can provide insights into the mechanism of DNAzyme catalysis. Aptamer binding is also accompanied with a conformational change known as adaptive binding.[134] Since the aptamer is infused in the Ag10c DNAzyme, Ag^+ binding may induce folding of the aptamer core. Herein, 2-aminopurine (2AP) was used to probe the folding of the Ag10c DNAzyme, and it was observed that indeed, the DNAzyme undergoes Ag^+ induced local folding.

3.2 Results and discussion

3.2.1 Catalytic activity of Ag10c is not dependent on formation of C-Ag^+-C base pair

The best known interaction between Ag^+ and DNA is the C-Ag^+-C base pair.[173,243] Therefore, it was worth testing if Ag^+ functions by this mechanism in Ag10c. Ag10c has only three potentially important cytosines (highlighted in red in Figure 3.1 A). The remaining ones are in the hairpin and unimportant for activity (section 2.2.4). Each of these three cytosines (i.e. C8, C13 and C16) was mutated to A, T, and G. The drop in the catalytic activity of the mutants is color coded to be <10 (black), ~10 (orange), ~100 (green), ~1000 (blue) and ~10,000 (red) folds. Any mutation to the C8 drops the activity by ~600-fold (Figure 3.1 B). The C13 is slightly more tolerable to mutations and the rate drop ranges from 20- to 400-fold, while any change to the C16 drops the rate by at least 1000-fold (Figure 3.1 B). Therefore, all these cytosines are critical for activity.

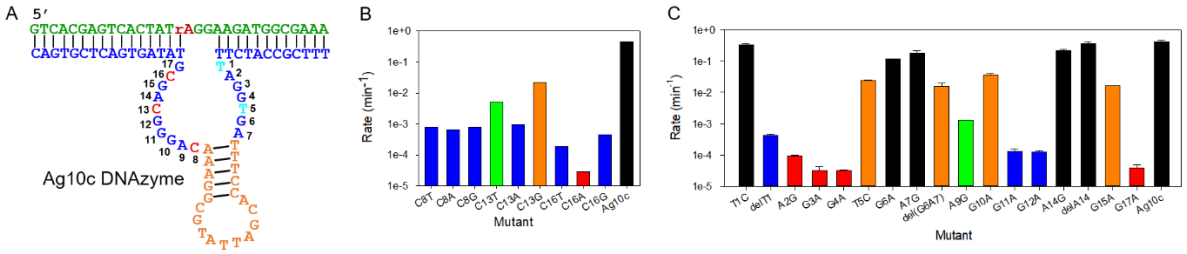

Figure 3.1 The secondary structure of (A) the Ag10c DNAzyme. The cytosine bases in the loop are marked in red, the thymines in cyan, and the rest of the purine bases in blue. Each base in the loop is numbered from 1 to 17. Cleavage activity of the mutants with modifications to (B) the cytosines in the loop, and (C) the other nucleotides. The rates were determined in 50 mM MOPS, pH 7.5, 200 mM $NaNO_3$ and 10 µM Ag^+. The drop in the activity of the mutants is color coded to be <10 (black), ~10 (orange), ~100 (green), ~1000 (blue) and ~10,000 (red) folds.

While this mutation study confirms the crucial role of these cytosines, it argues against C-Ag^+-C base pairing. If C-Ag^+-C were required for activity, mutating one of the C to G should

maintain the base pair and thus activity. However, all the C-to-G mutations inhibit the activity. Furthermore, C can also bind Ag^+ together with T.[244] There are two thymines in the enzyme loop (highlighted in cyan in Figure 3.1 A). For the same reason mentioned above, it is unlikely that C-Ag^+-T base pairs are formed, since otherwise the C-to-A mutation should be able to maintain the activity (Figure 3.1 B). Altogether, this indicates that the role of Ag^+ is more sophisticated than simple mismatch stabilization.[126] It was recently reported that Ag^+ can also be inserted between two guanines, and such binding does not disrupt the G-C Watson−Crick base pairing.[178] It has been reviewed in detail in section 1.5.2 that Ag^+ is capable of coordinating to all the natural bases. The exact way of Ag^+ binding in Ag10c remains unclear, only the formation of most well-known C-Ag^+-C(T) base pairs is ruled out by this point.

3.2.2 Critical residues for the catalytic activity

From the cytosine mutation studies, it is apparent that all three C residues present in the Ag10c loop are critical for its activity (section 3.2.1). To decipher which of the other loop nucleotides play an important role, A-to-G, G-to-A, and T-to-C mutations were tested for each of them (Figure 3.1 C). The ability to tolerate purine-to-purine or pyrimidine-to-pyrimidine mutations indicates the possibility of a structural role of the bases. It was found that the mutations to the T1, G6, A7 and A14 do not affect the activity of the DNAzyme as they show less than 10-fold decrease in the rate min^{-1}. Further deletion experiments indicated that the presence of T1 is critical, with its deletion conferring a decrease of ~ 1000 fold in the activity. Deleting G6A7 together decreases the activity only by 10-fold and deleting A14 does not affect the activity.

Apart from these four nucleotides, mutations to the rest of the loop nucleotides were more detrimental. The T5C, G10A and G15A mutation showed ~ 10 fold diminished activity. The activity was lowered by about ~ 100 fold by A9G mutation. The G11A and G12A brought the activity down by ~ 1000 fold while the A2G, G3A, G4A and G17A reduced the activity by ~ 10,000 fold. Overall, Ag10c is a well-defined enzyme and most of the nucleotides cannot be randomly changed.

3.2.3 The Ag10c binds two Ag^+ ions cooperatively

After confirming the critical nucleotides in the enzyme loop, the effect of Ag^+ was studied. Ag10c's cleavage kinetics was measured at various Ag^+ concentrations. It was found that all the samples followed a first order kinetics (Figure 3.2 A) and the cleavage rate for each concentration was calculated. Below 1 µM Ag^+, the activity is very low. With increase in [Ag^+], the DNAzyme quickly activates, reaching saturation as [Ag^+] approaches >5 µM (Figure 3.2 B). Upon plotting the rate (min^{-1}) of Ag10c versus the respective Ag^+ concentrations, a sigmoidal curve was obtained (Figure 3.2 B). This sigmoidal curve suggests multiple Ag^+ ions binding cooperatively to the DNAzyme. To calculate the number of Ag^+, a double log plot was made with $\leq$5 µM Ag^+ (Figure 3.2 C), which exhibited a slope of 1.9, suggesting that the DNAzyme binds two Ag^+ ions. The Ag^+ concentration was limited at 5 µM because the cleavage activity approaches saturation beyond this concentration. With a few exceptions of lanthanide ions,[123,125] most DNAzymes only use one metal for catalysis. In most DNAzymes, the metal interacts with the scissile phosphate as probed by phosphorothioate

modification.[98,99,124,245] However, Ag^+ is a highly thiophilic metal and its affinity with the normal DNA backbone phosphate is likely to be very low. Therefore, as discussed in detail in the further sections, Ag^+ might exert a completely different function in the Ag10c DNAzyme.

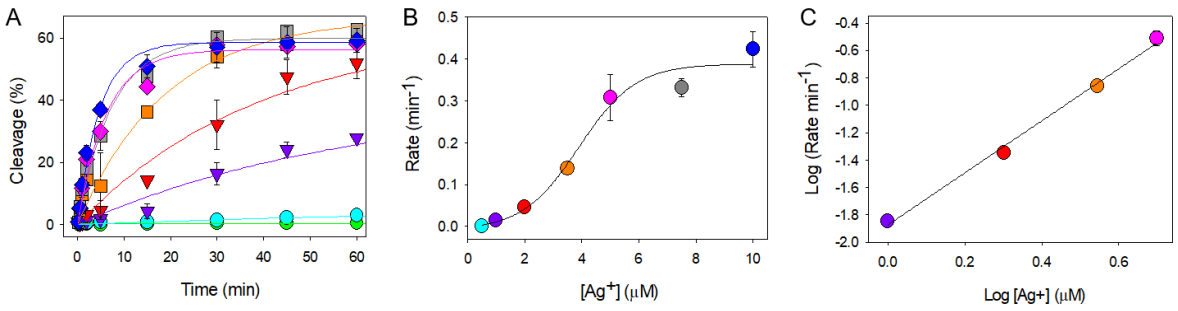

Figure 3.2 (A) Kinetics of the Ag10c DNAzyme in presence of various concentrations of Ag^+. The data is fit using the first-order kinetics model. (B) Cleavage rate of the Ag10c as a function of Ag^+ concentration, exhibiting a sigmoidal curve. (C) The double log plot for the same data in (B) at low Ag^+ concentrations. A slope of 1.9 suggests binding of two Ag^+ ions. The buffer contained 50 mM MOPS, pH 7.5, and 200 mM $NaNO_3$. Color code of Ag^+ concentration (μM): 0.1 (green), 0.5 (cyan), 1 (purple), 2 (red), 3.5 (orange), 5 (pink), 7.5 (grey) and 10 (blue).

3.2.4 Salt promotes Ag10c activity

Since DNA is a polyanion, salt concentration might have a strong influence on its interaction with Ag^+. So to further understand this DNAzyme, the buffer conditions were changed. The Ag^+ concentration was fixed to be 10 μM, and the rate was measured as a function of $NaNO_3$ concentration (Figure 3.3 A). Interestingly, $NaNO_3$ significantly promotes the Ag10c activity by ~10-fold. On plotting the rate (min^{-1}) versus Na^+ concentration, an apparent K_d of 87.6 mM Na^+ was obtained. A double log plot was made (Figure 3.3 B), yielding a slope of 1.26.

Therefore, one Na^+ interacts with the enzyme to promote its cleavage activity. To test whether this salt-accelerated activity is unique, the cleavage % of a few other RNA-cleaving DNAzymes was measured, including the 17E with Pb^{2+},[111] Lu12 with Ce^{3+},[122] and Tm7 with Tm^{3+}.[123]

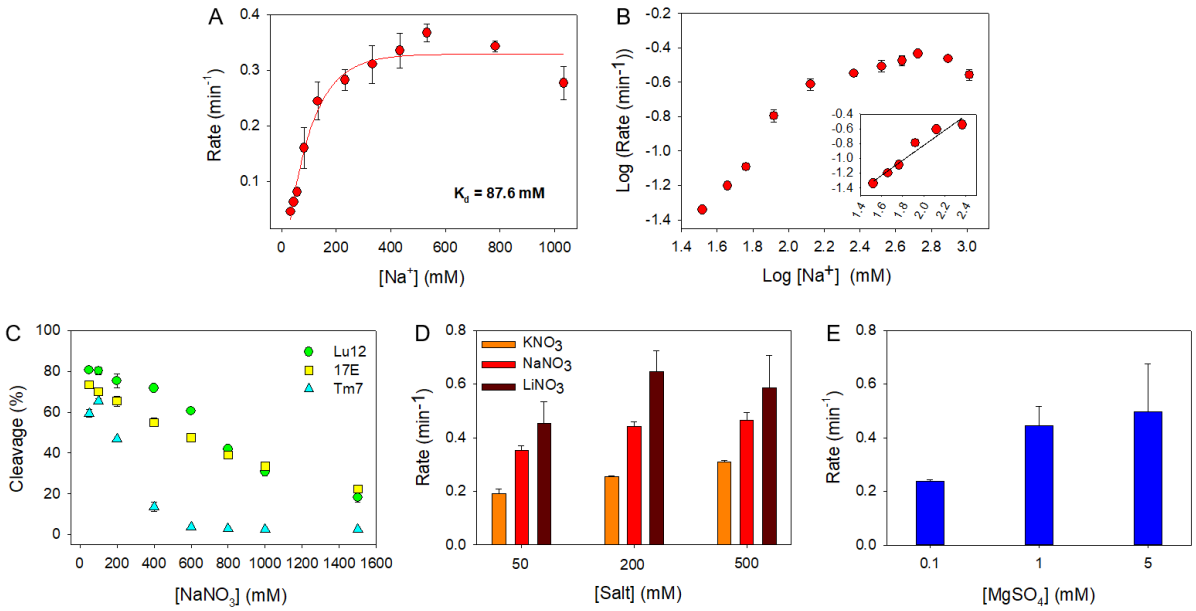

Figure 3.3 (A) The activity of the Ag10c DNAzyme with increasing concentration of $NaNO_3$ in the presence of 50 mM MOPS and 10 µM Ag^+ at pH 7.0. (B) The log of rate of Ag10c rises linearly with increasing log of [Na^+] up to around 300 mM [Na^+]. Inset: the low Na^+ concentration data fit to a straight line with a slope of 1.01. (C) Cleavage % of the Lu12, 17E and Tm7 DNAzymes with 1 µM Ce^{3+}, 1 µM Pb^{2+} and 10 µM Tm^{3+} respectively in 30 min in the presence of various concentrations of $NaNO_3$ and 50 mM MOPS pH 6.0. Activity of Ag10c in increasing concentrations of (D) $NaNO_3$, $LiNO_3$, KNO_3, and (E) $MgSO_4$ in the presence of 50 mM MOPS, pH 7.5 and 10 µM Ag^+.

However, they were all inhibited by salt (Figure 3.3 C). Salt has a number of effects on DNAzyme catalysis. First, at very low salt concentrations, salt is often required to stabilize the

DNAzyme complex to ensure that its melting temperature is above room temperature. Approximately 20 mM Na^+ is often sufficient for this purpose. Second, salt can screen the electrostatic interaction between metal ions and DNA, which can explain its inhibition effect in Figure 3.3 C. When the stability of the DNAzyme complex is no longer a limiting factor for activity, the charge screening effect may take over. Finally, at even higher salt concentrations (e.g., ~1 M), salt ions may influence the structure of water and the solubility of biopolymers.[246] The slightly reduced activity of Ag10c in Figure 3.3 A at >500 mM Na^+ might be related to this. This salt dependent study also suggests that the mechanism of Ag10c is indeed different from those of most previously reported DNAzymes. This finding has also led us to question whether Na^+ is a specific requirement for the activity of Ag10c. For example, a previously reported lanthanide-dependent DNAzyme named Ce13d actually requires both a lanthanide and Na^+.[101,129] A few recently reported DNAzymes work with Na^+ alone but not with other group 1A metals.[103,104] To study whether the Ag10c is also specific for Na^+, its activity was measured in Li^+ or K^+ with 10 μM Ag^+ (Figure 3.3 D). The Ag10c is active in all these salts. Therefore, these group 1A metals do not appear to play a specific chemical role (unlike in the case of Ce13d). They only act as a general salt to raise the ionic strength. At the same metal concentration, Li^+ promoted the highest cleavage rate among these three group 1A metals. This might be attributable to its highest charge density to allow the strongest electrostatic interaction with DNA. In RNA cleavage, metal ions might play the following roles. First, the metal bound water after deprotonation might act as a general base to help deprotonate the 2′-OH nucleophile. The second role is to interact with the scissile phosphate and stabilize the transition state phosphorane, which is highly negatively charged. This makes it worth suspecting that the role

of Na^+ (or Li^+, K^+, or Mg^{2+}) here is the latter since it is unlikely for the thiophilic Ag^+ to play such a role. Ag^+ is a very soft metal and has low affinity with the phosphate. The fact that Li^+ works the best also supports this hypothesis. Monovalent Na^+ does not bind to phosphate tightly, and it needs a few hundred mM to achieve the optimal activity. For comparison, most divalent metal ions such as Mg^{2+} work optimally at a concentration ~10 mM,[247–250] while trivalent lanthanides work optimally even at nM concentrations due to a very strong phosphate binding.[123,125] To further support the hypothesis of phosphate binding, Mg^{2+} was used in addition to 10 μM Ag^+ (Figure 3.3 E). Indeed, ~5 mM Mg^{2+} could accelerate the Ag10c activity to the same extent as that seen with 200 mM Li^+. Therefore, group 1A metals are not absolutely required, and their charge screening role can be played by a group 2A metal, as well. Taken together, it was concluded that Ag^+ does not interact with the scissile phosphate of Ag10c (as discussed in section 3.2.7, it interacts with some nucleobases of a more covalent nature). Instead, the phosphate is activated by the buffer salt and thus, salt does not compete with Ag^+ for its binding to the DNAzyme. Most other DNAzymes rely on the metal cofactor binding to the scissile phosphate via electrostatic interaction, and therefore, salt can compete and inhibit the reaction in their case.

3.2.5 Effect of pH on Ag10c activity

After studying the effect of salt, the mechanism was further probed by measuring the rate of Ag10c with varying pH. Below pH 5.5, the rate is <0.01 min^{-1}, and thus, pH of <5.5 was not measured. The cleavage rate increases with pH and starts to reach saturation as the pH

approaches 8 (Figure 3.4 A). The rise in log (rate min^{-1}) increases linearly with pH between 6.0 and 7.0 with a slope of ~1 (Figure 3.4 B).

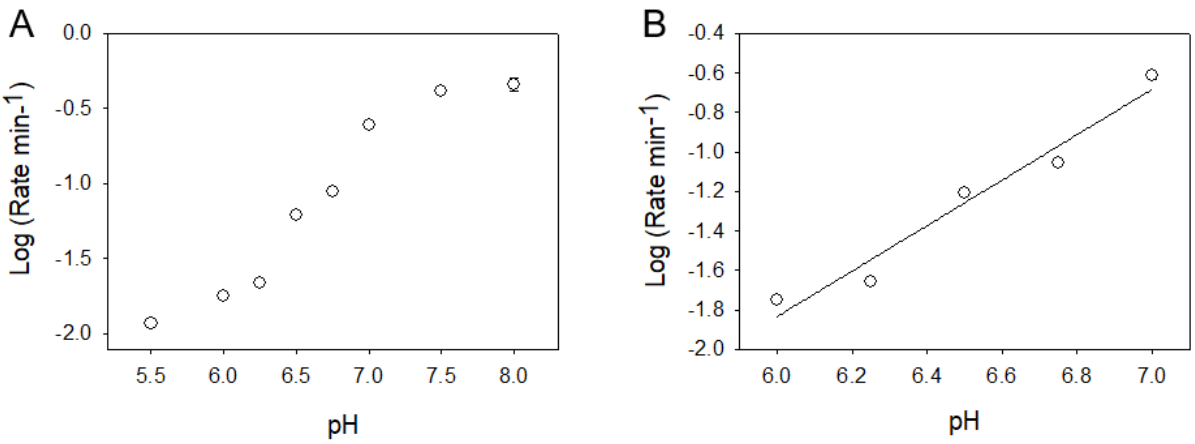

Figure 3.4 Log of the rate of Ag10c is plotted against (A) a wide pH rage and (B) a narrow linearly rising pH range. The pH- log (rate) slope is calculated to be 1.15. The rates are calculated in presence of 50 mM MOPS/MES, 200mM $NaNO_3$ and 10 µM Ag^+.

This suggests a single deprotonation step in the cleavage. This trend has been seen typically in most RNA-cleaving DNAzymes. The first pK_a of Ag^+ is around 10.0, and thus in the pH range tested Ag^+ is a fully hydrated ion, and the rate change is unlikely to be related to the hydrolysis of Ag^+. A critical step in the RNA cleavage reaction is the nucleophilic attack of the scissile phosphate by the 2'-OH nucleophile. The pH profile probed here is likely due to a nucleobase with a shifted pK_a (e.g., by interacting with Ag^+) acting as a general base and helping in the deprotonation of the 2'-OH to make it a stronger nucleophile, which has been commonly seen in ribozymes.[102]

3.2.6 Phosphorothioate (PS) modification to probe metal binding in Ag10c

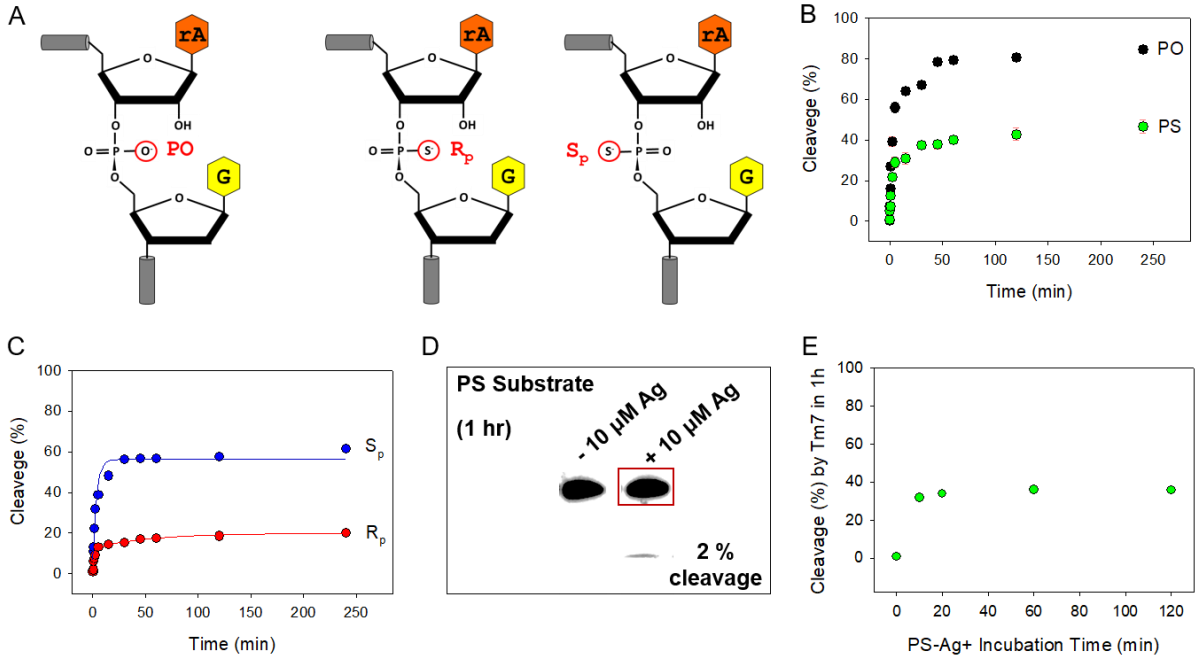

Figure 3.5 (A) Structure of the cleavage site dinucleotide junction in PO, R_p, and S_p substrates. The kinetics of Ag10c cleavage of (B) the PO and PS (mixture of R_p and S_p) substrates and (C) separated R_p and S_p substrates. (D) Gel image showing that, upon incubation of the PS substrate with 10 µM Ag^+ for 1 h, only 2 % of the PS substrate was cleaved. (E) After various periods (0, 2, 10, 30, and 60 min) of incubation of the PS substrate with Ag^+, the sample was treated with β-mercaptoethanol. Then the product was hybridized with the Tm7 DNAzyme. The cleavage yield after 1 h with 10 µM Er^{3+} is plotted here [buffer consisting of 50 mM MOPS (pH 7.5) and 50 mM NaNO3].

Further, the metal binding was probed by introducing a phosphorothioate (PS) modification at the scissile phosphate. PS refers to replacing one of the non-bridging oxygen atoms in the phosphate by sulfur. Once a PS is introduced, the phosphorus becomes a chiral center with two stereoisomers (called R_p and S_p).The schematic of the cleavage site dinucleotide junction in

normal phosphodiester (PO), R_p and S_p substrate is shown in Figure 3.5 A. With 10 μM Ag^+ and 200 mM $NaNO_3$, the PS substrate has only approximately half of the cleavage yield of the normal PO substrate (Figure 3.5 B), while the cleavage rate (0.37 ± 0.02 min^{-1}) was quite similar to the PO substrate (0.42 ± 0.01 min^{-1}). This lower cleavage yield of the PS substrate suggests that only one of the isomers is cleavable, which is quite typical for cleavage of RNA by ribozymes and DNAzymes.[124,231–233] Then, the two isomers were separated, following previously established protocols,[98] and their cleavage yield was separately measured (Figure 3.5 C). The cleavage yield was significantly higher with the S_p substrate than with the R_p substrate, which again is consistent with all previous reports.[124,231–233] Their average yield also agrees with that of their mixture (Figure 3.5 B, green trace). A careful examination of the kinetic profile indicates that the R_p substrate has an initial fast cleavage (but only up to ~15 % yield) followed by a much slower rise, while the S_p substrate has a more normal kinetic profile. Therefore, the cleavage of the R_p substrate was fitted with a two-rate model ($R^2 = 0.99$), yielding a faster rate of 1.17 ± 0.22 min^{-1} and a slower rate of 0.037 ± 0.03 min^{-1}. Note that this faster rate may be an overestimation because of its very low cleavage yield. The S_p substrate was fitted with a normal single-rate of 0.37 ± 0.01 min^{-1} ($R^2 = 0.94$). Typically, for such PS-modified experiments, a thiophilic metal such as Cd^{2+} or Mn^{2+} is used to rescue the activity of the inactive isomer (e.g., the R_p substrate). However, this system requires Ag^+, which has a thiophilicity that is much stronger than that of Cd^{2+} or Mn^{2+}. In this sense, this system is already under the rescued condition, and the thiophilicity of Ag^+ can cause complication in data analysis.The initial fast phase of the R_p substrate can be rationalized as follows. Due to the extremely strong thiophilicity of Ag^+, the following reactions can take place: 1) direct cleavage of the PS

substrate, 2) desulfurization of the substrate from PS to PO, which is then cleaved by the DNAzyme, and 3) direct cleavage by the DNAzyme.[251–254] Note that factors 1 and 2 are impossible for Cd^{2+} or Mn^{2+} under ambient conditions but take place with Hg^{2+}, Tl^{3+}, and Ag^{+}. To measure the amount of Ag^{+}-induced direct cleavage, 0.4 μM PS substrate was incubated with 10 μM Ag^{+} for 1 h, where only 2 % direct cleavage was observed (Figure 3.5 D). Next, to measure the amount of Ag^{+}-induced desulfurization, PS substrate was again incubated with Ag^{+}, but for various time periods of ≤60 min. At each time point, an aliquot was taken out and the reaction was stopped by chelating Ag^{+} with 1 mM β-mercaptoethanol. Then, the reaction mixture was annealed with the Tm7 DNAzyme followed by the addition of 10 μM Er^{3+}. The purpose was to examine the kinetics of desulfurization by Ag^{+}. The amount of cleavage by Tm7 after 1 h was measured (Figure 3.5 E). As the Tm7 cleaves only the 3′−5′ PO substrate but not the PS substrate,[123] the measured cleavage suggests that Ag^{+} desulfurizes the PS substrate into the cleavable PO substrate mainly within the first 2 min, but there is a slow yet noticeable rise in the level of desulfurization, taking place at least until 1 h. Therefore, the slower phase in Figure 3.5 C (red dots between 10 min and 4 h) can be attributed to the slow phase of desulfurization followed by Ag10c DNAzyme cleavage. The data indicates that at least 35 % of the PS was desulfurized to the 3′−5′ PO substrate in 1 h, and a similar amount should isomerized to the non-cleavable 2′−5′ PO substrate.[252] Considering that the cleavage yield by the Tm7 is not 100 % in 1 h, it can be reasoned that most of the PS substrate was desulfurized by Ag^{+}. Note that during desulfurization, the concentration of Ag^{+} is also decreased, and this also reduces the cleavage rate. At the same time, Ag^{+} can act as a rescue metal to bind to the sulfur, and this can also contribute to the cleavage. These overlapping factors make quantitative

dissection of cleavage contributions nearly impossible. These mechanisms can also act upon the S_p substrate. The fact that its cleavage yield is much higher than that of the R_p substrate indicates that the S_p substrate can be cleaved with a mechanism similar to that of the normal PO substrate. It has reached only 60 % cleavage yield likely also because of the desulfurization and isomerization to the inactive 2′−5′ substrate. While quantitative discussion is obscured by the strong thiophilicity of Ag^+, the higher yield of the S_p substrate can still allow to assign the metal binding site because it is known that only one metal is involved in phosphate binding here. Because the binding of Ag^+ to the scissile phosphate is already ruled out, it can be reasoned that Na^+ is used by the DNAzyme for this purpose. This is also consistent with the study mentioned above that used Li^+, K^+, and Mg^{2+} based on their charge density. These metals interact with the pro-R_p oxygen in the phosphate. The effect of monovalent metals in the HDV ribozyme was recently studied, where the cation charge density was also articulated.[232]

3.2.7 A silver aptamer embedded in Ag10c

All the above experiments described above indicate that Na^+ interacts with the scissile phosphate. As such, the role of Ag^+ still remains elusive. Therefore, it was hypothesized that the DNAzyme loop might be a silver aptamer. To confirm this, DMS foot printing was carried out. For this purpose, the DNAzyme complex in Figure 3.6 A was used, and the enzyme strand was fluorophore labeled instead of the substrate. DMS methylates the N7 position of guanine, conferring instability. This results in opening of the purine ring that is vulnerable to displacement and β-elimination by a base such as piperidine.[255] If a guanine is protected by

folding into a particular structure (i.e., N7 inaccessible to DMS), it might be protected from methylation and thus cleavage. This does not mean that the guanine has to directly participate in metal coordination. As long as the structure is folded and the N7 position is inaccessible, a protection should be observed. If a treated DNA is analyzed using PAGE, each exposed guanine in the DNA would produce a band in the gel. Upon titration with an increasing concentration of Ag^+, G3, G4, G6, G10−G12, and G15 were found to be more and more protected, while the two guanines in the hairpin stem (GS1 and GS2) and G17 remain unaffected (Figure 3.6 C). Strong participation of G3, G4, G11, and G12 in the binding pocket of Ag^+ also corresponds well with the >1000-fold decrease in activity upon their mutation and also indicates that they may be directly involved in Ag^+ binding. It is interesting to note that G17 was not protected from DMS but is critical for the catalytic activity of Ag10c (>1000-fold decrease in rate upon mutation), suggesting it might have a direct role in catalysis but might not be part of the aptamer. When other metal ions were used, no such protection was observed, further supporting the specific binding to Ag^+ (Figure 3.6 D). This experiment not only indicates the existence of a highly specific Ag^+ aptamer but also supports the idea that it is the role of Na^+ rather than Ag^+ to interact with the scissile phosphate. The protection of the guanines was quantitatively measured as a function of silver concentration (Figure 3.6 B). The measured K_d values range from 45 to 65 μM Ag^+ for the G residues involved in the binding pocket. This K_d is higher than that measured from its cleavage activity of ∼4 μM Ag^+ in Figure 3.2 B. This can be attributed to the different DNAzyme concentrations used for these assays. Only 400 nM Ag10c complex was used in the gel-based activity assay, while 4 μM Ag10c was used here in the foot printing

experiment. The 4 μM DNAzyme would require at least 8 μM Ag^+ to bind, thus leading to a much higher apparent K_d.

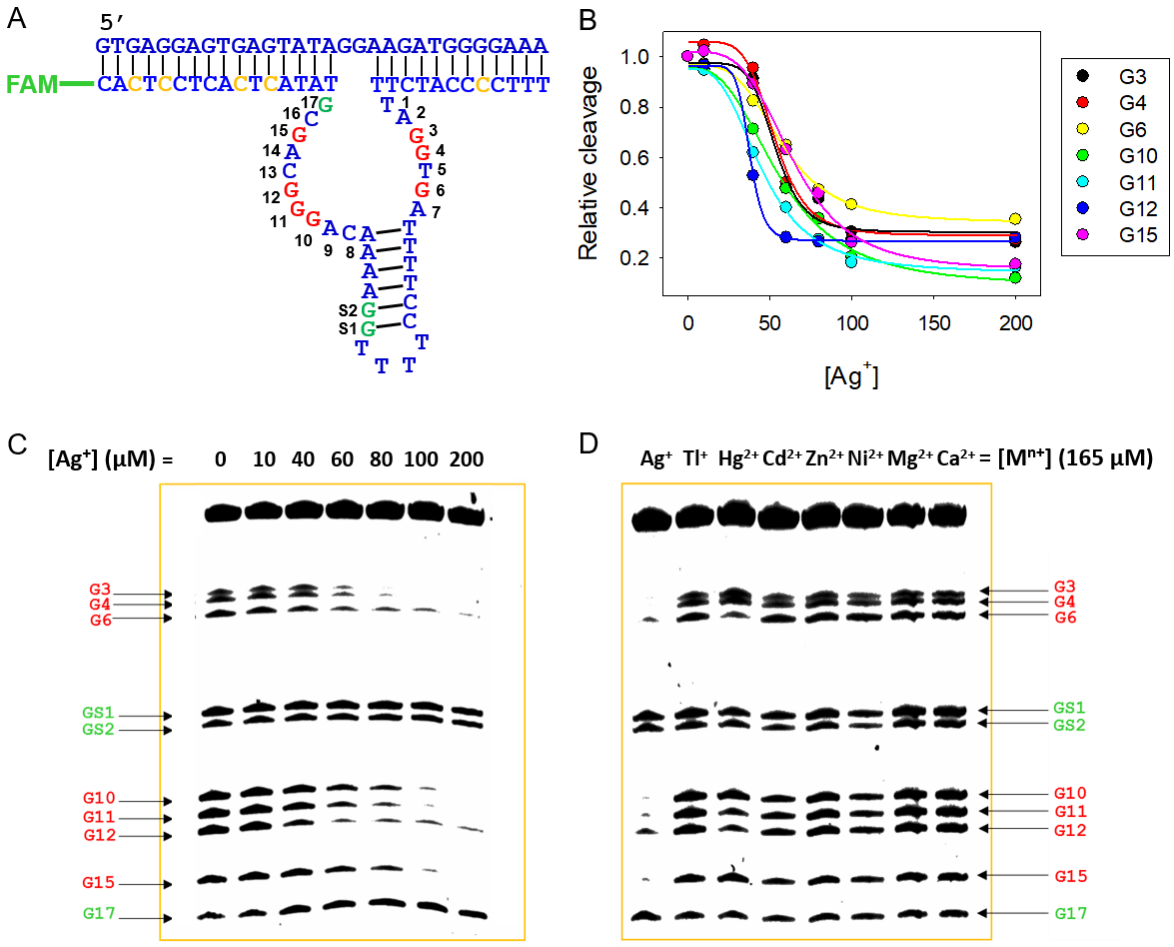

Figure 3.6 (A) The Ag10c DNAzyme complex used for DMS foot printing with a FAM labeled in the enzyme strand. (B) The relative cleavage of the G residues shown to be involved in the binding pocket of Ag^+ by the DMS experiment plotted on the y-axis against the increasing Ag^+ concentration on the x-axis. The band intensity for each G residue at 0 Ag^+ concentration is taken as 1 and as the [Ag^+] increases the reducing band intensity is respectively normalised. Gel images of the Ag10c DNAzyme in presence of (C) increasing concentration of Ag^+ and (D) 165 μM of different metals in the DMS foot-printing experiment. The above experiments were done in the presence of 200 mM $NaNO_3$.

Also, an apparent K_d of ~200 nM Ag^+ was measured from an Ag10c-based fluorescent biosensor (Figure 4.2 B).[256] In that case, the signal was generated from substrate cleavage followed by release of the cleaved fragment, and the Ag10c concentration was only 50 nM. These differences could have led to a much lower K_d for the sensor.

3.2.8 Ag10c DNAzyme undergoes Ag^+ induced local folding

The Ag10c contains a well-defined Ag^+ binding aptamer as indicated by DMS foot printing. Since this aptamer is infused with the Ag10c DNAzyme, Ag^+ binding may induce folding within the whole DNAzyme. Herein, 2-aminopurine (2AP) was used to probe its local folding in the presence of Ag^+.

The Ag10c DNAzyme and 2AP labeling. 2-aminopurine (2AP) is a fluorescent adenine analog and its emission is strongly affected by the local base stacking environment.[257] 2AP has been extensively used to study the folding of ribozymes and DNAzymes,[234,257–260] as well as aptamers.[261–263] While adenine is essentially non-fluorescent, free 2AP bases are strongly fluorescent. When embedded in a DNA sequence, its fluorescence is strongly quenched and the extent of quenching is affected by its local base stacking environment.[257] The structures of the bases adenine and 2-aminopurine are shown in Figure 3.7 B and C respectively. The Ag^+-specific Ag10c DNAzyme complex contains a substrate strand and an enzyme strand.[256] The typical substrate contains a single adenine RNA linkage (rA, Fig. 3.1 A) serving as the cleavage site. The enzyme strand has a hairpin flanked by two loops forming a pocket. In the presence

of Ag^+, the substrate is cleaved into two pieces. Based on the prior cleavage activity assays, the Ag10c binds two Ag^+ ions cooperatively via an aptamer pocket for the cleavage reaction.[171] The metal binding property is usually unaffected by deleting a single oxygen atom. To probe its folding, the Ag10c was labeled with 2AP at three different positions (in the substrate strand and in the enzyme strand) one at a time (Figure 3.7 A). For all the 2AP experiments, the RNA bearing substrate was replaced by its uncleavable full-DNA analog. This was to avoid cleavage during metal titration, and this method has been commonly used for studying the folding and structure of other DNAzymes.[238,264]

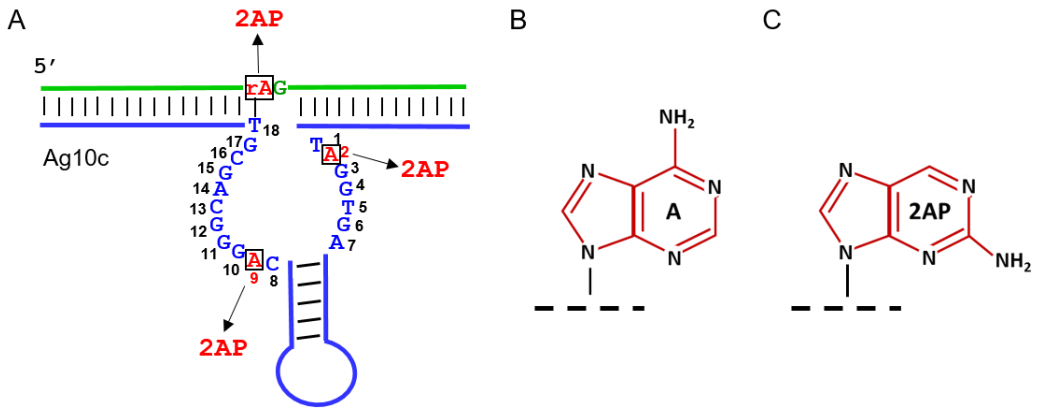

Figure 3.7 (A) The secondary structure of the Ag10c DNAzyme highlighting a hairpin and two loops in the enzyme strand. Three adenines are highlighted, each of which was replaced by a 2AP base (one at a time). The structures of the bases (B) adenine and (C) 2AP.

Labeling a 2AP at the cleavage site. Before carrying out any 2AP related studies in the Ag10c DNAzyme, the effect of Ag^+ on the emission of the free 2AP base was monitored (Figure 3.8 A). A progressive decrease in the 2AP fluorescence was observed by titrating Ag^+, reaching 80 % quenching with 100 μM Ag^+.[46] Thiophilic Hg^{2+} and Tl^+ were also studied. Hg^{2+} quenched

the 2AP fluorescence like Ag^+, while little quenching occurred with Tl^+. After studying the free 2AP base, 2AP was labeled in the Ag10c DNAzyme. An obvious position to probe for Ag^+-induced folding was the cleavage junction, as based on previous 2AP studies for another DNAzyme.[234] Therefore, the cleavage site adenine was replaced with a 2AP base (Figure 3.7 A), and Ag^+ was titrated into the complex. As shown in Figure 6.8 B, Ag^+ increased the emission of the 2AP in a concentration dependent manner. Since free 2AP bases are quenched by Ag^+ in this concentration range, this increase is attributable to DNAzyme folding (e.g. relaxing of the local base stacking of the 2AP). By plotting the 370 nm emission peak intensity against Ag^+ concentration, 80 % fluorescence enhancement was observed (Figure 6.8 C). It is interesting to note that the titration curve appears sigmoidal, indicative of cooperative binding of multiple Ag^+ ions. The binding curve was fitted to the Hill equation, and a Hill coefficient of 3.64 was obtained. This Hill co-efficient is larger than 2, which was determined from activity-based assays.[171] This might be related to the quenching effect (e.g. observed in Figure 6.8 A), overlapping with the enhancement leading to this difference. It is noticeable that the apparent dissociation constant, or K_d, measured by the 2AP was ~50 μM Ag^+, which was higher than that from the cleavage activity assay (~4 μM). The DNAzyme sequences in these assays were very similar and the use of non-cleavable 2AP labeled substrate is unlikely to significantly affect metal binding based on another DNAzyme study done in the Liu lab.[234] This difference in K_d was attributed to the different DNA concentrations used for each assay. The 2AP assay here used 1 μM DNAzyme due to its relatively weak fluorescence, while a 400 nM DNAzyme was used in the activity assays. The apparent K_d was even lower (e.g. ~200 nM Ag^+) when a

fluorescent sensor was used at only 50 nM. However still, it cannot be ruled out that labeling the 2AP has affected Ag^+ binding at this moment.

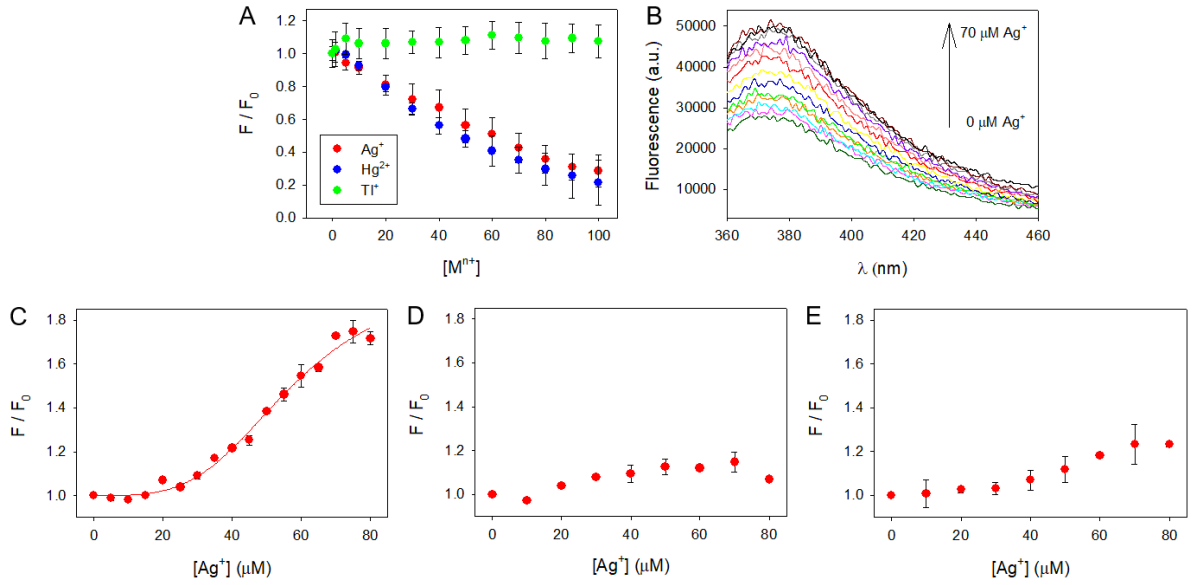

Figure 3.8 (A) The relative fluorescence of free 2AP base (1 μM) at 370 nm against the increasing concentration of Ag^+, Tl^+ or Hg^{2+}. (B) The fluorescence emission spectra of the Ag10c DNAzyme complex with a 2AP labeled at the substrate cleavage site. The rise in the relative fluorescence at 370 nm of DNAzyme complexes with the 2AP-labeled substrate hybridized to (C) the wild-type Ag10c, (D) the A2G, and (E) the G4A mutants with increasing [Ag^+] in buffer (50 mM MES, pH 6.0 with 50 mM $NaNO_3$).

Previous biochemical assays indicated that most nucleotides in the enzyme loops are critical for cleavage activity, and mutating them into other nucleotides negated the activity (Figure 3.1 C).[171] To test if folding and activity are related, two inactive mutants were tested as controls: A2G and G4A (see Figure 3.7 A for their positions). Interestingly, compared to the 80 % fluorescence rise for the wild-type, both mutants raised fluorescence only by ~20 % (Figure 3.8

D and E), indicating that the cleavage junction was still in a much more confined and stacked state after adding Ag^+. This further suggests that the folding at the cleavage site was indeed affected by such mutations, which might be a reason for their loss of cleavage activity. At the same time, these controls also indicated that the observed folding in the wild-type Ag10c was specific to Ag^+ binding.

Modulating local base stacking environment. Based on the data in Figure 3.8 C, 80 % fluorescence enhancement was achieved with 80 µM Ag^+. Next, it was tested if the fluorescence signal could be increased further by modulating the local environment around the 2AP label.

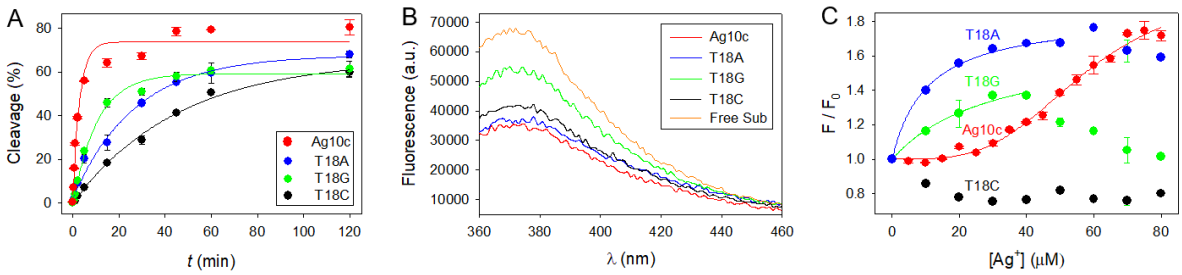

Figure 3.9 (A) The kinetics of substrate cleaved by the wild-type Ag10c DNAzyme and the three mutants (T18A, T18G, and T18C) in 50 mM MOPS, pH 7.5, 200 mM $NaNO_3$. (B) The fluorescence emission spectra of the 2AP modified substrate alone and in complex with T18A, T18G, T18C and Ag10c enzyme strands, in the absence of Ag^+. (C) The relative rise in fluorescence of the 2AP emission at 370 nm for these mutants upon adding increasing [Ag^+] in buffer (50 mM MES, pH 6.0 with 50 mM $NaNO_3$).

Based on Mfold predictions,[265] the cleavage site adenine (or 2AP in the current system) might base pair with the T18 residue of the enzyme strand (Figure 3.7 A). Note that both 2AP and adenine can pair with thymine.[257] This base pairing may confer a restriction on the accessibility

as well as flexibility of the 2AP. To test the importance of this putative base pair, the T18 residue in the enzyme strand was mutated to A, G or C, respectively. Before 2AP fluorescence was measured, the cleavage activity of each mutant was tested (Figure 3.9 A). In this case, the normal cleavable substrate was used. All the mutants remained active and the activity followed the order of the wild-type (~0.4 min^{-1}) > T18G (0.092 min^{-1}) > T18A (0.04 min^{-1}) > T18C (0.02 min^{-1}). Although the activity dropped slightly with the mutants (e.g. maximal dropping only 20-fold), they could still bind silver and thus the subsequent 2AP studies were biochemically relevant. Next, each mutant was respectively hybridized to the 2AP-modified substrate. Compared to the free substrate, all the DNAzyme complexes had lower initial fluorescence before adding Ag^+. This indicates that the 2AP was more confined upon by hybridization, suggesting successful formation of DNAzyme complexes. Among the four DNAzyme complexes, the T18G mutant gave the highest initial fluorescence in the absence of Ag^+, suggesting that its 2AP was in the most relaxed state (least stacking). For the other three, their initial fluorescence intensities were similar to one another (Figure 3.9 B). It is interesting to note that the initial fluorescence of the T18A mutant was similar to that of the wild-type Ag10c rather than that of T18G. This does not comply with the 2AP base pairing affinity ranking i.e. 'T > C > A ≈ G'.[266,267] Therefore, the predicted Watson-Crick base pairing of T18 and the 2AP was doubtful. The T18 nucleotide might have other roles rather than forming a base pair with cleavage site adenine. Upon titrating the mutant complexes with Ag^+ (Figure 3.9 C), the T18A and T18G mutants saturated at around 30 μM Ag^+, with a maximum increase of 68 % and 37 %, respectively. On the other hand, the T18C exhibited a 25 % decrease in fluorescence. It is quite striking that none of these mutants exhibited a common sigmoidal trend, typical of

multiple Ag^+ binding in the wild-type. It is interesting to note that the data for the T18G mutant (Fig. 3.9 C, green dots) had a breaking point near 40 mM Ag^+, which might be attributable to misfolding at high Ag^+ concentrations. Therefore, only the initial rising part of the data was fitted for it. It appears that any mutation made to T18 had an adverse effect on the activity and completely changed the pattern of Ag^+ binding and folding. This data reinforced the reasoning for the incompliance of the initial fluorescence of T mutants with the 2AP base pairing affinity, and that the T18 remains unpaired in the absence of Ag^+. It suggests that the role of T18 is stabilization of the interaction between Ag^+ and its aptamer, rather than base pairing with a cleavage site adenine. Addition of Ag^+ facilitates T18's involvement in the aptamer binding pocket, and relaxes base stacking at the cleavage site. On the other hand, mutations to T18 disrupted the typical aptamer pocket formation, and Ag^+ bound the mutated DNAzymes differently. Overall, the best fluorescence enhancement in the wild-type Ag10c. This is quite different from the Ce13d DNAzyme recently studied, where mutations to the same thymine has suggested its base pairing is with the 2AP.[234] Also in Ce13d, the mutations to this thymine position has improved the amount the fluorescence increased, from 34 % for the wild-type to 130 % in the best mutant upon adding Na^+.[229]

Probing local folding by labeling the enzyme strand. In all the above studies, the 2AP label was placed at the substrate cleavage site. However, it was intriguing to study the folding of the enzyme loop too. The previous biochemical mutation assays indicated that the A2G mutation decreased the activity by ~10,000-fold, and the A9G mutation decreased the activity by ~100-

fold.[171] Since these two positions are important for activity, each of these adenines was replaced with 2AP, one at a time (Figure 3.7 A).

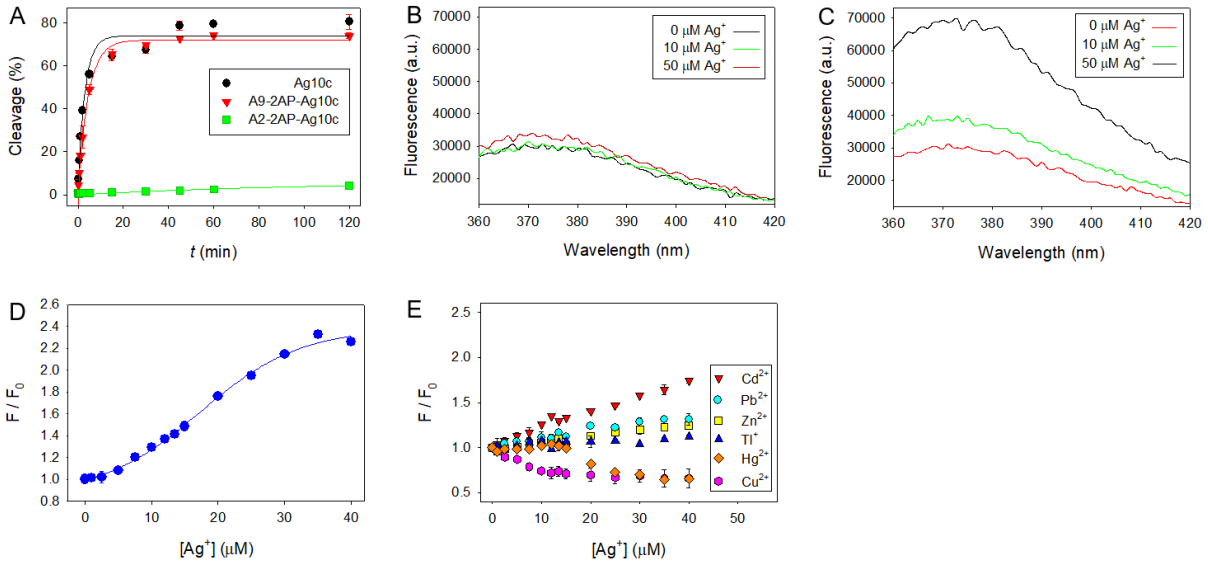

Figure 3.10 (A) The kinetics of the Ag10c DNAzyme and its mutants bearing A2P modifications at the A2 or A9 positions at pH 7.5 in the presence of 200 mM $NaNO_3$ and 10 μM Ag^+. The fluorescence emission spectra the (B) A2 modified and (C) A9 modified Ag10c complex in the presence of 0, 10, 20 and 50 μM Ag^+. The relative increase in the fluorescence at 370 nm against the increasing concentration of (D) Ag^+, and (E) Cd^{2+}, Pb^{2+}, Zn^{2+}, Tl^+, Hg^{2+} and Cu^{2+} with the A9-d2AP-Ag10c DNAzyme complex in 50 mM MES, pH 6.0, 50 mM $NaNO_3$.

First, the activity of the 2AP-modified enzymes were tested using the normal RNA containing substrate. The A2-to-2AP mutant had negligible activity, while the A9-to-2AP mutant was very active with a rate of ~ 0.22 min^{-1}, which is comparable to that of the wild-type (~0.4 min^{-1}, Figure 3.10 A). This indicates that the A2 site might directly participate in catalysis or Ag^+ binding, while the A9 site does less so. Then, DNAzyme complexes of the modified Ag10c

strands with the unlabeled full-DNA substrate were prepared. Upon addition of Ag^+ to the A2-to-2AP complex, little change in fluorescence occurred (Figure 3.10 B). This result corresponds well with the ~10,000-fold decrease in cleavage kinetics of this mutant and could thus be attributed to the loss of Ag^+ binding to the DNAzyme, due to the 2AP modification. The A9-to-2AP sample showed a noticeable fluorescence rise upon Ag^+ titration (Figure 3.10 C). Therefore, labeling 2AP at this position did not affect its folding or activity. This motivated us to perform a more careful titration with this sample. A progressive increase in fluorescence was observed, with a final increase of ~ 140 % saturating at around ~ 40 μM Ag^+ (Figure 3.10 D). This suggests that addition of Ag^+ induces relaxation of the base stacking near the A9 position. It is quite interesting that fluorescence rise was observed here, since normally one would expect aptamer binding to induce a more compact structure and thus, decrease fluorescence. Indeed, decreased fluorescence was observed for the Ce13d DNAzyme for Na^+ binding in a 2AP modified enzyme loop.[234] In this case, it appears that the loop already had some structure and the A9 position was released from such a structure upon forming the aptamer binding pocket. Upon plotting the rise in relative fluorescence at 370 nm on the y-axis against Ag^+ concentration, the data could be fitted well into the Hill equation with a Hill coefficient of 2.17 ($R^2 = 0.99$, Figure 3.10 D). This was consistent with the binding of 2 Ag^+ ions and it matched well with the number of Ag^+ ions estimated through the activity assays.[171] The K_d of the Ag^+ binding was calculated to be ~ 18 μM, which was also in better agreement with the K_d observed from the previous activity assay. It was then confirmed if the rise in fluorescence was specific to Ag^+ or not. Therefore, increasing concentrations of Cd^{2+}, Zn^{2+}, Cu^{2+}, Pb^{2+}, Hg^{2+} or Tl^+, were titrated with the A9-to-2AP DNAzyme complex (Figure 3.10 E). These metals were chosen

since they are also thiophilic similar to Ag^+. It was found that no other metals except Cd^{2+} demonstrated a significant rise in the fluorescence. Unlike Ag^+, the rise exhibited a linear trend with Cd^{2+}, indicating a non-specific interaction of Cd^{2+}. None of these above mentioned metal ions promoted any cleavage activity.[256] This suggested that the observed rise in fluorescence in the presence of Ag^+ was due to specific aptamer folding of the DNAzyme complex.

3.3 Summary

In this study, biochemical characterization of the Ag10c DNAzyme was performed. Many interesting observations were made. Firstly, through systematic mutation studies, it was concluded that Ag10c has a well-defined secondary structure and most of the nucleotides in its catalytic loop are important for activity and cannot be randomly changed. Secondly, fundamental mechanistic insights were gained into Ag10c catalysis. Through Ag^+-dependent activity assays, the role of Ag^+ was rationalized. It was established that this Ag10c DNAzyme uses two metals for catalysis: one Na^+ (or other group 1A metals or Mg^{2+}) binds to the pro-R_p oxygen of the scissile phosphate; and two Ag^+ ions bind cooperatively to Ag10c aptamer loop. This is the second such example. The first was the Ce13d DNAzyme, which uses Ce^{3+} (or other lanthanides) to bind to the phosphate, and it also has an aptamer loop for Na^+.[129] It was also confirmed that Ag10c undergoes a single deprotonation step during catalysis. Through this study, a new theme of DNAzyme catalysis has emerged that may be used by soft metals to escape interaction with the scissile phosphate and yet confer effective catalysis. Such a fundamental understanding, has opened up the platform to explore and select novel soft metal-

dependent DNAzymes. Thirdly, using DMS footprinting, a well-defined silver aptamer was confirmed, which can fold into a compact structure by binding Ag^+. This work has provided a new aptamer for Ag^+ and this aptamer is completely different from the well-known C-Ag^+-C structure.[243] The mutation studies strongly argue against the formation of any C-Ag^+-C base pair. As mentioned above, this is the second example of an aptamer embedded in a DNAzyme obtained via *in-vitro* selection, and is different from those intentional aptazymes selected starting with an existing enzyme scaffold.[128,268] For a given metal, there are many solutions for producing aptamer sequences. Such a complex binding structure is reminiscent of metal binding aptamers in riboswitches,[269] where the aptamers are coupled with functions related to regulation of gene expression. This study will prove to be of help for intentionally adjusting DNAzyme selection conditions to obtain more such metal aptamers (for e.g. high salt concentration to promote the formation of aptamers). Now, such more complex sequences can be created *in-vitro*, which will give us more insights into the metal binding ability of nucleic acids. Lastly, 2AP fluorescence was used to study the folding of the Ag^+-specific RNA-cleaving DNAzyme Ag10c. This DNAzyme is unique since it contains an aptamer for Ag^+. Local folding was observed by increased 2AP fluorescence at the dinucleotide junction of Ag10c, while none of the inactive mutants exhibited such a response at the same 2AP position. In addition, Ag^+ also induced a rise in 2AP fluorescence when labeled in the enzyme loop (the A9 position), while other metals did not give such a fluorescence increase. The control experiments with the mutated DNAzyme and inactive metals confirmed specific aptamer binding. It was concluded that the substrate cleavage site remains unpaired in the absence of Ag^+. Upon addition of Ag^+, T18 gets involved in the Ag^+ binding pocket leading to increased 2AP fluorescence at the

cleavage site. Therefore, the cleavage site and the A9 position, both undergo a conformational change from stacked to less stacked, upon Ag^+ binding. As previously studied, this aptamer is not related to the typical C-Ag^+-C base pairing, and is a new way of binding Ag^+. Silver is an important analyte, and this aptamer will likely be useful for developing silver sensors. The binding of two metals produces a sigmoidal response curve, and such a response might also be analytically useful. The study here suggests the possibility of designing folding-based biosensors for Ag^+ using this DNAzyme.

3.4 Materials and Methods

3.4.1 Chemicals

All of the fluorescently labeled DNA samples were purchased from Integrated DNA Technologies (Coralville, IA), and the rest DNA samples including the 2AP labelled DNA sequences were from Eurofins (Huntsville, AL). The sequences and modifications are listed in Table 3.1. Metal ions that were used for analysis include silver(I) nitrate, potassium(I) chloride, lithium(I) chloride, thallium(I) chloride, lead(II) acetate, magnesium(II) sulfate, manganese(II) chloride tetrahydrate, iron(II) chloride tetrahydrate, cobalt(II) chloride hexahydrate, copper(II) chloride dehydrate, zinc(II) chloride, calcium(II) chloride, nickel(II) chloride, strontium(II) chloride, cadmium(II) chloride, mercury(II) perchlorate, yttrium(III) chloride hexahydrate, gallium(III) chloride, cerium(III) chloride, iron(III) chloride hexahydrate. All these salts were purchased from Sigma-Aldrich except the iron and silver salts were purchased from Alfa Aesar. The purity of the metals used is 99.99 %. Tris (Hydroxymethyl) aminomethane (Tris), 2-(N-

morpholino) ethanesulfonic acid, (MES) free acid monohydrate, 3-(*N*-morpholino) propanesulfonic acid (MOPS), sodium chloride, sodium nitrate and sodium iodide were from Mandel Scientific (Guelph, ON, Canada). Acrylamide/bisacrylamide 40 % solution (29:1), urea, and 10 X TBE solution were purchased from Bio Basic Inc.

Table 3.1 List of DNA sequences used in chapter 3.

* denotes the phosphorothioate (PS) modification

DNA	**Sequences (5′ – 3′)**
PO-Substrate	GTCACGAGTCACTATrAGGAAGATGGCGAAA/FAM/
PS-Substrate	GTCACGAGTCACTATrA*GGAAGATGGCGAAA/FAM/
Rp-Substrate	GTCACGAGTCACTATrA*GGAAGATGGCGAAA/FAM/
Sp-Substrate	GTCACGAGTCACTATrA*GGAAGATGGCGAAA/FAM/
Substrate-FP	GTGAGGAGTGAGTATAGGAAGATGGGGAAA
2AP Substrate	GTCACGAGTCACTAT/2AP/GGAAGATGGCGAAA
Ag10c	CGCCATCTTTAGGTGATTTCCACGATTATGCGGAAACAGGGCAG CGTATAGTGACTCG
Ag10c(a)	CGCCATCTTTAGGTGATACAGGGCAGCGTATAGTGACTCG
Ag10c(b)	CGCCATCTTTAGGTGAAAAGGACGATTATGCCCTTTCAGGGCAG CGTATAGTGACTCG
Ag10c(c)	CGCCATCTTTAGGTGATTTCCGATTAGGAAACAGGGCAGCGTAT AGTGACTCGTGAC
Ag10c(d)	CGCCATCTTTAGGTGATTTCCTTTTGGAAACAGGGCAGCGTATA GTGACTCG
Ag10c(e)	CGCCATCTTTAGGTGATTTCCGCAGATTATGCGGAAACAGGGCA GCGTATAGTGACTCG

Ag10c(f)	CGCCATCTTTAGGTGATTTCCGCATTTTTGCGGAAACAGGGCAG CGTATAGTGACTCG
Ag10cT1C	CGCCATCTTCAGGTGATTTCCACGATTATGCGGAAACAGGGCAG CGTATAGTGACTCG
Ag10cdelT1	CGCCATCTT.AGGTGATTTCCACGATTATGCGGAAACAGGGCAG CGTATAGTGACTCG
Ag10cA2G	CGCCATCTTTGGGTGATTTCCACGATTATGCGGAAACAGGGCAG CGTATAGTGACTCG
Ag10cG3A	CGCCATCTTTAAGTGATTTCCACGATTATGCGGAAACAGGGCAG CGTATAGTGACTCG
Ag10cG4A	CGCCATCTTTAGATGATTTCCACGATTATGCGGAAACAGGGCAG CGTATAGTGACTCG
Ag10cT5C	CGCCATCTTTAGGCGATTTCCACGATTATGCGGAAACAGGGCAG CGTATAGTGACTCG
Ag10cG6A	CGCCATCTTTAGGTAATTTCCACGATTATGCGGAAACAGGGCAG CGTATAGTGACTCG
Ag10cA7G	CGCCATCTTTAGGTGGTTTCCACGATTATGCGGAAACAGGGCAG CGTATAGTGACTCG
Ag10cdel(G6A7)	CGCCATCTTTAGGT..TTTCCACGATTATGCGGAAACAGGGCAGC GTATAGTGACTCG
Ag10cC8T	CGCCATCTTTAGGTGATTTCCACGATTATGCGGAAATAGGGCAG CGTATAGTGACTCG
Ag10cC8A	CGCCATCTTTAGGTGATTTCCACGATTATGCGGAAAAAGGGCAG CGTATAGTGACTCG
Ag10cC8G	CGCCATCTTTAGGTGATTTCCACGATTATGCGGAAAGAGGGCAG CGTATAGTGACTCG
Ag10cA9G	CGCCATCTTTAGGTGATTTCCACGATTATGCGGAAACGGGGCAG CGTATAGTGACTCG
Ag10cG10A	CGCCATCTTTAGGTGATTTCCACGATTATGCGGAAACAAGGCAG CGTATAGTGACTCG

Ag10cG11A	CGCCATCTTTAGGTGATTTCCACGATTATGCGGAAACAGAGCAG CGTATAGTGACTCG
Ag10cG12A	CGCCATCTTTAGGTGATTTCCACGATTATGCGGAAACAGGACAG CGTATAGTGACTCG
Ag10cC13T	CGCCATCTTTAGGTGATTTCCACGATTATGCGGAAACAGGGTAG CGTATAGTGACTCG
Ag10cC13A	CGCCATCTTTAGGTGATTTCCACGATTATGCGGAAACAGGGAAG CGTATAGTGACTCG
Ag10cC13G	CGCCATCTTTAGGTGATTTCCACGATTATGCGGAAACAGGGGAG CGTATAGTGACTCG
Ag10cA14G	CGCCATCTTTAGGTGATTTCCACGATTATGCGGAAACAGGGCGG CGTATAGTGACTCG
Ag10cdel14A	CGCCATCTTTAGGTGATTTCCACGATTATGCGGAAACAGGGC.GC GTATAGTGACTCG
Ag10cG15A	CGCCATCTTTAGGTGATTTCCACGATTATGCGGAAACAGGGCAA CGTATAGTGACTCG
Ag10cC16T	CGCCATCTTTAGGTGATTTCCACGATTATGCGGAAACAGGGCAG TGTATAGTGACTCG
Ag10cC16A	CGCCATCTTTAGGTGATTTCCACGATTATGCGGAAACAGGGCAG AGTATAGTGACTCG
Ag10cC16G	CGCCATCTTTAGGTGATTTCCACGATTATGCGGAAACAGGGCAG GGTATAGTGACTCG
Ag10cG17A	CGCCATCTTTAGGTGATTTCCACGATTATGCGGAAACAGGGCAG CATATAGTGACTCG
Ag10c-FP	TTTCCCCATCTTTAGGTGATTTCCTTTTGGAAACAGGGCAGCGTA TACTCACTCCTCAC/FAM/
Ag10cT18A	TTTCGCCATCTTTAGGTGATTTCCTTTTGGAAACAGGGCAGCGA ATAGTGACTCGTGAC
Ag10cT18G	TTTCGCCATCTTTAGGTGATTTCCTTTTGGAAACAGGGCAGCGG ATAGTGACTCGTGAC

Ag10cT18C	TTTCGCCATCTTTAGGTGATTTCCTTTTGGAAACAGGGCAGCGC ATAGTGACTCGTGAC
A9-2AP-Ag10c	TTTCGCCATCTTTAGGTGATTTCCTTTTGGAAAC/2AP/GGGCAGC GTATAGTGACTCGTGAC
A2-2AP-Ag10c	TTTCGCCATCTTT/2AP/GGTGATTTCCTTTTGGAAACAGGGCAGC GTATAGTGACTCGTGAC

3.4.2 Activity assays

For a typical gel-based activity assay, the DNAzyme complex were prepared by annealing the FAM-labeled substrate (10 µM) and enzyme (30 µM) in buffer 50 mM MES (pH 6.0, 25 mM $NaNO_3$) by heating at 85 °C for 1 min and then slowly cooled at room temperature until ~30 °C. The complex was then frozen at -20 °C for at least 2 hours. To initiate the reaction at room temperature, a final of 0.05 - 200 µM Ag^+ or another metal ion (as required) was incubated with 0.4 µM DNAzyme complex in a total 10 µL reaction mixture in buffer 50 mM Na.Acetate (pH 5.0 - 5.5) / 50 mM MES (pH 6.0 - 6.5) / 50 mM MOPS (pH 7.0 – 8.0) with salt concentration varying from 25 - 200 mM $NaNO_3$, for the required time ranging from 10 s – 8 h. The samples were quenched with 8 M urea at designated time points and run in 15 % dPAGE at 120 V for 80 min. The gel images were taken with Bio-Rad ChemiDoc MP imaging system. For determining the rate of cleavage, the gel band intensities of the cleaved vs. uncleaved substrate were quantified and the data obtained were fitted (using *Sigma Plot 12.0*) according to the first-order rate equation $Y_t = Y_o + a(1\text{-}e^{-kx})$, where Y_t and Y_o are the cleavage fractions at a given

reaction time '*t*' or '*0*' min, respectively, '*a*' is a constant i.e. the scaling parameter and '*k*' is the observed rate constant.

3.4.3 Dimethyl sulphate (DMS) footprinting

DMS footprinting was performed following previously published protocols.[129] Briefly, the 3-end FAM-labeled enzyme (Ag10c-FP-FAM) and the noncleavable all-DNA substrate was used. The DNAzyme complex (4 μM Ag10c-FP-FAM and 20 μM Sub-dA) was formed by annealing in 50 mM MOPS buffer (pH 7.5) containing 0 or 200 mM NaNO3. Before footprinting, the DNAzyme complex (10 μL) was incubated with a final concentration of 0, 10, 40, 60, 80, 100, or 200 μM of a metal ion such as Ag^{+}, Hg^{2+}, Cd^{2+}, Ni^{2+}, Tl^{+}, Zn^{2+}, Mg^{2+}, or Ca^{2+} for 15 min. To methylate the guanosine, 1 μL of freshly prepared 4 % DMS was added to 10 μL of the DNAzyme−metal complex, followed by a 15 min incubation in the dark. Then, the reaction was quenched by adding 200 μL of a solution containing β-mercaptoethanol (1 M) and NaOAc (600 mM, pH 5.2), followed by ethanol precipitation and cleavage by 10 % piperidine. Finally, the products were separated by 15 % dPAGE for analysis.

3.4.4 2AP titration

For the 2AP experiments, three DNAzyme constructs were tested to identify the ideal location for the label, with modification in either the substrate or the enzyme strand (named as '2AP Substrate', 'A2-2AP-Ag10c' and 'A9-2AP-Ag10c' in Table 1). To prepare the E-S complex

for the 2AP experiment, the unlabeled (3 µM) and the labeled (1 µM) strands were mixed in buffer 50 mM MES, pH 6.0, 50 mM $NaNO_3$. The two strands were annealed by heating at 85°C for 1 min, followed by slow cooling at room temperature until ~30 °C. The complex was then frozen at -20 °C overnight. Each E-S complex sample had a volume of 200 µL and a concentration of 1 µM in a micro quartz cuvette (path length = 10 mm). The sample was then titrated using increasing concentrations of metal ions, followed by measuring the 2AP spectra using a fluorimeter (Horiba FluoroMax 4) by exciting at λ = 310 nm and measuring its emission from λ = 360 - 460 nm. Every time a metal solution was titrated in the complex, the fluorescence reading was treated with the dilution factor to make up for any loss in fluorescence due to increase in volume. These corrected fluorescence values were then plotted. The binding curve (relative max. fluorescence vs. metal concentration) obtained through the above method was fitted to the Hill equation, $Y = Y_o + \frac{A * X^b}{C^b + X^b}$. Here '*Y'* and '$Y_O$*'* are the relative 2AP fluorescence units at M^+ concentration '*X'* and '*0'* µM respectively, *'A'* and *'C'* are constants and *'b'* is the Hill coefficient.

4. Chapter 4 – Ag10c based Ag^+ Biosensor[c]

4.1 Introduction

Metallic silver and its alloys and compounds have been used in jewelry, solar cells, antimicrobial agents, dental amalgams, photography, electronic components, glass coatings, and catalysis, among other applications.[270] Such widespread usage has led to environmental contamination. Silver is a heavy metal and poses a health threat as it tends to bio-accumulate, causing Argyria (the blue skin syndrome) and damage to the skin, eyes, liver, kidneys, and intestinal tracts.[271] While silver can be measured by instrumentation methods such as inductively coupled plasma mass spectrometry (ICPMS), it is also important to develop biosensors for on-site detection, which may also help recover this valuable metal.[272,273] Over the past 2 decades, DNA has emerged as a highly versatile platform for metal sensing based on either metal/nucleobase binding interactions or metal-assisted DNAzyme catalysis.[209,274–278] A number of DNA based Ag^+ sensors have been demonstrated till date. The use of C-rich sequences to form C-Ag^+-C base pairs in the presence of Ag^+ is the most popular one. This highly specific FRET based turn off sensor exhibits concentration dependent quenching.[173] Another method for sensitive and specific detection of Ag^+ involves the use of the fluorescent analogue of cytosine, pyrrolocytosine (PdC). PdC is known to show intrinsic fluorescence in its unpaired form but its fluorescence is known to decrease when it base pairs with a complementary nucleotide.[279–283] In the presence of Ag^+, PdC was designed to base pair to form

[c] This chapter is the basis for a published manuscript: Saran R.; Liu, J. A Silver DNAzyme. *Anal. Chem.* **2016**, 88, 4014-4020.

PdC-Ag^+-C, strongly decreasing its fluorescence in a concentration dependent manner and thus facilitating the detection of Ag^+ ions with a limit of detection (LOD) of 9.2 nM.[145] C-rich DNA is often used as template for the synthesis of fluorescent AgNCs, and this has also been implied for Ag^+ quantification. Ag^+ triggers poly-C templated AgNCs to form dimers, consequently switching their fluorescence emission from red to green, and allowing specific detection of Ag^+ down to 10 nM.[197] As mentioned before (section 1.5.2), Ag^+ can stabilize i-motif at physiological pH and once Ag^+ is chelated away by cysteine, i-motif unfolds.[175] Taking advantage of this, an i-motif DNA based label-free Ag^+ sensor has been demonstrated (LOD 17 nM) taking help of the fluorescent stain thiazole orange (TO).[201] It is well known that Ag^+ can strongly coordinate with guanine.[178] Interestingly, the Ag^+ binding sites in guanine are also important for G4 formation and thus, addition of Ag^+ ions can destabilize and disrupt the G4 structure. Based on this phenomenon, Ag^+ induced abolished peroxidase activity of G-quadruplex-hemin DNAzymes (LOD 64 nM),[202] Ag^+ induced dispersion of aggregated G-quadruplex capped AuNPs (LOD 7nM),[204] Ag^+ induced decreased fluorescence of G-quadruplex - N-methyl-mesoporphyrin IX (NMM) complex (LOD 400 nM)[284] as well as G-quadruplex-Triphenylmethane (TPM) complex (LOD 80 nM),[285] has been harnessed for developing highly sensitive and selective Ag^+ sensing systems. It is fascinating that weak fluorescence of lanthanide/nucleotide coordination polymers is strongly increased by Ag^+ in aqueous solution. The Ag^+ triggered increase in the luminescence of AMP/Tb^{3+} co-ordination polymer has been utilized for demonstrating a selective and sensitive Ag^+ sensor with a LOD of 60 nM.[286] /Ag^+ Similarly, Ag^+ induced enhanced luminescence of Tb^{3+} sensitized poly-G DNA has been shown to form the basis of a selective Ag^+ sensor with a LOD of 57.6 nM.[200]

Although DNAzymes have been used for Ag^+ sensing, these systems utilize cytosine-Ag^+ as well as the cysteine-Ag^+ coordination, but Ag^+ does not play a catalytic role.[287] RNA-cleaving DNAzymes are particularly interesting in this respect. Many DNAzymes already known have been used to build metal biosensors. They can achieve extremely high metal sensitivity i.e. low nM (parts-per-billion) and sometimes even pM (parts-per-trillion) levels, and are versatile in biosensor design.[208,214] Herein, for the first time, a RNA-cleaving DNAzyme (Ag10c) based Ag^+ biosensor is reported and is also demonstrated to be highly sensitive and selective.

4.2 Results and discussion

4.2.1 Biosensor design

From the studies mentioned in previous chapters, it is clear that Ag10c is highly specific for Ag^+ with fast catalytic rate, allowing us to build a biosensor for Ag^+. Among the various signaling strategies known, a catalytic beacon method was employed for its high sensitivity.[113,275] A fluorescence 'turn-on' strategy was adopted to develop a DNAzyme beacon for real-time analysis. The 3′-end of the enzyme strand was labeled with a Black Hole Quencher (named Ag10c-Q), which upon hybridization, quenches the fluorescence of the FAM fluorophore labeled on the 5′-end of the substrate (5′-FAM-Sub). In the presence of Ag^+, the substrate strand is expected to cleave into two pieces at the cleavage site. In comparison to the full-length substrate, the expected cleaved fragment has a lower melting temperature (T_m) and

thus lower affinity for the enzyme strand. If the T_m of the FAM modified cleaved substrate fragment is lower than the room temperature (RT), it would dissociate from the enzyme strand, and the fluorescence would thus be rescued after its release (Figure 4.1 A).

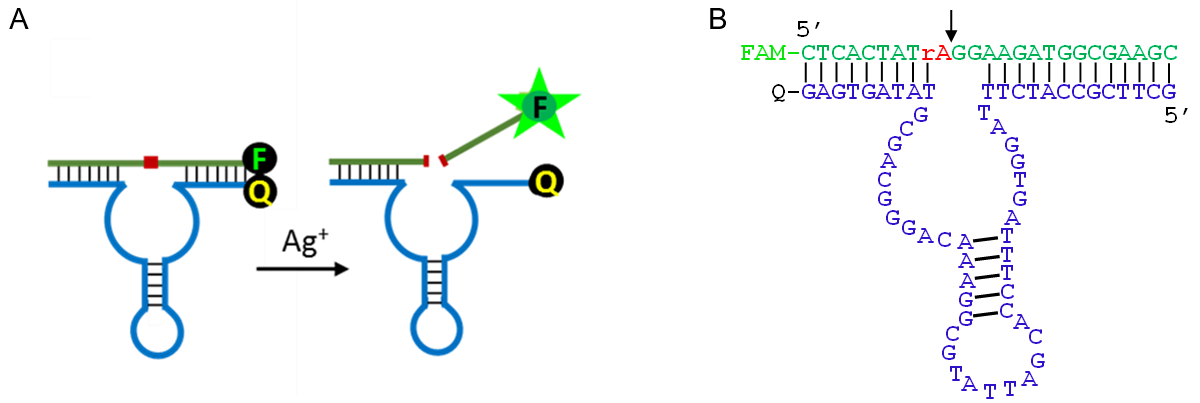

Figure 4.1 (A) Schematic representation of the Ag^+ DNAzyme beacon design. (B) The secondary structure of the Ag10c-Q DNAzyme beacon.

The secondary structure of the Ag10c-Q DNAzyme beacon is shown in Figure 4.1 B. For Ag10c-Q, the sequence of the substrate binding arms of the Ag10c enzyme is modified, the length of the 5′ substrate binding arm is increased by 1 nucleotide while that of the 3' substrate binding arm is reduced by 7 nucleotides to suit the experiment. As calculated by the software 'OligoAnalyzer 3.1' from Integrated DNA Technologies (IDT),[288] the T_m of the 5′ fragment of the cleaved substrate is predicted to be ~ 40 °C, while that of the 3' fragment is expected to be ~ 7 °C. Therefore, the sensor was designed with an extremely low T_m of the 3′ cleaved substrate fragment, to facilitate its release from the enzyme strand, so that the fluorescence rescue can be considered as a direct reflection of the Ag^+ induced substrate cleavage.

4.2.2 Limit of detection

This experiment was executed by monitoring the signaling kinetics of the beacon with increasing concentration of Ag^+ in 50 mM MOPS (pH 7.5, 200 mM $NaNO_3$). With 50 nM of the sensor complex, in the absence of Ag^+, the background was quite stable, indicating a stable DNAzyme complex. The rate of fluorescence enhancement rapidly and progressively increased with higher Ag^+ concentrations with the dynamic range reaching ~400 nM Ag^+ (Figure 4.2 A). The initial rates of the fluorescence traces were quantified and plotted against their respective Ag^+ concentrations in Figure 4.2 B. The low Ag^+ concentration region is shown in the inset of Figure 4.2 B.

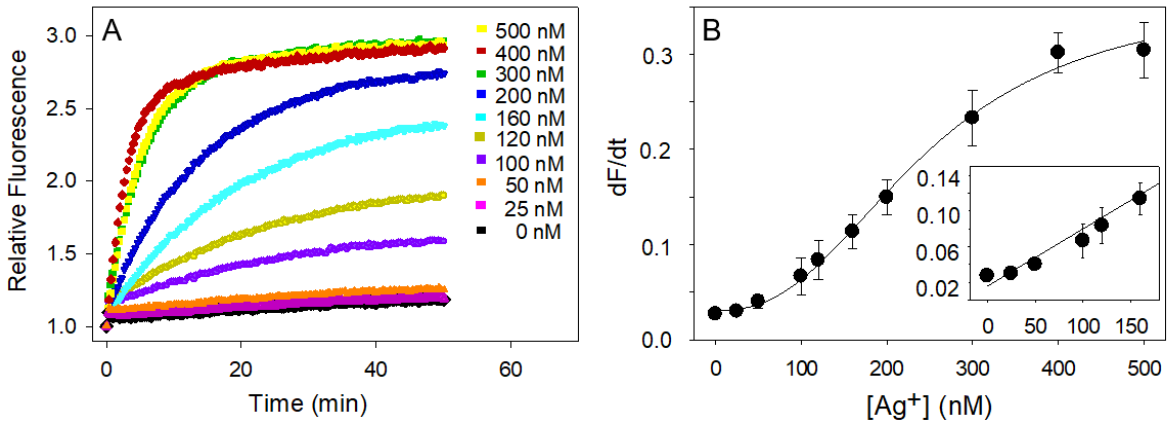

Figure 4.2 (A) Sensor signaling kinetics at various concentrations of Ag^+. (B) Quantification of Ag^+ based on the initial rate of fluorescence enhancement. Inset: the low Ag^+ concentration region fitted with a linear response.

A limit of detection (LOD) of 24.9 nM Ag^+ was calculated based on 3σ/slope (σ is the standard deviation of the background signal). This LOD is 37-fold lower than the maximum permissible

contamination level of silver in water i.e. 0.1 mg/L or 930 nM defined by the World Health Organization. This represents the first instance of a sensitive RNA-cleaving DNAzyme based Ag^{+} biosensor.

4.2.3 Metal specificity

To test for selectivity, the sensor was then challenged with various monovalent, divalent and trivalent cations.

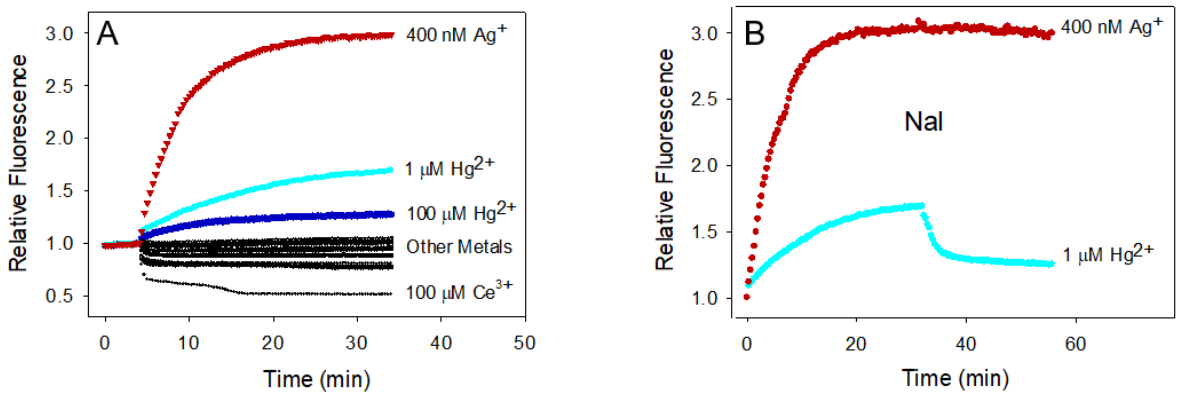

Figure 4.3 Sensor signaling kinetics with (A) various metal ions: 1 and 100 mM K^{+}, Li^{+}, Rb^{+}, Na^{+}, Cs^{+}; 1 and 10 mM Ca^{2+}, Mg^{2+}, 1 and 100 µM Mn^{2+}, Fe^{2+}, Cu^{2+}, Zn^{2+}, Ni^{2+}, Co^{2+}, Cd^{2+}, Pb^{2+}, Sr^{2+}, Ce^{3+} and Fe^{3+}. (B) Sensor response to 400 nM Ag^{+} and 1 µM Hg^{2+} where the black arrows indicate the time of addition of 10 µM NaI. The fluorescence dropping in the Hg^{2+} reaction indicates its signaling was not due to cleavage. All the reactions were performed in 50 mM MOPS, pH 7.5 with 200 mM $NaNO_3$. The final sensor concentration was 50 nM.

The signal remained at the background level with most ions, while a few caused fluorescence quenching. The only one (except Ag^{+}) with fluorescence increase was Hg^{2+}, both at 1 µM and

100 µM concentrations (Figure 4.3 A). Since the gel-based assay with similar concentrations of Hg^{2+} did not produce any cleavage (Figure 2.7), it was speculated that the fluorescence increase was from Hg^{2+}-induced DNA misfolding. Hg^{2+} has strong affinity with DNA pyrimidine bases, which may fold the FAM label away from the quencher, thus enhancing the fluorescence. If this hypothesis is true, such a rise in fluorescence should be reversible if the Hg^{2+} ions are made unavailable. To test it, the rise in fluorescence was initiated with 1 µM Hg^{2+} or 400 nM Ag^{+}. Upon signal stabilization, 10 µM NaI was added to both reactions (Figure 4.3 B). Indeed, in the Hg^{2+} reaction, the signal went back to the background level due to HgI_2 formation, while no change was seen in the Ag^{+} reaction upon formation of AgI, proving that the sensor was irreversibly cleaved by silver ions. While Pb^{2+} showed a slight cleavage in gel-based assay, its rate is >3000-fold slower than Ag^{+}, and Pb^{2+} is a strong fluorescence quencher at high concentrations. These factors may explain the lack of Pb^{2+} response in this rate-based signaling method.

4.2.4 Testing in Lake Huron water

Further, it was tested if this sensor works in real word water samples. For this, the sensor was tested in Lake Huron water with 50 mM MOPS buffer (pH 7.5, 90 % of lake water in the final reaction, Figure 4.4 A). The response was quite similar to that obtained in clean buffers, and a LOD of 21.8 nM was calculated (Figure 4.4 B). Therefore, the lake water matrix did not interfere with the detection. The Great Lake's water often contains below 1 mM Cl^{-}, and therefore it is understandable that the sensitivity of the sensor was not affected.

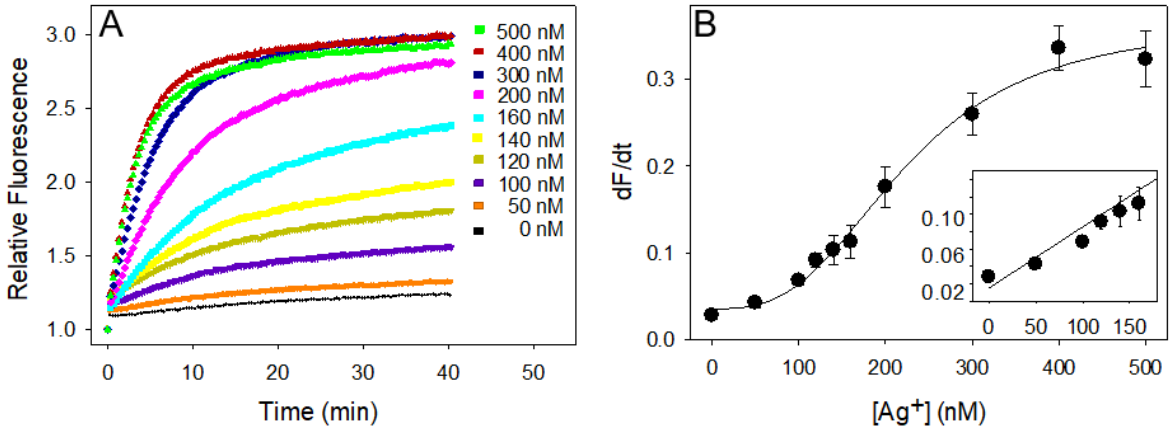

Figure 4.4 (A) Sensor signaling kinetics at various concentrations of Ag^+ spiked Ag^+ in Lake Huron water. (B) Quantification of Ag^+ based on the initial rate of fluorescence enhancement in 50 mM MOPS buffer (pH 7.5) made in Lake Huron water. The DNAzyme concentration was 50 nM for all the above experiments.

4.3 Summary

It was demonstrated that the DNAzyme Ag10c is a useful analytical probe for silver. A FRET based system was used with the DNAzyme Ag10c for developing a sensing system to detect low concentrations of Ag^+ ions. The limit of detection of the sensor was reported to be 24.9 nM, which is far below the permissible limit of silver in water. It was also confirmed that the sensor is very selective for silver ions. Finally, the robustness of the sensor was proved in real world samples by demonstrating its selectivity and sensitivity in Lake Huron's water. This study puts forth a rare example of DNAzyme beacons being used for sensing of monovalent ions. It highlights the possibility of using DNAzyme beacons for sensing transition metal ions upto low nanomolar concentrations. It further strengthens the idea of developing biosensors for on-site detection, which may also help in recovering valuable metals.

4.4 Materials and Methods

4.4.1 Chemicals

Sensing related DNA samples were from Integrated DNA Technologies (IDT, Coralville, IA). The rest of the DNAs were from Eurofins (Huntsville, AL). The sequences of DNA used are listed in Table 4.1. Metal ions that were used for analysis include silver(I) nitrate, potassium(I) chloride, lithium(I) chloride, thallium(I) chloride, lead(II) acetate, magnesium(II) sulfate, manganese(II) chloride tetrahydrate, iron(II) chloride tetrahydrate, cobalt(II) chloride hexahydrate, copper(II) chloride dehydrate, zinc(II) chloride, calcium(II) chloride, nickel(II) chloride, strontium(II) chloride, cadmium(II) chloride, mercury(II) perchlorate, yttrium(III) chloride hexahydrate, gallium(III) chloride, cerium(III) chloride, iron(III) chloride hexahydrate. All these salts were purchased from Sigma-Aldrich except the iron and silver salts were purchased from Alfa Aesar. The purity of the metals used is 99.99 %. Their solutions were made by directly dissolving their salts in Milli-Q water. 3-(*N*-morpholino) propanesulfonic acid (MOPS) was from Mandel Scientific Inc. (Guelph, Ontario, Canada).

Table 4.1 List of DNA sequences used in chapter 4.

DNA	Sequence (5′-3′)
5'-FAM-Sub	FAM-CTCACTATrAGGAAGATGGCGAAGC

Ag10c-Q	GCTTCGCCATCTTTAGGTGATTTCCACGATTATGCGGAAACAGGGC AGCGTATAGTGAG-BHQ1

4.4.2 Fluorescence-based Ag^+ sensing

Sensor signaling kinetics were measured in 96-well plates using a microplate reader (SpectraMax M3). The sensing complex was formed by annealing 5′-FAM-Sub (10 μM) and the quencher-labeled enzyme (Ag10c-Q, 20 μM) in buffer (50 mM MOPS, pH 7.0 with 25 mM $NaNO_3$). 100 μl of 50 nM FAM-Q DNAzyme in 50 mM MOPS (pH 7.5, 200 mM $NaNO_3$) was used for each well. A 2 μL amount of target ions was added to initiate the cleavage reaction after 5 min of background reading. Samples were continuously monitored after addition for at least 30 min with 20 sec intervals. For the reaction with NaI, a final concentration of 10 μM NaI was used.

5. Chapter 5 – Summary and Future work

5.1 Summary

Owing to its serviceable properties such as reversible denaturation, high sequence programmability, amphipathic nature, and high stability, deoxyribonucleic acid (DNA) has been well recognized as a generic material along with being the genetic material. The catalytic potential embedded in DNA has been uncovered with the isolation of DNAzymes (catalytic DNA sequences). Among these, the RNA-cleaving DNAzymes can cleave a specific RNA bond in the presence of a selective cofactor. Multi and monovalent cations give rise to very interesting interactions with DNA, and act as excellent cofactors for DNAzyme catalysis. Within this thesis I explored the evolution and characterization of an Ag^+-dependent RNA-cleaving DNAzyme.

The research work presented in this thesis, begins with Chapter 2 which describes an Ag^+-dependent *in-vitro* selection. This experiment resulted into the very first occurrence of a monovalent transition metal Ag^+-dependent RNA-cleaving DNAzyme, called Ag10c. It was also reported that Ag10c is shown to achieve a catalytic rate of 0.41 min^{-1} with just 10 µM Ag^+, which is the highest reported till now in the category of monovalent ion dependent RNA-cleaving DNAzymes. Subsequently, the DNAzyme Ag10c was shown to exhibit remarkable selectivity for silver ions, amongst all the other metal ions tested.

Many interesting observations were made in chapter 3, from detailed biochemical characterization of the Ag10c DNAzyme. Systematic mutation studies were carried out to confirm that Ag10c has a well-defined secondary structure, and most of the nucleotides in its catalytic loop are important for activity and cannot be randomly changed. Using DMS

footprinting, it was confirmed that the Ag10c catalytic loop bears a well-defined silver aptamer that can fold into a compact structure by binding Ag^+. This work has provided a new aptamer for Ag^+ and this aptamer is completely different from the well-known C-Ag^+-C structure.[243] This was confirmed by mutation studies, which strongly argue against the formation of any C-Ag^+-C base pair. Further, fundamental mechanistic studies have been reported which helped in gaining insights into Ag10c catalysis. Ag^+-dependent activity assays were performed to rationalize the role of Ag^+. It was established that the Ag10c DNAzyme uses two metals for catalysis: one Na^+ (or other group 1A metals or Mg^{2+}) binds to the pro-R_p oxygen of the scissile phosphate, and two Ag^+ ions bind cooperatively to Ag10c aptamer loop. It was demonstrated that Ag10c undergoes a single deprotonation step during catalysis. Further, 2AP fluorescence experiments have been described, which were undertaken to study the folding of the Ag^+-specific RNA-cleavage Ag10c DNAzyme. Local folding was observed by increased 2AP fluorescence at the dinucleotide junction of Ag10c, while none of the inactive mutants exhibited such a response at the same 2AP position. In addition, Ag^+ also induced a rise in 2AP fluorescence when labeled at the enzyme loop (the A9 position), while other metals did not give such a fluorescence increase. Specific aptamer binding was confirmed with the help of control experiments with mutated Ag10c and inactive metals. It was concluded that the substrate cleavage site remains unpaired in the absence of Ag^+. Upon addition of Ag^+, T18 gets involved in the Ag^+ binding pocket leading to increased 2AP fluorescence at the cleavage site. Therefore, the cleavage site and the A9 position, both undergo a conformational change from stacked to less stacked, upon Ag^+ binding.

It was demonstrated in chapter 4, that the DNAzyme Ag10c is a useful analytical probe for silver. A FRET based system was used with Ag10c for sensing low concentrations of Ag^+ ions. The limit of detection of the sensor was demonstrated to be 24.9 nM, which is far below the permissible limit of silver in water. It was also confirmed that the sensor is very selective for silver ions. The robustness of the sensor in real world samples was proved by demonstrating its high selectivity and sensitivity in Lake Huron's water. This study puts forth a rare example of DNAzyme beacons being used for sensing of monovalent ions.

5.2 Original Contributions

The research work presented herein, offers various insights into DNAzyme discovery and catalysis, as well as DNAzyme-based metal sensing. At the same time, the outcomes of this study foster the development of innovative strategies for obtaining novel DNAzymes, aptamers and biosensors.

Firstly, I have discovered a novel RNA-cleaving DNAzyme Ag10c, which is dependent on the monovalent transition metal ion Ag^+, for its activity. Among the array of DNAzymes known previously, all the RNA cleaving DNAzymes which are dependent on thiophilic metal ions e.g. Hg^{2+},[121] Cd^{2+}, and Cu^{2+},[98,99,226] for their activity, required non-canonical DNA modifications e.g. phosphorothioate (PS) bond at the scissile phosphate, modified nucleotide bases, etc. In spite of Ag^+ being a thiophilic metal ion, no such modification was required for Ag10c catalysis. Therefore, with this study, the first in vitro-selected unmodified RNA-cleaving DNAzyme that cleaves efficiently in the presence of a thiophilic metal was reported. This study

leverages the possibility of selecting DNAzymes for soft thiophilic metals using the natural RNA dinucleotide cleavage junction.

Secondly, my research work reports the fastest DNAzyme kinetics till now in the category of monovalent ion dependent RNA cleaving DNAzymes i.e. 0.4 min^{-1} at 10 μM Ag^{+}. The previously known Na^{+}-dependent DNAzymes have much slower rates at much higher Na^{+} concentration.[104,215,216] This study dedicates a much needed attention at the role of monovalent ions in DNAzyme catalysis.

Thirdly, through this research I have discovered a novel Ag^{+} aptamer embedded in the catalytic loop of Ag10c. The isolation of metal ion specific nucleic acid aptamers is difficult through SELEX as it is tricky to immobilize the metal ions. Therefore their occurrence is rare. As far as aptamers embedded in DNAzymes are concerned, there are only two examples, the NaA43 and Ce13d DNAzymes,[101,104] both consisting of Na^{+} binding aptamer.[129,130,234,235] No such aptamer bearing DNAzyme exists for thiophilic or transition metal ions, apart from Ag10c. This contribution not only expands the repertoire of metal ion specific aptamers, it floats an elegant strategy to discover novel aptamers, especially for thiophilic or transition metal ions.

Fourthly, within this research, I have reported a novel and specific interaction of Ag^{+} with DNA, which is free from the well-known C-Ag^{+}-C base pairing.[172,173] . This fact supports the possibility of exploring novel metal-nucleotide interactions and furnishes the option of using these new interactions in application oriented research problems.

Fifthly, I have reported a new theme of RNA-cleaving DNAzyme catalysis that may be used by soft metals to escape interaction with the scissile phosphate and yet confer effective catalysis. Interestingly mechanism of Ag10c involves a group 1A metal ion or Mg^{2+} interacting

with the scissile RNA phosphate, and two Ag^+ ions binding cooperatively to Ag10c aptamer loop and conferring local folding of the aptamer into a more compact structure. The only previous example of a similar mechanism is Ce13d DNAzyme, which uses Ce^{3+} (or other lanthanides) to bind to the cleavage dinucleotide phosphate, and it also has an aptamer loop for Na^+.[129] Such a fundamental understanding, has opened up the platform to explore and select novel soft metal-dependent DNAzymes.

Lastly, I have developed a new fluorescence based biosensor for Ag^+ which selectively and sensitively detects aqueous Ag^+ with a LOD of 24.9 nM. This biosensor relies on the specific interaction between Ag^+ and its specific aptamer, while most of the previous biosensors depend on Ag^+ mediated base pairs.[173] The proof of the robustness of this biosensor in Lake Huron's water, endorses the exploration of this novel interaction in more real world applications.

5.3 Future Work

The research work presented in this thesis stages multiple aspects that can be potentially investigated in greater detail. It also offers multiple new schemes that can be utilized to design and execute effective strategies in the future.

Firstly, the presence of an Ag^+ aptamer within the Ag10c loop, is a perfect opportunity to work towards the extraction of a standalone Ag^+ aptamer. As mentioned before, the occurrence of metal ion specific aptamers is rare. With the background knowledge regarding Ag10c folding studies carried out in this research work, it will be easier to develop strategies

(e.g. use of fluorescent or colorimetric dyes) to confirm if the extracted sequence folds adequately upon Ag^+ binding. Development of such an aptamer would prove to be very beneficial in gaining a deeper insight into the interactions between Ag^+ and DNA. Alongside, silver is an important analyte, and such a standalone aptamer would be very useful in crafting folding-based Ag^+ biosensors.

Secondly, the discovery of Ag10c has fished out a template DNAzyme which can be used to build a reselection library for evolving new metal ion specific RNA-cleaving DNAzymes. Re-selection is a prudent method, in which the DNA library is designed by introducing variations in previously known DNAzyme sequences. Tactical variations in selection parameters like cofactor concentration, library-cofactor incubation time, pH, temperature, etc. can foster the evolution of more rapid, sensitive, selective Ag^+/ other thiophilic/ transition metal-dependent DNAzymes. For real-world application needs like biomedical diagnostics or chemical sensing, this method can also be used to focus on evolving DNAzymes which are capable of working in more stringent/relaxed conditions of real-world samples e.g. blood serum, lake waters, etc.

Thirdly, as mentioned before, this study stages a new theme of DNAzyme catalysis, which can be effectively used to design specific selection conditions for obtaining soft metal-dependent DNAzymes and aptamers. In this scheme, a group 1A or Mg^{2+} metal ion acts at the scissile phosphate while the soft metal Ag^+ interacts with the nucleotides in the catalytic loop. By intentionally setting relevant selection conditions e.g. use of high salt concentration, etc. soft metals can be made to escape interaction with the scissile phosphate and yet confer effective

catalysis. This work will open up multiple possibilities of discovering novel soft metal-dependent DNAzymes and soft metal specific aptamers embedded in DNAzymes.

Lastly, from the purview of fundamental science, there is still scope for a deeper understanding of the mechanism of cleavage conferred by Ag10c. Time-resolved techniques e.g. singe molecule fluorescence experiments, can be applied to decipher the detailed progress of the conformational changes taking place in the DNAzyme as the reaction proceeds. To know the exact structural changes at high resolution, Nuclear Magnetic Resonance (NMR) or X-Ray Diffraction (XRD) of single crystals can be pursued. Such kind of an extensive study would prove to be very helpful in enhancing the general understanding of RNA cleaving DNAzyme catalysis, and also provide a strong grasp of the interactions between Ag^+ and DNA.

Bibliography

(1) Izatt, R. M.; Christensen, J. J.; Rytting, J. H. Sites and Thermodynamic Quantities Associated with Proton and Metal Ion Interaction with Ribonucleic Acid, Deoxyribonucleic Acid, and Their Constituent Bases, Nucleosides, and Nucleotides. *Chem. Rev.* **1971**, *71* (5), 439–481.

(2) Sigel, H. Interactions of Metal Ions with Nucleotides and Nucleic Acids and Their Constituents. *Chem. Soc. Rev.* **1993**, *22* (4), 255.

(3) Sigel, R. K. O.; Sigel, H. A Stability Concept for Metal Ion Coordination to Single-Stranded Nucleic Acids and Affinities of Individual Sites. *Acc. Chem. Res.* **2010**, *43* (7), 974–984.

(4) Freisinger, E.; Sigel, R. K. O. From Nucleotides to Ribozymes—A Comparison of Their Metal Ion Binding Properties. *Coord. Chem. Rev.* **2007**, *251* (13–14), 1834–1851.

(5) Pechlaner, M.; Sigel, R. K. O. Characterization of Metal Ion-Nucleic Acid Interactions in Solution; 2012; pp 1–42.

(6) Sigel, H.; Griesser, R. Nucleoside 5′-Triphosphates: Self-Association, Acid–base, and Metal Ion-Binding Properties in Solution. *Chem. Soc. Rev.* **2005**, *34* (10), 875.

(7) Miyake, Y.; Togashi, H.; Tashiro, M.; Yamaguchi, H.; Oda, S.; Kudo, M.; Tanaka, Y.; Kondo, Y.; Sawa, R.; Fujimoto, T.; et al. Mercury ^{II} -Mediated Formation of Thymine−Hg ^{II} −Thymine Base Pairs in DNA Duplexes. *J. Am. Chem. Soc.* **2006**, *128* (7), 2172–2173.

(8) Reedijk, J. Why Does Cisplatin Reach Guanine-N7 with Competing S-Donor Ligands Available in the Cell? *Chem. Rev.* **1999**, *99* (9), 2499–2510.

(9) Wrobel, K. K.; Rodriguez Flores, C.; Chan, Q.; Wrobel, K. K.; Rodríguez Flores, C.; Chan, Q.; Wrobel, K. K. Ribonucleoside Labeling with Os(VI): A Methodological Approach to Evaluation of RNA Methylation by HPLC-ICP-MS. *Metallomics* **2010**, *2* (2), 140–146.

(10) Trefulka, M.; Bartošík, M.; Paleček, E. Facile End-Labeling of RNA with Electroactive Os(VI)

Complexes. *Electrochem. commun.* **2010**, *12* (12), 1760–1763.

(11) Che, Y.; Yang, X.; Zang, L. Ultraselective Fluorescent Sensing of Hg2+ through Metal Coordination-Induced Molecular Aggregation. *Chem. Commun.* **2008**, No. 12, 1413.

(12) Helm, L.; Merbach, A. E. Inorganic and Bioinorganic Solvent Exchange Mechanisms. *Chem. Rev.* **2005**, *105* (6), 1923–1960.

(13) Reedijk, J. Metal-Ligand Exchange Kinetics in Platinum and Ruthenium Complexes SIGNIFICANCE FOR EFFECTIVENESS AS ANTICANCER DRUGS. *Platin. Met. Rev.* **2008**, *52* (1), 2–11.

(14) Tuerk, C.; Gold, L. Systematic Evolution of Ligands by Exponential Enrichment: RNA Ligands to Bacteriophage T4 DNA Polymerase. *Science (80-.).* **1990**, *249* (4968), 505–510.

(15) Ellington, A. D.; Szostak, J. W. In Vitro Selection of RNA Molecules That Bind Specific Ligands. *Nature* **1990**, *346* (6287), 818–822.

(16) Nutiu, R.; Li, Y. In Vitro Selection of Structure-Switching Signaling Aptamers. *Angew. Chemie - Int. Ed.* **2005**, *44* (7), 1061–1065.

(17) Rajendran, M.; Ellington, A. D. Selection of Fluorescent Aptamer Beacons That Light up in the Presence of Zinc. *Anal. Bioanal. Chem.* **2008**, *390* (4), 1067–1075.

(18) Wang, H.; Cheng, H.; Wang, J.; Xu, L.; Chen, H.; Pei, R. Selection and Characterization of DNA Aptamers for the Development of Light-up Biosensor to Detect Cd(II). *Talanta* **2016**, *154*, 498–503.

(19) Wu, Y.; Zhan, S.; Wang, L.; Zhou, P. Selection of a DNA Aptamer for Cadmium Detection Based on Cationic Polymer Mediated Aggregation of Gold Nanoparticles. *Analyst* **2014**, *139* (6), 1550–1561.

(20) Qu, H.; Csordas, A. T.; Wang, J.; Oh, S. S.; Eisenstein, M. S.; Soh, H. T. Rapid and Label-Free Strategy to Isolate Aptamers for Metal Ions. *ACS Nano* **2016**, *10* (8), 7558–7565.

(21) Sun, H.; Chen, H.; Zhang, X.; Liu, Y.; Guan, A.; Li, Q.; Yang, Q.; Shi, Y.; Xu, S.; Tang, Y. Colorimetric Detection of Sodium Ion in Serum Based on the G-Quadruplex Conformation Related DNAzyme Activity. *Anal. Chim. Acta* **2016**, *912*, 133–138.

(22) Bhattacharyya, D.; Arachchilage, G. M.; Basu, S. Metal Cations in G-Quadruplex Folding and Stability. *Front. Chem.* **2016**, *4*, UNSP 38.

(23) Mekmaysy, C. S.; Petraccone, L.; Garbett, N. C.; Ragazzon, P. A.; Gray, R.; Trent, J. O.; Chaires, J. B. Effect of O(6)-Methylguanine on the Stability of G-Quadruplex. *J. Am. Chem. Soc.* **2008**, *130* (21), 6710–+.

(24) Caceres, C.; Wright, G.; Gouyette, C.; Parkinson, G.; Subirana, J. A. A Thymine Tetrad in d(TGGGGT) Quadruplexes Stabilized with Tl+/Na+ Ions. *Nucleic Acids Res.* **2004**, *32* (3), 1097–1102.

(25) Gill, M. L.; Strobel, S. A.; Loria, J. P. (TI)-T-205 NMR Methods for the Characterization of Monovalent Cation Binding to Nucleic Acids. *J. Am. Chem. Soc.* **2005**, *127* (47), 16723–16732.

(26) Gill, M. L.; Strobel, S. A.; Loria, J. P. Crystallization and Characterization of the Thallium Form of the Oxytricha Nova G-Quadruplex. *Nucleic Acids Res.* **2006**, *34* (16), 4506–4514.

(27) Wong, A.; Ida, R.; Wu, G. Direct NMR Detection of the "Invisible" Alkali Metal Cations Tightly Bound to G-Quadruplex Structures. *Biochem. Biophys. Res. Commun.* **2005**, *337* (1), 363–366.

(28) Hud, N. V; Schultze, P.; Sklenar, V.; Feigon, J. Binding Sites and Dynamics of Ammonium Ions in a Telomere Repeat DNA Quadruplex. *J. Mol. Biol.* **1999**, *285* (1), 233–243.

(29) Kankia, B. I.; Marky, L. A. Folding of the Thrombin Aptamer into a G-Quadruplex with Sr2+: Stability, Heat, and Hydration. *J. Am. Chem. Soc.* **2001**, *123* (44), 10799–10804.

(30) Chen, F. M. Sr2+ Facilitates Intermolecular G-Quadruplex Formation of Telomeric Sequences. *Biochemistry* **1992**, *31* (15), 3769–3776.

(31) Shi, X. D.; Fettinger, J. C.; Davis, J. T. Homochiral G-Quadruplexes with Ba2+ but Not with

K+: The Cation Programs Enantiomeric Self-Recognition. *J. Am. Chem. Soc.* **2001**, *123* (27), 6738–6739.

(32) Qu, K.; Zhao, C.; Ren, J.; Qu, X. Human Telomeric G-Quadruplex Formation and Highly Selective Fluorescence Detection of Toxic Strontium Ions. *Mol. Biosyst.* **2012**, *8* (3), 779–782.

(33) Yang, C.; Liu, L.; Zeng, T.; Yang, D.; Yao, Z.; Zhao, Y.; Wu, H.-C. Highly Sensitive Simultaneous Detection of Lead(II) and Barium(II) with G-Quadruplex DNA in Alpha-Hemolysin Nanopore. *Anal. Chem.* **2013**, *85* (15), 7302–7307.

(34) Leung, K.-H.; Ma, V. P.-Y.; He, H.-Z.; Chan, D. S.-H.; Yang, H.; Leung, C.-H.; Ma, D.-L. A Highly Selective G-Quadruplex-Based Luminescent Switch-on Probe for the Detection of Nanomolar Strontium(II) Ions in Sea Water. *Rsc Adv.* **2012**, *2* (22), 8273–8276.

(35) Ciesiolka, J.; Gorski, J.; Yarus, M. Selection of an Rna Domain That Binds Zn2+. *Rna-a Publ. Rna Soc.* **1995**, *1* (5), 538–550.

(36) Ciesiolka, J.; Yarus, M. Small RNA-Divalent Domains. *Rna-a Publ. Rna Soc.* **1996**, *2* (8), 785–793.

(37) Kawakami, J.; Imanaka, H.; Yokota, Y.; Sugimoto, N. In Vitro Selection of Aptamers That Act with Zn2+. *J. Inorg. Biochem.* **2000**, *82* (1–4), 197–206.

(38) Hofmann, H. P.; Limmer, S.; Hornung, V.; Sprinzl, M. Ni2+-Binding RNA Motifs with an Asymmetric Purine-Rich Internal Loop and a G-A Base Pair. *Rna-a Publ. Rna Soc.* **1997**, *3* (11), 1289–1300.

(39) Knobloch, B.; Sigel, H. A Quantitative Appraisal of the Ambivalent Metal Ion Binding Properties of Cytidine in Aqueous Solution and an Estimation of the Anti-Syn Energy Barrier of Cytidine Derivatives. *J. Biol. Inorg. Chem.* **2004**, *9* (3), 365–373.

(40) Da Costa, C. P.; Sigel, H. Acid-Base and Metal Ion Binding Properties of Guanylyl(3 '-> 5 ')Guanosine (GpG(-)) and 2 '-Deoxyguanylyl(3 '-5 ')-2 '-Deoxyguanosine [d(GpG)(-)] in

Aqueous Solution. *Inorg. Chem.* **2003**, *42* (11), 3475–3482.

(41) Nishiyabu, R.; Hashimoto, N.; Cho, T.; Watanabe, K.; Yasunaga, T.; Endo, A.; Kaneko, K.; Niidome, T.; Murata, M.; Adachi, C.; et al. Nanoparticles of Adaptive Supramolecular Networks Self-Assembled from Nucleotides and Lanthanide Ions. *J. Am. Chem. Soc.* **2009**, *131* (6), 2151–2158.

(42) Zhou, W.; Saran, R.; Liu, J. Metal Sensing by DNA. *Chem. Rev.* **2017**, *117* (12), 8272–8325.

(43) Hoang, M.; Huang, P.-J. J.; Liu, J. G-Quadruplex DNA for Fluorescent and Colorimetric Detection of Thallium(I). *Acs Sensors* **2016**, *1* (2), 137–143.

(44) Torigoe, H.; Okamoto, I.; Dairaku, T.; Tanaka, Y.; Ono, A.; Kozasa, T. Thermodynamic and Structural Properties of the Specific Binding between Ag+ Ion and C:C Mismatched Base Pair in Duplex DNA to Form C-Ag-C Metal-Mediated Base Pair. *Biochimie* **2012**, *94* (11), 2431–2440.

(45) Torigoe, H.; Ono, A.; Kozasa, T. Hg-II Ion Specifically Binds with T:T Mismatched Base Pair in Duplex DNA. *Chem. Eur. J.* **2010**, *16* (44), 13218–13225.

(46) Zhou, W.; Ding, J.; Liu, J. 2-Aminopurine-Modified DNA Homopolymers for Robust and Sensitive Detection of Mercury and Silver. *Biosens. Bioelectron.* **2017**, *87*, 171–177.

(47) Kruger, K.; Grabowski, P. J.; Zaug, A. J.; Sands, J.; Gottschling, D. E.; Cech, T. R. Self-Splicing RNA: Autoexcision and Autocyclization of the Ribosomal RNA Intervening Sequence of Tetrahymena. *Cell* **1982**, *31* (1), 147–157.

(48) Golden, B. L. Two Distinct Catalytic Strategies in the Hepatitis Delta Virus Ribozyme Cleavage Reaction. *Biochemistry* **2011**, *50* (44), 9424–9433.

(49) Lai, M. M. C. The Molecular Biology of Hepatitis Delta Virus. *Annu. Rev. Biochem.* **1995**, *64* (1), 259–286.

(50) Ferre-D'Amare, A. R.; Scott, W. G. Small Self-Cleaving Ribozymes. *Cold Spring Harb.*

Perspect. Biol. **2010**, *2* (10), a003574–a003574.

(51) Winkler, W. C.; Nahvi, A.; Roth, A.; Collins, J. A.; Breaker, R. R. Control of Gene Expression by a Natural Metabolite-Responsive Ribozyme. *Nature* **2004**, *428* (6980), 281–286.

(52) Ferré-D'Amaré, A. R. The Hairpin Ribozyme. *Biopolymers* **2004**, *73* (1), 71–78.

(53) Fedor, M. J. Structure and Function of the Hairpin Ribozyme. *J. Mol. Biol.* **2000**, *297* (2), 269–291.

(54) Guo, H. C.; Collins, R. A. Efficient Trans-Cleavage of a Stem-Loop RNA Substrate by a Ribozyme Derived from Neurospora VS RNA. *EMBO J.* **1995**, *14* (2), 368–376.

(55) Kennell, J. C.; Saville, B. J.; Mohr, S.; Kuiper, M. T.; Sabourin, J. R.; Collins, R. A.; Lambowitz, A. M. The VS Catalytic RNA Replicates by Reverse Transcription as a Satellite of a Retroplasmid. *Genes Dev.* **1995**, *9* (3), 294–303.

(56) Haugen, P.; Simon, D. M.; Bhattacharya, D. The Natural History of Group I Introns. *Trends Genet.* **2005**, *21* (2), 111–119.

(57) Eskes, R.; Liu, L.; Ma, H.; Chao, M. Y.; Dickson, L.; Lambowitz, A. M.; Perlman, P. S. Multiple Homing Pathways Used by Yeast Mitochondrial Group II Introns. *Mol. Cell. Biol.* **2000**, *20* (22), 8432–8446.

(58) Guo, H.; Karberg, M.; Long, M.; Jones, J. P.; Sullenger, B.; Lambowitz, A. M. Group II Introns Designed to Insert into Therapeutically Relevant DNA Target Sites in Human Cells. *Science* **2000**, *289* (5478), 452–457.

(59) Mondragón, A. Structural Studies of RNase P. *Annu. Rev. Biophys.* **2013**, *42* (1), 537–557.

(60) Guerrier-Takada, C.; Gardiner, K.; Marsh, T.; Pace, N.; Altman, S. The RNA Moiety of Ribonuclease P Is the Catalytic Subunit of the Enzyme. *Cell* **1983**, *35* (3 Pt 2), 849–857.

(61) Beebe, J. A.; Kurz, J. C.; Fierke, C. A. Magnesium Ions Are Required by *Bacillus Subtilis* Ribonuclease P RNA for Both Binding and Cleaving Precursor TRNA ^{Asp} †. *Biochemistry* **1996**,

35 (32), 10493–10505.

(62) Pan, T. Higher Order Folding and Domain Analysis of the Ribozyme from Bacillus Subtilis Ribonuclease P. *Biochemistry* **1995**, *34* (3), 902–909.

(63) Shechner, D. M.; Grant, R. A.; Bagby, S. C.; Koldobskaya, Y.; Piccirilli, J. A.; Bartel, D. P. Crystal Structure of the Catalytic Core of an RNA-Polymerase Ribozyme. *Science (80-.).* **2009**, *326* (5957), 1271–1275.

(64) Wochner, A.; Attwater, J.; Coulson, A.; Holliger, P. Ribozyme-Catalyzed Transcription of an Active Ribozyme. *Science (80-.).* **2011**, *332* (6026), 209–212.

(65) Biondi, E.; Poudyal, R. R.; Forgy, J. C.; Sawyer, A. W.; Maxwell, A. W. R.; Burke, D. H. Lewis Acid Catalysis of Phosphoryl Transfer from a Copper(II)-NTP Complex in a Kinase Ribozyme. *Nucleic Acids Res.* **2013**, *41* (5), 3327–3338.

(66) Seelig, B.; Jäschke, A. A Small Catalytic RNA Motif with Diels-Alderase Activity. *Chem. Biol.* **1999**, *6* (3), 167–176.

(67) Breaker, R. R.; Joyce, G. F. A DNA Enzyme That Cleaves RNA. *Chem. Biol.* **1994**, *1* (4), 223–229.

(68) Flynn-charlebois, A.; Prior, T. K.; Hoadley, K. A.; Silverman, S. K. In Vitro Evolution of an RNA-Cleaving DNA Enzyme into an RNA Ligase Switches the Selectivity from 3 ′ -5 ′ to 2 ′ -5 ′ In Vitro Evolution of RNA Ligase Deoxyribozymes . Using. *Jacs* **2003**, No. c, 5346–5350.

(69) Flynn-Charlebois, A.; Wang, Y. M.; Prior, T. K.; Rashid, I.; Hoadley, K. A.; Coppins, R. L.; Wolf, A. C.; Silverman, S. K. Deoxyribozymes with 2 ’-5 ’ RNA Ligase Activity. *J. Am. Chem. Soc.* **2003**, *125* (9), 2444–2454.

(70) Purtha, W. E.; Coppins, R. L.; Smalley, M. K.; Silverman, S. K. General Deoxyribozyme-Catalyzed Synthesis of Native 3 ’-5 ’ RNA Linkages. *J. Am. Chem. Soc.* **2005**, *127* (38), 13124–13125.

(71) Coppins, R. L.; Silverman, S. K. A Deoxyribozyme That Forms a Three-Helix-Junction Complex with Its RNA Substrates and Has General RNA Branch-Forming Activity. *J. Am. Chem. Soc.* **2005**, *127* (9), 2900–2907.

(72) Wang, Y. M.; Silverman, S. K. Deoxyribozymes That Synthesize Branched and Lariat RNA. *J. Am. Chem. Soc.* **2003**, *125* (23), 6880–6881.

(73) Pratico, E. D.; Wang, Y.; Silverman, S. K. A Deoxyribozyme That Synthesizes 2',5'-Branched RNA with Any Branch-Site Nucleotide. *Nucleic Acids Res.* **2005**, *33* (11), 3503–3512.

(74) Wang, Y.; Silverman, S. K. Efficient One-Step Synthesis of Biologically Related Lariat RNAs by a Deoxyribozyme. *Angew. Chemie Int. Ed.* **2005**, *44* (36), 5863–5866.

(75) Höbartner, C.; Pradeepkumar, P. I.; Silverman, S. K. Site-Selective Depurination by a Periodate-Dependent Deoxyribozyme. *Chem. Commun.* **2007**, No. 22, 2255–2257.

(76) Sheppard, T. L.; Ordoukhanian, P.; Joyce, G. F. A DNA Enzyme with N-Glycosylase Activity. *Proc. Natl. Acad. Sci.* **2000**, *97* (14), 7802–7807.

(77) Carmi, N.; Shultz, L. A.; Breaker, R. R. In Vitro Selection of Self-Cleaving DNAs. *Chem. Biol.* **1996**, *3* (12), 1039–1046.

(78) Carmi, N.; Balkhi, S. R.; Breaker, R. R. Cleaving DNA with DNA. *Proc. Natl. Acad. Sci. U. S. A.* **1998**, *95* (5), 2233–2237.

(79) Carmi, N.; Breaker, R. R. Characterization of a DNA-Cleaving Deoxyribozyme. *Bioorg. Med. Chem.* **2001**, *9* (10), 2589–2600.

(80) Cuenoud, B.; Szostak, J. W. A DNA Metalloenzyme with DNA Ligase Activity. *Nature* **1995**, *375* (6532), 611–614.

(81) Sreedhara, A.; Li, Y.; Breaker, R. R. Ligating DNA with DNA. *J. Am. Chem. Soc.* **2004**, *126* (11), 3454–3460.

(82) Mui, T. P.; Silverman, S. K. Convergent and General One-Step DNA-Catalyzed Synthesis of

Multiply Branched DNA. *Org. Lett.* **2008**, *10* (20), 4417–4420.

(83) Levy, M.; Ellington, A. D. In Vitro Selection of a Deoxyribozyme That Can Utilize Multiple Substrates. *J. Mol. Evol.* **2002**, *54* (2), 180–190.

(84) Levy, M.; Ellington, A. D. Selection of Deoxyribozyme Ligases That Catalyze the Formation of an Unnatural Internucleotide Linkage. *Bioorg. Med. Chem.* **2001**, *9* (10), 2581–2587.

(85) Li, Y.; Breaker, R. R. Phosphorylating DNA with DNA. *Proc. Natl. Acad. Sci.* **1999**, *96* (6), 2746–2751.

(86) McManus, S. A.; Li, Y. Multiple Occurrences of an Efficient Self-Phosphorylating Deoxyribozyme Motif †. *Biochemistry* **2007**, *46* (8), 2198–2204.

(87) Wang, W.; Billen, L. P.; Li, Y. F. Sequence Diversity, Metal Specificity, and Catalytic Proficiency of Metal-Dependent Phosphorylating DNA Enzymes. *Chem. Biol.* **2002**, *9* (4), 507–517.

(88) Li, Y.; Liu, Y.; Breaker, R. R. Capping DNA with DNA †. *Biochemistry* **2000**, *39* (11), 3106–3114.

(89) Burmeister, J.; von Kiedrowski, G.; Ellington, A. D. Cofactor-Assisted Self-Cleavage in DNA Libraries with a 3′–5′-Phosphoramidate Bond. *Angew. Chemie Int. Ed. English* **1997**, *36* (12), 1321–1324.

(90) Li, Y. F.; Sen, D. A Catalytic DNA for Porphyrin Metallation. *Nat. Struct. Biol.* **1996**, *3* (9), 743–747.

(91) Travascio, P.; Bennet, A. J.; Wang, D. Y.; Sen, D. A Ribozyme and a Catalytic DNA with Peroxidase Activity: Active Sites versus Cofactor-Binding Sites. *Chem. Biol.* **1999**, *6* (11), 779–787.

(92) Travascio, P.; Li, Y.; Sen, D. DNA-Enhanced Peroxidase Activity of a DNA-Aptamer-Hemin Complex. *Chem. Biol.* **1998**, *5* (9), 505–517.

(93) Chinnapen, D. J.-F.; Sen, D. A Deoxyribozyme That Harnesses Light to Repair Thymine Dimers in DNA. *Proc. Natl. Acad. Sci.* **2004**, *101* (1), 65–69.

(94) Pradeepkumar, P. I.; Höbartner, C.; Baum, D. A.; Silverman, S. K. DNA-Catalyzed Formation of Nucleopeptide Linkages. *Angew. Chemie Int. Ed.* **2008**, *47* (9), 1753–1757.

(95) Chandra, M.; Silverman, S. K. DNA and RNA Can Be Equally Efficient Catalysts for Carbon−Carbon Bond Formation. *J. Am. Chem. Soc.* **2008**, *130* (10), 2936–2937.

(96) Silverman, S. K. In Vitro Selection, Characterization, and Application of Deoxyribozymes That Cleave RNA. *Nucleic Acids Res.* **2005**, *33* (19), 6151–6163.

(97) Liu, J.; Brown, A. K.; Meng, X.; Cropek, D. M.; Istok, J. D.; Watson, D. B.; Lu, Y. A Catalytic Beacon Sensor for Uranium with Parts-per-Trillion Sensitivity and Millionfold Selectivity. *Proc. Natl. Acad. Sci. U. S. A.* **2007**, *104* (7), 2056–2061.

(98) Huang, P.-J. J.; Liu, J. Rational Evolution of Cd^{2+} -Specific DNAzymes with Phosphorothioate Modified Cleavage Junction and Cd^{2+} Sensing. *Nucleic Acids Res.* **2015**, *43* (12), 6125–6133.

(99) Huang, P.-J. J.; Liu, J. An Ultrasensitive Light-up Cu^{2+} Biosensor Using a New DNAzyme Cleaving a Phosphorothioate-Modified Substrate. *Anal. Chem.* **2016**, *88* (6), 3341–3347.

(100) Bruesehoff, P. J.; Li, J.; Angustine, A. J.; Lu, Y. Improving Metal Ion Specificity during in Vitro Selection of Catalytic DNA. *Comb. Chem. High Throughput Screen.* **2002**, *5* (4), 327–335.

(101) Huang, P.-J. J.; Lin, J.; Cao, J.; Vazin, M.; Liu, J. Ultrasensitive DNAzyme Beacon for Lanthanides and Metal Speciation. *Anal. Chem.* **2014**, *86* (3), 1816–1821.

(102) Ward, W. L.; Plakos, K.; DeRose, V. J. Nucleic Acid Catalysis: Metals, Nucleobases, and Other Cofactors. *Chem. Rev.* **2014**, *114* (8), 4318–4342.

(103) Zhou, W.; Saran, R.; Chen, Q.; Ding, J.; Liu, J. A New Na^{+} -Dependent RNA-Cleaving DNAzyme with over 1000-Fold Rate Acceleration by Ethanol. *ChemBioChem* **2016**, *17* (2), 159–163.

(104) Torabi, S.-F.; Wu, P.; McGhee, C. E.; Chen, L.; Hwang, K.; Zheng, N.; Cheng, J.; Lu, Y. In Vitro Selection of a Sodium-Specific DNAzyme and Its Application in Intracellular Sensing. *Proc. Natl. Acad. Sci. U. S. A.* **2015**, *112* (19), 5903–5908.

(105) Zhou, W.; Saran, R.; Chen, Q.; Ding, J.; Liu, J. A New Na(+)-Dependent RNA-Cleaving DNAzyme with over 1000-Fold Rate Acceleration by Ethanol. *Chembiochem* **2016**, *17* (2), 159–163.

(106) Saran, R.; Liu, J. A Comparison of Two Classic Pb^{2+}-Dependent RNA-Cleaving DNAzymes. *Inorg. Chem. Front.* **2016**, *3* (4).

(107) Zhou, W.; Zhang, Y.; Ding, J.; Liu, J. In Vitro Selection in Serum: RNA-Cleaving DNAzymes for Measuring Ca2+ and Mg2+. *Acs Sensors* **2016**, *1* (5), 600–606.

(108) Saran, R.; Chen, Q.; Liu, J. Searching for a DNAzyme Version of the Leadzyme. *J. Mol. Evol.* **2015**, *81* (5–6), 235–244.

(109) Breaker, R. R.; Joyce, G. F. A Dna Enzyme with Mg2+-Dependent Rna Phosphoesterase Activity. *Chem. Biol.* **1995**, *2* (10), 655–660.

(110) Feldman, A. R.; Sen, D. A New and Efficient DNA Enzyme for the Sequence-Specific Cleavage of RNA. *J. Mol. Biol.* **2001**, *313* (2), 283–294.

(111) Santoro, S. W.; Joyce, G. F. A General Purpose RNA-Cleaving DNA Enzyme. *Proc. Natl. Acad. Sci.* **1997**, *94* (9), 4262–4266.

(112) Li, J. In Vitro Selection and Characterization of a Highly Efficient Zn(II)-Dependent RNA-Cleaving Deoxyribozyme. *Nucleic Acids Res.* **2000**, *28* (2), 481–488.

(113) Li, J.; Lu, Y. A Highly Sensitive and Selective Catalytic DNA Biosensor for Lead Ions. *J. Am. Chem. Soc.* **2000**, *122* (42), 10466–10467.

(114) Faulhammer, D.; Famulok, M. Characterization and Divalent Metal-Ion Dependence of in Vitro Selected Deoxyribozymes Which Cleave DNA/RNA Chimeric Oligonucleotides. *J. Mol. Biol.*

1997, *269* (2), 188–202.

(115) Peracchi, A. Preferential Activation of the 8–17 Deoxyribozyme by Ca^{2+} Ions. *J. Biol. Chem.* **2000**, *275* (16), 11693–11697.

(116) Faulhammer, D.; Famulok, M. The Ca2+ Ion as a Cofactor for a Novel RNA-Cleaving Deoxyribozyme. *Angew. Chemie Int. Ed. English* **1996**, *35* (2324), 2837–2841.

(117) Cruz, R. P. G.; Withers, J. B.; Li, Y. F. Dinucleotide Junction Cleavage Versatility of 8-17 Deoxyribozyme. *Chem. Biol.* **2004**, *11* (1), 57–67.

(118) Kasprowicz, A.; Stokowa-Soltys, K.; Wrzesinski, J.; Jezowska-Bojczuk, M.; Ciesiolka, J. In Vitro Selection of Deoxyribozymes Active with Cd2+ Ions Resulting in Variants of DNAzyme 8-17. *Dalt. Trans.* **2015**, *44* (17), 8138–8149.

(119) Faulhammer, D.; Famulok, M. The Ca2+ Ion as a Cofactor for a Novel RNA-Cleaving Deoxyribozyme. *Angew. Chemie Int. Ed. English* **1996**, *35* (2324), 2837–2841.

(120) Zhou, W.; Saran, R.; Huang, P.-J. J.; Ding, J.; Liu, J. An Exceptionally Selective DNA Cooperatively Binding Two Ca^{2+} Ions. *ChemBioChem* **2017**, *18* (6), 518–522.

(121) Hollenstein, M.; Hipolito, C.; Lam, C.; Dietrich, D.; Perrin, D. M. A Highly Selective DNAzyme Sensor for Mercuric Ions. *Angew. Chemie Int. Ed.* **2008**, *47* (23), 4346–4350.

(122) Huang, P.-J. J.; Vazin, M.; Liu, J. In Vitro Selection of a New Lanthanide-Dependent DNAzyme for Ratiometric Sensing Lanthanides. *Anal. Chem.* **2014**, *86* (19), 9993–9999.

(123) Huang, P.-J. J.; Vazin, M.; Matuszek, Ż.; Liu, J. A New Heavy Lanthanide-Dependent DNAzyme Displaying Strong Metal Cooperativity and Unrescuable Phosphorothioate Effect. *Nucleic Acids Res.* **2015**, *43* (1), 461–469.

(124) Vazin, M.; Huang, P.-J. J.; Matuszek, Ż.; Liu, J. Biochemical Characterization of a Lanthanide-Dependent DNAzyme with Normal and Phosphorothioate-Modified Substrates. *Biochemistry* **2015**, *54* (39), 6132–6138.

(125) Huang, P.-J. J.; Vazin, M.; Liu, J. *In Vitro* Selection of a DNAzyme Cooperatively Binding Two Lanthanide Ions for RNA Cleavage. *Biochemistry* **2016**, *55* (17), 2518–2525.

(126) Liu, J.; Lu, Y. Rational Design of "Turn-On" Allosteric DNAzyme Catalytic Beacons for Aqueous Mercury Ions with Ultrahigh Sensitivity and Selectivity. *Angew. Chemie Int. Ed.* **2007**, *46* (40), 7587–7590.

(127) Achenbach, J. C.; Nutiu, R.; Li, Y. F. Structure-Switching Allosteric Deoxyribozymes. *Anal. Chim. Acta* **2005**, *534* (1), 41–51.

(128) Seetharaman, S.; Zivarts, M.; Sudarsan, N.; Breaker, R. R. Immobilized RNA Switches for the Analysis of Complex Chemical and Biological Mixtures. *Nat. Biotechnol.* **2001**, *19* (4), 336–341.

(129) Zhou, W.; Zhang, Y.; Huang, P.-J. J.; Ding, J.; Liu, J. A DNAzyme Requiring Two Different Metal Ions at Two Distinct Sites. *Nucleic Acids Res.* **2016**, *44* (1), 354–363.

(130) Torabi, S.-F.; Lu, Y. Identification of the Same Na(+)-Specific DNAzyme Motif from Two In Vitro Selections Under Different Conditions. *J. Mol. Evol.* **2015**, *81* (5–6), 225–234.

(131) Liu, J.; Lu, Y. Fluorescent DNAzyme Biosensors for Metal Ions Based on Catalytic Molecular Beacons. In *Fluorescent Energy Transfer Nucleic Acid Probes*; Humana Press: New Jersey, 2006; Vol. 335, pp 275–288.

(132) Liu, J. W.; Lu, Y. Improving Fluorescent DNAzyme Biosensors by Combining Inter- and Intramolecular Quenchers. *Anal. Chem.* **2003**, *75* (23), 6666–6672.

(133) Liu, J.; Lu, Y. Design of Asymmetric DNAzymes for Dynamic Control of Nanoparticle Aggregation States in Response to Chemical Stimuli. *Org. Biomol. Chem.* **2006**, *4* (18), 3435–3441.

(134) Hermann, T.; Patel, D. J. Biochemistry - Adaptive Recognition by Nucleic Acid Aptamers. *Science (80-.).* **2000**, *287* (5454), 820–825.

(135) Ueyama, H.; Takagi, M.; Takenaka, S. A Novel Potassium Sensing in Aqueous Media with a Synthetic Oligonucleotide Derivative. Fluorescence Resonance Energy Transfer Associated with Guanine Quartet-Potassium Ion Complex Formation. *J. Am. Chem. Soc.* **2002**, *124* (48), 14286–14287.

(136) Tyagi, S.; Kramer, F. R. Molecular Beacons: Probes That Fluoresce upon Hybridization. *Nat. Biotechnol.* **1996**, *14* (3), 303–308.

(137) Yamamoto, R.; Kumar, P. K. R. Molecular Beacon Aptamer Fluoresces in the Presence of Tat Protein of HIV-1. *Genes to Cells* **2000**, *5* (5), 389–396.

(138) Li, J. W. J.; Fang, X. H.; Tan, W. H. Molecular Aptamer Beacons for Real-Time Protein Recognition. *Biochem. Biophys. Res. Commun.* **2002**, *292* (1), 31–40.

(139) Vicens, M. C.; Sen, A.; Vanderlaan, A.; Drake, T. J.; Tan, W. H. Investigation of Molecular Beacon Aptamer-Based Bioassay for Platelet-Derived Growth Factor Detection. *Chembiochem* **2005**, *6* (5), 900–907.

(140) Yang, R.; Jin, J.; Long, L.; Wang, Y.; Wang, H.; Tan, W. Reversible Molecular Switching of Molecular Beacon: Controlling DNA Hybridization Kinetics and Thermodynamics Using Mercury(II) Ions. *Chem. Commun.* **2009**, No. 3, 322–324.

(141) Wang, Y.; Li, J.; Wang, H.; Jin, J.; Liu, J.; Wang, K.; Tan, W.; Yang, R. Silver Ions-Mediated Conformational Switch: Facile Design of Structure-Controllable Nucleic Acid Probes. *Anal. Chem.* **2010**, *82* (15), 6607–6612.

(142) Zhu, J.; Zhang, L.; Dong, S.; Wang, E. How to Split a G-Quadruplex for DNA Detection: New Insight into the Formation of DNA Split G-Quadruplex. *Chem. Sci.* **2015**, *6* (8), 4822–4827.

(143) Dai, N.; Kool, E. T. Fluorescent DNA-Based Enzyme Sensors. *Chem. Soc. Rev.* **2011**, *40* (12), 5756–5770.

(144) Chen, P.; He, C. A. A General Strategy to Convert the MerR Family Proteins into Highly

Sensitive and Selective Fluorescent Biosensors for Metal Ions. *J. Am. Chem. Soc.* **2004**, *126* (3), 728–729.

(145) Park, K. S.; Lee, J. Y.; Park, H. G. Mismatched Pyrrolo-DC-Modified Duplex DNA as a Novel Probe for Sensitive Detection of Silver Ions. *Chem. Commun.* **2012**, *48* (38), 4549.

(146) Liu, J. W.; Lu, Y. Fast Colorimetric Sensing of Adenosine and Cocaine Based on a General Sensor Design Involving Aptamers and Nanoparticles. *Angew. Chemie-International Ed.* **2006**, *45* (1), 90–94.

(147) Tang, X.; Liu, H.; Zou, B.; Tian, D.; Huang, H. A Fishnet Electrochemical Hg2+ Sensing Strategy Based on Gold Nanoparticle-Bioconjugate and Thymine-Hg2+ -Thymine Coordination Chemistry. *Analyst* **2012**, *137* (2), 309–311.

(148) Park, M.; Ha, H. D.; Kim, Y. T.; Jung, J. H.; Kim, S.-H.; Kim, D. H.; Seo, T. S. Combination of a Sample Pretreatment Microfluidic Device with a Photoluminescent Graphene Oxide Quantum Dot Sensor for Trace Lead Detection. *Anal. Chem.* **2015**, *87* (21), 10969–10975.

(149) Fu, X. B.; Qu, F.; Li, N. B.; Luo, H. Q. A Label-Free Thrombin Binding Aptamer as a Probe for Highly Sensitive and Selective Detection of Lead(II) Ions by a Resonance Rayleigh Scattering Method. *Analyst* **2012**, *137* (5), 1097–1099.

(150) Han, D.; Lim, S. Y.; Kim, B. J.; Piao, L.; Chung, T. D. Mercury(II) Detection by SERS Based on a Single Gold Microshell. *Chem. Commun.* **2010**, *46* (30), 5587–5589.

(151) Yue, Q.; Shen, T.; Wang, J.; Wang, L.; Xu, S.; Li, H.; Liu, J. A Reusable Biosensor for Detecting Mercury(II) at the Subpicomolar Level Based on “Turn-on” Resonance Light Scattering. *Chem. Commun.* **2013**, *49* (17), 1750–1752.

(152) Zhang, L.; Wong, J. X. H.; Li, X.; Li, Y.; Yi, H.-Z. Detection and Quantitation of Heavy Metal Ions on Bona Fide DVDs Using DNA Molecular Beacon Probes. *Anal. Chem.* **2015**, *87* (10), 5062–5067.

(153) Xiang, Y.; Tong, A.; Lu, Y. Abasic Site-Containing DNAzyme and Aptamer for Label-Free Fluorescent Detection of Pb2+ and Adenosine with High Sensitivity, Selectivity, and Tunable Dynamic Range. *J. Am. Chem. Soc.* **2009**, *131* (42), 15352–15357.

(154) Xiang, Y.; Wang, Z.; Xing, H.; Wong, N. Y.; Lu, Y. Label-Free Fluorescent Functional DNA Sensors Using Unmodified DNA: A Vacant Site Approach. *Anal. Chem.* **2010**, *82* (10), 4122–4129.

(155) Zhang, L.; Zhang, Y.; Wei, M.; Yi, Y.; Li, H.; Yao, S. A Label-Free Fluorescent Molecular Switch for Cu2+ Based on Metal Ion-Triggered DNA-Cleaving DNAzyme and DNA Intercalator. *New J. Chem.* **2013**, *37* (4), 1252–1257.

(156) Ferrari, D.; Peracchi, A. A Continuous Kinetic Assay for RNA-Cleaving Deoxyribozymes, Exploiting Ethidium Bromide as an Extrinsic Fluorescent Probe. *Nucleic Acids Res.* **2002**, *30* (20), e112–e112.

(157) Zhang, L.; Han, B.; Li, T.; Wang, E. Label-Free DNAzyme-Based Fluorescing Molecular Switch for Sensitive and Selective Detection of Lead Ions. *Chem. Commun.* **2011**, *47* (11), 3099–3101.

(158) Ho, H. A.; Leclerc, M. Optical Sensors Based on Hybrid Aptamer/Conjugated Polymer Complexes. *J. Am. Chem. Soc.* **2004**, *126* (5), 1384–1387.

(159) Chang, C.-C.; Lin, S.; Wei, S.-C.; Chu-Su, Y.; Lin, C.-W. Surface Plasmon Resonance Detection of Silver Ions and Cysteine Using DNA Intercalator-Based Amplification. *Anal. Bioanal. Chem.* **2012**, *402* (9), 2827–2835.

(160) Dong, Z.-M.; Zhao, G.-C. Quartz Crystal Microbalance Aptasensor for Sensitive Detection of Mercury(II) Based on Signal Amplification with Gold Nanoparticles. *Sensors* **2012**, *12* (6), 7080–7094.

(161) Torabi, S.-F.; Lu, Y. Small-Molecule Diagnostics Based on Functional DNA Nanotechnology: A Dipstick Test for Mercury. *Faraday Discuss.* **2011**, *149*, 125–135.

(162) Mazumdar, D.; Liu, J.; Lu, G.; Zhou, J.; Lu, Y. Easy-to-Use Dipstick Tests for Detection of Lead in Paints Using Non-Cross-Linked Gold Nanoparticle-DNAzyme Conjugates. *Chem. Commun.* **2010**, *46* (9), 1416–1418.

(163) Fang, Z.; Huang, J.; Lie, P.; Xiao, Z.; Ouyang, C.; Wu, Q.; Wu, Y.; Liu, G.; Zeng, L. Lateral Flow Nucleic Acid Biosensor for Cu2+ Detection in Aqueous Solution with High Sensitivity and Selectivity. *Chem. Commun.* **2010**, *46* (47), 9043–9045.

(164) and, N. E. T.; Lagowski*, J. J. Metal Ammonia Solutions: Solutions Containing Argentide Ions. **2001**.

(165) Köhler, J.; Whangbo, M.-H. Late Transition Metal Anions Acting as P-Metal Elements. *Solid State Sci.* **2008**, *10* (4), 444–449.

(166) Lee, C.; Whangbo, M.-H.; Köhler, J. Analysis of Electronic Structures and Chemical Bonding of Metal-Rich Compounds. 2. Presence of Dimer (T - T) $^{4-}$ and Isolated T^{2-} Anions in the Polar Intermetallic Cr_5B_3 -Type Compounds AE_5T_3 (AE = Ca, Sr; T = Au, Ag, Hg, Cd, Zn). *Zeitschrift für Anorg. und Allg. Chemie* **2010**, *636* (1), 36–40.

(167) Greenwood, N. N. (Norman N.; Earnshaw, A. (Alan). *Chemistry of the Elements*; Butterworth-Heinemann, 1997.

(168) Shannon, R. D.; IUCr. Revised Effective Ionic Radii and Systematic Studies of Interatomic Distances in Halides and Chalcogenides. *Acta Crystallogr. Sect. A* **1976**, *32* (5), 751–767.

(169) Persson, I.; Nilsson, K. B. Coordination Chemistry of the Solvated Silver(I) Ion in the Oxygen Donor Solvents Water, Dimethyl Sulfoxide, and N , N ‘ -Dimethylpropyleneurea. *Inorg. Chem.* **2006**, *45* (18), 7428–7434.

(170) Cryst, A. Charge Densities of Selected Ions. **1976**, 13–15.

(171) Saran, R.; Kleinke, K.; Zhou, W.; Yu, T.; Liu, J. A Silver-Specific DNAzyme with a New Silver Aptamer and Salt-Promoted Activity. *Biochemistry* **2017**, *56* (14), 1955–1962.

(172) Funai, T.; Miyazaki, Y.; Aotani, M.; Yamaguchi, E.; Nakagawa, O.; Wada, S.; Torigoe, H.; Ono, A.; Urata, H. AgI Ion Mediated Formation of a C-A Mispair by DNA Polymerases. *Angew. Chemie-International Ed.* **2012**, *51* (26), 6464–6466.

(173) Ono, A.; Cao, S.; Togashi, H.; Tashiro, M.; Fujimoto, T.; Machinami, T.; Oda, S.; Miyake, Y.; Okamoto, I.; Tanaka, Y. Specific Interactions between Silver(i) Ions and Cytosine–cytosine Pairs in DNA Duplexes. *Chem. Commun.* **2008**, No. 39, 4825.

(174) Gehring, K.; Leroy, J.-L.; Guéron, M. A Tetrameric DNA Structure with Protonated Cytosine-Cytosine Base Pairs. *Nature* **1993**, *363* (6429), 561–565.

(175) Day, H. A.; Huguin, C.; Waller, Z. A. E. Silver Cations Fold I-Motif at Neutral PH. *Chem. Commun.* **2013**, *49* (70), 7696–7698.

(176) Loo, K.; Degtyareva, N.; Park, J.; Sengupta, B.; Reddish, M.; Rogers, C. C.; Bryant, A.; Petty, J. T. Ag + -Mediated Assembly of 5 ′ -Guanosine Monophosphate. **2010**, 4320–4326.

(177) Tu, A. T.; Reinosa, J. A. The Interaction of Silver Ion with Guanosine, Guanosine Monophosphate, and Related Compounds. Determination of Possible Sites of Complexing. *Biochemistry* **1966**, *5* (10), 3375–3383.

(178) Swasey, S. M.; Leal, L. E.; Lopez-Acevedo, O.; Pavlovich, J.; Gwinn, E. G. Silver (I) as DNA Glue: Ag^{+}-Mediated Guanine Pairing Revealed by Removing Watson-Crick Constraints. *Sci. Rep.* **2015**, *5* (May), 1–9.

(179) Ihara, T.; Ishii, T.; Araki, N.; Wilson, A. W.; Jyo, A. Silver Ion Unusually Stabilizes the Structure of a Parallel-Motif DNA Triplex. *J. Am. Chem. Soc.* **2009**, *131* (11), 3826–3827.

(180) Megger, D. A.; Fonseca Guerra, C.; Bickelhaupt, F. M.; Müller, J. Silver(I)-Mediated Hoogsteen-Type Base Pairs. *J. Inorg. Biochem.* **2011**, *105* (11), 1398–1404.

(181) Šponer, J.; Sabat, M.; Burda, J. Y.; Leszczynski, J.; Hobza, P.; Lippert, B. Metal Ions in Non-Complementary DNA Base Pairs: An Ab Initio Study of Cu(I), Ag(I), and Au(I) Complexes with

the Cytosine-Adenine Base Pair. *J. Biol. Inorg. Chem.* **1999**, *4* (5), 537–545.

(182) Menzer, S.; Sabat, M.; Lippert, B. Ag(I) Modified Base Pairs Involving Complementary (G, C) and Noncomplementary (A, C) Nucleobases. On the Possible Structural Role of Aqua Ligands in Metal-Modified Nucleobase Pairs. *J. Am. Chem. Soc.* **1992**, *114* (12), 4644–4649.

(183) Polonius, F. A.; Müller, J. An Artificial Base Pair, Mediated by Hydrogen Bonding and Metal-Ion Binding. *Angew. Chemie - Int. Ed.* **2007**, *46* (29), 5602–5604.

(184) Urata, H.; Yamaguchi, E.; Nakamura, Y.; Wada, S. Pyrimidine–pyrimidine Base Pairs Stabilized by Silver(i) Ions. *Chem. Commun.* **2011**, *47* (3), 941–943.

(185) Mandal, S.; Hebenbrock, M.; Müller, J. A Dinuclear Silver(I)-Mediated Base Pair in DNA Formed from 1,N6-Ethenoadenine and Thymine. *Inorganica Chim. Acta* **2018**, *472*, 229–233.

(186) Mandal, S.; Hepp, A.; Müller, J. F186

Dinuclear Silver(I)-Mediated Base Pair Involving the DNA Lesion 1,N(6)-Ethenoadenine. *Dalton Trans.* **2015**, *44* (8), 3540–3543.

(187) Mandal, S.; Hebenbrock, M.; Müller, J. Relative Strand Orientation in a DNA Duplex Controls the Nuclearity of a Metal-Mediated Base Pair. *Chem. - A Eur. J.* **2017**, *23* (25), 5962–5965.

(188) Hensel, S.; Megger, N.; Schweizer, K.; Müller, J. Second Generation Silver(I)-Mediated Imidazole Base Pairs. *Beilstein J. Org. Chem.* **2014**, *10* (I), 2139–2144.

(189) Johannsen, S.; Megger, N.; Böhme, D.; Sigel, R. K. O.; Müller, J. Solution Structure of a DNA Double Helix with Consecutive Metal-Mediated Base Pairs. *Nat. Chem.* **2010**, *2* (3), 229–234.

(190) Petrovec, K.; Ravoo, B. J.; Müller, J. Cooperative Formation of Silver(i)-Mediated Base Pairs. *Chem. Commun.* **2012**, *48* (97), 11844.

(191) Franska, M. Cytidine-Ag(+)-Purine Base Complexes as Studied by Electrospray Ionization Mass Spectrometry. *Eur. J. Mass Spectrom.* **2010**, *16* (5), 587–594.

(192) Petty, J. T.; Zheng, J.; Hud, N. V; Dickson, R. M. DNA-Templated Ag Nanocluster Formation.

J. Am. Chem. Soc. **2004**, *126* (16), 5207–5212.

(193) Obliosca, J. M.; Liu, C.; Yeh, H.-C. Fluorescent Silver Nanoclusters as DNA Probes. *Nanoscale* **2013**, *5* (18), 8443–8461.

(194) Choi, S.; Dickson, R. M.; Yu, J. Developing Luminescent Silver Nanodots for Biological Applications. *Chem. Soc. Rev.* **2012**, *41* (5), 1867–1891.

(195) Liu, J. DNA-Stabilized, Fluorescent, Metal Nanoclusters for Biosensor Development. *Trac-Trends Anal. Chem.* **2014**, *58*, 99–111.

(196) Schultz, D.; Gardner, K.; Oemrawsingh, S. S. R.; Markesevic, N.; Olsson, K.; Debord, M.; Bouwmeester, D.; Gwinn, E. Evidence for Rod-Shaped DNA-Stabilized Silver Nanocluster Emitters. *Adv. Mater.* **2013**, *25* (20), 2797–2803.

(197) Lee, J.; Park, J.; Hee Lee, H.; Park, H.; Kim, H. I.; Kim, W. J. Fluorescence Switch for Silver Ion Detection Utilizing Dimerization of DNA-Ag Nanoclusters. *Biosens. Bioelectron.* **2015**, *68*, 642–647.

(198) Gwinn, E. G.; O'Neill, P.; Guerrero, A. J.; Bouwmeester, D.; Fygenson, D. K. Sequence-Dependent Fluorescence of DNA-Hosted Silver Nanoclusters. *Adv. Mater.* **2008**, *20* (2), 279–+.

(199) Ono, A.; Cao, S.; Togashi, H.; Tashiro, M.; Fujimoto, T.; Machinami, T.; Oda, S.; Miyake, Y.; Okamoto, I.; Tanaka, Y. Specific Interactions between Silver(I) Ions and Cytosine-Cytosine Pairs in DNA Duplexes. *Chem. Commun. (Camb).* **2008**, No. 39, 4825–4827.

(200) Kleinke, K.; Saran, R.; Liu, J. Label-Free Ag+ Detection by Enhancing DNA Sensitized Tb3+ Luminescence. *Sensors* **2016**, *16* (9), 1370.

(201) Kang, B. H.; Gao, Z. F.; Li, N.; Shi, Y.; Li, N. B.; Luo, H. Q. Thiazole Orange as a Fluorescent Probe: Label-Free and Selective Detection of Silver Ions Based on the Structural Change of i-Motif DNA at Neutral PH. *Talanta* **2016**, *156*, 141–146.

(202) Zhou, X. H.; Kong, D. M.; Shen, H. X. Ag+ and Cysteine Quantitation Based on G-Quadruplex

- Hemin DNAzymes Disruption by Ag+. *Anal. Chem.* **2010**, *82* (3), 789–793.

(203) Zhou, X. H.; Kong, D. M.; Shen, H. X. G-Quadruplex-Hemin DNAzyme-Amplified Colorimetric Detection of Ag+ion. *Anal. Chim. Acta* **2010**, *678* (1), 124–127.

(204) Liu, G.; Zhang, Q.; Qian, Y.; Yu, S.; Li, F. Highly Specific Sensing of Silver Based on Aggregation of G-Quadruplex-Capped Gold Nanoparticles. *Anal. Methods* **2013**, *5* (3), 648–652.

(205) Joyce, G. F. Directed Evolution of Nucleic Acid Enzymes. *Annu. Rev. Biochem.* **2004**, *73* (1), 791–836.

(206) Breaker, R. R. *In Vitro* Selection of Catalytic Polynucleotides. *Chem. Rev.* **1997**, *97* (2), 371–390.

(207) Sen, D.; Geyer, C. R. DNA Enzymes. *Curr. Opin. Chem. Biol.* **1998**, *2* (6), 680–687.

(208) Lu*, Y. Metalloprotein and Metallo-DNA/RNAzyme Design: Current Approaches, Success Measures, and Future Challenges. **2006**.

(209) Schlosser, K.; Li, Y. Biologically Inspired Synthetic Enzymes Made from DNA. *Chem. Biol.* **2009**, *16* (3), 311–322.

(210) Silverman, S. K. Catalytic DNA: Scope, Applications, and Biochemistry of Deoxyribozymes. *Trends Biochem. Sci.* **2016**, *41* (7), 595–609.

(211) Lu, Y. New Transition-Metal-Dependent DNA-Zymes as Efficient Endonucleases and as Selective Metal Biosensors. *Chem. Eur. J.* **2002**, *8* (20), 4589–4596.

(212) Sigel, R. K. O.; Pyle, A. M. Alternative Roles for Metal Ions in Enzyme Catalysis and the Implications for Ribozyme Chemistry. *Chem. Rev.* **2007**, *107* (1), 97–113.

(213) Hwang, K.; Hosseinzadeh, P.; Lu, Y. Biochemical and Biophysical Understanding of Metal Ion Selectivity of DNAzymes. *Inorganica Chim. Acta* **2016**, *452*, 12–24.

(214) Liu, J. Lanthanide-Dependent RNA-Cleaving DNAzymes as Metal Biosensors. *Can. J. Chem.* **2015**, *93* (3), 273–278.

(215) Roth, A.; Breaker, R. R. An Amino Acid as a Cofactor for a Catalytic Polynucleotide. *Proc. Natl. Acad. Sci. U. S. A.* **1998**, *95* (11), 6027–6031.

(216) Geyer, C. R.; Sen, D. Evidence for the Metal-Cofactor Independence of an RNA Phosphodiester-Cleaving DNA Enzyme. *Chem. Biol.* **1997**, *4* (8), 579–593.

(217) Urata, H.; Yamaguchi, E.; Nakamura, Y.; Wada, S. Pyrimidine-Pyrimidine Base Pairs Stabilized by Silver(I) Ions. *Chem. Commun. (Camb).* **2011**, *47* (3), 941–943.

(218) Freeman, R.; Finder, T.; Willner, I. Multiplexed Analysis of Hg^{2+} and Ag^{+} Ions by Nucleic Acid Functionalized CdSe/ZnS Quantum Dots and Their Use for Logic Gate Operations. *Angew. Chemie Int. Ed.* **2009**, *48* (42), 7818–7821.

(219) Wen, Y.; Xing, F.; He, S.; Song, S.; Wang, L.; Long, Y.; Li, D.; Fan, C. A Graphene-Based Fluorescent Nanoprobe for Silver(i) Ions Detection by Using Graphene Oxide and a Silver-Specific Oligonucleotide. *Chem. Commun.* **2010**, *46* (15), 2596.

(220) Li, T.; Shi, L.; Wang, E.; Dong, S. Silver-Ion-Mediated DNAzyme Switch for the Ultrasensitive and Selective Colorimetric Detection of Aqueous Ag^{+} and Cysteine. *Chem. - A Eur. J.* **2009**, *15* (14), 3347–3350.

(221) Su, Y.-T.; Lan, G.-Y.; Chen, W.-Y.; Chang, H.-T. Detection of Copper Ions through Recovery of the Fluorescence of DNA-Templated Copper/Silver Nanoclusters in the Presence of Mercaptopropionic Acid. *Anal. Chem.* **2010**, *82* (20), 8566–8572.

(222) Richards, C. I.; Choi, S.; Hsiang, J.-C.; Antoku, Y.; Vosch, T.; Bongiorno, A.; Tzeng, Y.-L.; Dickson, R. M. Oligonucleotide-Stabilized Ag Nanocluster Fluorophores. *J. Am. Chem. Soc.* **2008**, *130* (15), 5038–5039.

(223) Dahm, S. C.; Derrick, W. B.; Uhlenbeck, O. C. Evidence for the Role of Solvated Metal Hydroxide in the Hammerhead Cleavage Mechanism. *Biochemistry* **1993**, *32* (48), 13040–13045.

(224) Sauls, F. C. A Simple Determination of the Ag_2O Solubility Product by Potentiometric Determinations of Both Ag^{+1} and OH^{-1}. *J. Chem. Educ.* **2013**, *90* (9), 1212–1214.

(225) Burgess, J. Metal Ions in Solution Ellis Horwood Ltd. *Chichester Google Sch.* **1978**.

(226) Huang, P.-J. J.; Liu, J. Sensing Parts-per-Trillion Cd^{2+} , Hg^{2+} , and Pb^{2+} Collectively and Individually Using Phosphorothioate DNAzymes. *Anal. Chem.* **2014**, *86* (12), 5999–6005.

(227) Santoro, S. W.; Joyce, G. F.; Sakthivel, K.; Gramatikova, S.; Barbas, C. F. RNA Cleavage by a DNA Enzyme with Extended Chemical Functionality. *J. Am. Chem. Soc.* **2000**, *122* (11), 2433–2439.

(228) Kim, H.-K.; Liu, J.; Li, J.; Nagraj, N.; Li, M.; Pavot, C. M.-B.; Lu, Y. Metal-Dependent Global Folding and Activity of the 8-17 DNAzyme Studied by Fluorescence Resonance Energy Transfer. *J. Am. Chem. Soc.* **2007**, *129* (21), 6896–6902.

(229) Kim, H.-K.; Rasnik, I.; Liu, J.; Ha, T.; Lu, Y. Dissecting Metal Ion-Dependent Folding and Catalysis of a Single DNAzyme. *Nat. Chem. Biol.* **2007**, *3* (12), 763–768.

(230) Schlosser, K.; Li, Y. A Versatile Endoribonuclease Mimic Made of DNA: Characteristics and Applications of the 8-17 RNA-Cleaving DNAzyme. *Chembiochem* **2010**, *11* (7), 866–879.

(231) Wang, S.; Karbstein, K.; Peracchi, A.; Beigelman, L.; Herschlag, D. Identification of the Hammerhead Ribozyme Metal Ion Binding Site Responsible for Rescue of the Deleterious Effect of a Cleavage Site Phosphorothioate †. *Biochemistry* **1999**, *38* (43), 14363–14378.

(232) Thaplyal, P.; Ganguly, A.; Hammes-Schiffer, S.; Bevilacqua, P. C. Inverse Thio Effects in the Hepatitis Delta Virus Ribozyme Reveal That the Reaction Pathway Is Controlled by Metal Ion Charge Density. *Biochemistry* **2015**, *54* (12), 2160–2175.

(233) Thaplyal, P.; Ganguly, A.; Golden, B. L.; Hammes-Schiffer, S.; Bevilacqua, P. C. Thio Effects and an Unconventional Metal Ion Rescue in the Genomic Hepatitis Delta Virus Ribozyme. *Biochemistry* **2013**, *52* (37), 6499–6514.

(234) Zhou, W.; Ding, J.; Liu, J. A Highly Specific Sodium Aptamer Probed by 2-Aminopurine for Robust Na+sensing. *Nucleic Acids Res.* **2016**, *44* (21), 10377–10385.

(235) Zhou, W.; Ding, J.; Liu, J. A Selective Na^{+} Aptamer Dissected by Sensitized Tb^{3+} Luminescence. *ChemBioChem* **2016**, *17* (16), 1563–1570.

(236) WILSON, T. J.; LILLEY, D. M. J. Metal Ion Binding and the Folding of the Hairpin Ribozyme. *RNA* **2002**, *8* (5), S1355838202020514.

(237) Tinsley, R. A.; Harris, D. A.; Walter, N. G. Magnesium Dependence of the Amplified Conformational Switch in the Trans-Acting Hepatitis Delta Virus Ribozyme †. *Biochemistry* **2004**, *43* (28), 8935–8945.

(238) Liu, J.; Lu, Y. FRET Study of a Trifluorophore-Labeled DNAzyme. *J. Am. Chem. Soc.* **2002**, *124* (51), 15208–15216.

(239) He, Y.; Lu, Y. Metal-Ion-Dependent Folding of a Uranyl-Specific DNAzyme: Insight into Function from Fluorescence Resonance Energy Transfer Studies. *Chem. - A Eur. J.* **2011**, *17* (49), 13732–13742.

(240) Lam, J. C. F.; Li, Y. Influence of Cleavage Site on Global Folding of an RNA-Cleaving DNAzyme. *ChemBioChem* **2010**, *11* (12), 1710–1719.

(241) Jung, J.; Han, K. Y.; Koh, H. R.; Lee, J.; Choi, Y. M.; Kim, C.; Kim, S. K. Effect of Single-Base Mutation on Activity and Folding of 10-23 Deoxyribozyme Studied by Three-Color Single-Molecule ALEX FRET. *J. Phys. Chem. B* **2012**, *116* (9), 3007–3012.

(242) Cepeda-Plaza, M.; Null, E. L.; Lu, Y. Metal Ion as Both a Cofactor and a Probe of Metal-Binding Sites in a Uranyl-Specific DNAzyme: A Uranyl Photocleavage Study. *Nucleic Acids Res.* **2013**, *41* (20), 9361–9370.

(243) Ono, A.; Torigoe, H.; Tanaka, Y.; Okamoto, I. Binding of Metal Ions by Pyrimidine Base Pairs in DNA Duplexes. *Chem. Soc. Rev.* **2011**, *40* (12), 5855.

(244) Urata, H.; Yamaguchi, E.; Nakamura, Y.; Wada, S. Pyrimidine–pyrimidine Base Pairs Stabilized by Silver(<scp>i</Scp>) Ions. *Chem. Commun.* **2011**, *47* (3), 941–943.

(245) Nawrot, B.; Widera, K.; Sobczak, M.; Wojcik, M.; Stec, W. Effect of RP and SPPhosphorothioate Substitution at the Scissile Site on the Cleavage Activity of Deoxyribozyme 10-23. *Curr. Org. Chem.* **2008**, *12* (12), 1004–1009.

(246) Barciszewski, J.; Jurczak, J.; Porowski, S.; Specht, T.; Erdmann, V. A. The Role of Water Structure in Conformational Changes of Nucleic Acids in Ambient and High-Pressure Conditions. *Eur. J. Biochem.* **2001**, *260* (2), 293–307.

(247) Sigel, R. K. O.; Sigel, H. A Stability Concept for Metal Ion Coordination to Single-Stranded Nucleic Acids and Affinities of Individual Sites. *Acc. Chem. Res.* **2010**, *43* (7), 974–984.

(248) Schlosser, K.; Gu, J.; Sule, L.; Li, Y. Sequence-Function Relationships Provide New Insight into the Cleavage Site Selectivity of the 8-17 RNA-Cleaving Deoxyribozyme. *Nucleic Acids Res.* **2008**, *36* (5), 1472–1481.

(249) Santoro, S. W.; Joyce, G. F. Mechanism and Utility of an RNA-Cleaving DNA Enzyme †. *Biochemistry* **1998**, *37* (38), 13330–13342.

(250) Brown, A. K.; Li, J.; Pavot, C. M. B.; Lu, Y. A Lead-Dependent DNAzyme with a Two-Step Mechanism. *Biochemistry* **2003**, *42* (23), 7152–7161.

(251) Huang, P.-J. J.; Wang, F.; Liu, J. Cleavable Molecular Beacon for Hg^{2+} Detection Based on Phosphorothioate RNA Modifications. *Anal. Chem.* **2015**, *87* (13), 6890–6895.

(252) Huang, P.-J. J.; Vazin, M.; Liu, J. Desulfurization Activated Phosphorothioate DNAzyme for the Detection of Thallium. *Anal. Chem.* **2015**, *87* (20), 10443–10449.

(253) Cunningham, L. A.; Li, J.; Lu, Y. Spectroscopic Evidence for Inner-Sphere Coordination of Metal Ions to the Active Site of a Hammerhead Ribozyme. *J. Am. Chem. Soc.* **1998**, *120* (18), 4518–4519.

(254) Oivanen, M.; Ora, M.; Almer, H.; Stromberg, R.; Lonnberg, H. Hydrolytic Reactions of the Diastereomeric Phosphoromonothioate Analogs of Uridylyl(3',5')Uridine: Kinetics and Mechanisms for Desulfurization, Phosphoester Hydrolysis, and Transesterification to the 2',5'-Isomers. *J. Org. Chem.* **1995**, *60* (17), 5620–5627.

(255) Maxam, A. M.; Gilbert, W. [57] Sequencing End-Labeled DNA with Base-Specific Chemical Cleavages; 1980; pp 499–560.

(256) Saran, R.; Liu, J. A Silver DNAzyme. *Anal. Chem.* **2016**, *88* (7), 4014–4020.

(257) Jones, A. C.; Neely, R. K. 2-Aminopurine as a Fluorescent Probe of DNA Conformation and the DNA–enzyme Interface. *Q. Rev. Biophys.* **2015**, *48* (02), 244–279.

(258) Gray, R. D.; Petraccone, L.; Trent, J. O.; Chaires, J. B. Characterization of a K^+-Induced Conformational Switch in a Human Telomeric DNA Oligonucleotide Using 2-Aminopurine Fluorescence. *Biochemistry* **2010**, *49* (1), 179–194.

(259) Soulière, M. F.; Haller, A.; Rieder, R.; Micura, R. A Powerful Approach for the Selection of 2-Aminopurine Substitution Sites to Investigate RNA Folding. *J. Am. Chem. Soc.* **2011**, *133* (40), 16161–16167.

(260) Wilcox, J. L.; Bevilacqua, P. C. A Simple Fluorescence Method for p K_a Determination in RNA and DNA Reveals Highly Shifted p K_a's. *J. Am. Chem. Soc.* **2013**, *135* (20), 7390–7393.

(261) Li, M.; Sato, Y.; Nishizawa, S.; Seino, T.; Nakamura, K.; Teramae, N. 2-Aminopurine-Modified Abasic-Site-Containing Duplex DNA for Highly Selective Detection of Theophylline. *J. Am. Chem. Soc.* **2009**, *131* (7), 2448–2449.

(262) Li, N.; Ho, C.-M. Aptamer-Based Optical Probes with Separated Molecular Recognition and Signal Transduction Modules. *J. Am. Chem. Soc.* **2008**, *130* (8), 2380–2381.

(263) Heppell, B.; Lafontaine, D. A. Folding of the SAM Aptamer Is Determined by the Formation of a K-Turn-Dependent Pseudoknot †. *Biochemistry* **2008**, *47* (6), 1490–1499.

(264) Kim, H.-K.; Li, J.; Nagraj, N.; Lu, Y. Probing Metal Binding in the 8-17 DNAzyme by Tb^{III} Luminescence Spectroscopy. *Chem. - A Eur. J.* **2008**, *14* (28), 8696–8703.

(265) Zuker, M. No Title. **2003**, *31* (13).

(266) Law, S. M.; Eritja, R.; Goodman, M. F.; Breslauer, K. J. Spectroscopic and Calorimetric Characterizations of DNA Duplexes Containing 2-Aminopurine †. *Biochemistry* **1996**, *35* (38), 12329–12337.

(267) Hall, K. B. Chapter 13 – 2-Aminopurine as a Probe of RNA Conformational Transitions. In *Methods in Enzymology*; 2009; Vol. 469, pp 269–285.

(268) Famulok, M.; Hartig, J. S.; Mayer, G. Functional Aptamers and Aptazymes in Biotechnology, Diagnostics, and Therapy. *Chem. Rev.* **2007**, *107* (9), 3715–3743.

(269) Furukawa, K.; Ramesh, A.; Zhou, Z.; Weinberg, Z.; Vallery, T.; Winkler, W. C.; Breaker, R. R. Bacterial Riboswitches Cooperatively Bind Ni 2+ or Co 2+ Ions and Control Expression of Heavy Metal Transporters. *Mol. Cell* **2015**, *57* (6), 1088–1098.

(270) Drake, P. L.; Hazelwood, K. J. Exposure-Related Health Effects of Silver and Silver Compounds: A Review. *Ann. Occup. Hyg.* **2005**, *49* (7), 575–585.

(271) Ratte, H. T. Annual Review Bioaccumulation and Toxicity of Silver Compounds: A Review. *Environ. Toxicol. Chem.* **1999**, *18* (1), 89–108.

(272) Coskun, A.; Akkaya, E. U. Ion Sensing Coupled to Resonance Energy Transfer: A Highly Selective and Sensitive Ratiometric Fluorescent Chemosensor for Ag(I) by a Modular Approach. *J. Am. Chem. Soc.* **2005**, *127* (30), 10464–10465.

(273) Chatterjee, A.; Santra, M.; Won, N.; Kim, S. B. S.; Kim, J. K.; Kim, S. B. S.; Ahn, K. H. Selective Fluorogenic and Chromogenic Probe for Detection of Silver Ions and Silver Nanoparticles in Aqueous Media. *J. Am. Chem. Soc.* **2009**, *131* (6), 2040–2041.

(274) Zhang, X.-B.; Kong, R.-M.; Lu, Y. Metal Ion Sensors Based on DNAzymes and Related DNA

Molecules. *Annu. Rev. Anal. Chem.* **2011**, *4* (1), 105–128.

(275) Liu, J.; Cao, Z.; Lu, Y. Functional Nucleic Acid Sensors. *Chem. Rev.* **2009**, *109* (5), 1948–1998.

(276) Song, S.; Qin, Y.; He, Y.; Huang, Q.; Fan, C.; Chen, H.-Y. Functional Nanoprobes for Ultrasensitive Detection of Biomolecules. *Chem. Soc. Rev.* **2010**, *39* (11), 4234.

(277) Katz, E.; Willner, I. Integrated Nanoparticle-Biomolecule Hybrid Systems: Synthesis, Properties, and Applications. *Angew. Chemie Int. Ed.* **2004**, *43* (45), 6042–6108.

(278) Wang, H.; Yang, R.; Yang, L.; Tan, W. Nucleic Acid Conjugated Nanomaterials for Enhanced Molecular Recognition. *ACS Nano* **2009**, *3* (9), 2451–2460.

(279) Wilhelmsson, L. M. Fluorescent Nucleic Acid Base Analogues. *Q. Rev. Biophys.* **2010**, *43* (02), 159–183.

(280) Liu, C.; Martin, C. T. Fluorescence Characterization of the Transcription Bubble in Elongation Complexes of T7 RNA Polymerase. *J. Mol. Biol.* **2001**, *308* (3), 465–475.

(281) Li, T.; Fu, R.; Park, H. G. Pyrrolo-DC Based Fluorescent Aptasensors for the Molecular Recognition of Targets. *Chem. Commun.* **2010**, *46* (19), 3271–3273.

(282) Zhang, H.; Wang, M.; Gao, Q.; Qi, H.; Zhang, C. Fluorescent Detection of Single Nucleotide Polymorphism Utilizing a Hairpin DNA Containing a Nucleotide Base Analog Pyrrolo-Deoxycytidine as a Fluorescent Probe. *Talanta* **2011**, *84* (3), 771–776.

(283) Liu, C.; Martin, C. T. Promoter Clearance by T7 RNA Polymerase. Initial Bubble Collapse and Transcript Dissociation Monitored by Base Analog Fluorescence. *J. Biol. Chem.* **2002**, *277* (4), 2725–2731.

(284) Xu, S.; Zhang, Y.; Luo, X.; Wang, Y.; Chen, S.; Wang, J.; Yuan, H.; Xu, A.; Wu, L. Fluorescent G-Quadruplex-NMM DNA Probe for the Detection of Silver Nanoparticles in Aqueous Media. *Anal. Methods* **2015**, *7* (5), 1672–1675.

(285) Guo, J. H.; Kong, D. M.; Shen, H. X. Design of a Fluorescent DNA IMPLICATION Logic Gate

and Detection of Ag+ and Cysteine with Triphenylmethane Dye/G-Quadruplex Complexes. *Biosens. Bioelectron.* **2010**, *26* (2), 327–332.

(286) Tan, H.; Chen, Y. Ag+-Enhanced Fluorescence of Lanthanide/Nucleotide Coordination Polymers and Ag+ Sensing. *Chem. Commun.* **2011**, *47* (45), 12373.

(287) Li, T.; Shi, L.; Wang, E.; Dong, S. Silver-Ion-Mediated DNAzyme Switch for the Ultrasensitive and Selective Colorimetric Detection of Aqueous Ag+ and Cysteine. *Chemistry* **2009**, *15* (14), 3347–3350.

(288) OligoAnalyzer 3.1 | IDT https://www.idtdna.com/calc/analyzer (accessed May 9, 2018).

(289) Lu, Y. New Transition-Metal-Dependent DNAzymes as Efficient Endonucleases and as Selective Metal Biosensors. *Chem. - A Eur. J.* **2002**, *8* (20), 4588–4596.

(290) Dimroth, K.; Witzel, H.; Hülsen, W.; Mirbach, H. Über Die Hydrolyse von Ribonucleinsäuren in Gegenwart von Metallhydroxyden. *Justus Liebigs Ann. Chem.* **1959**, *620* (1), 94–108.

(291) Farkas, W. R. Depolymerization of Ribonucleic Acid by Plumbous Ion. *Biochim. Biophys. Acta* **1968**, *155* (2), 401-.

(292) Wintermeyer, W.; Zachau, H. G. Mg2+-Catalyzed Specific Splitting of Transfer-Rna. *Biochim. Biophys. Acta* **1973**, *299* (1), 82–90.

(293) Werner, C.; Krebs, B.; Keith, G.; Dirheimer, G. Specific Cleavages of Pure TRNAs by Plumbous Ions. *Biochim. Biophys. Acta - Nucleic Acids Protein Synth.* **1976**, *432* (2), 161–175.

(294) Brown, R. S.; Dewan, J. C.; Klug, A. Crystallographic and Biochemical Investigation of the Lead(II)-Catalyzed Hydrolysis of Yeast Phenylalanine TRNA. *Biochemistry* **1985**, *24* (18), 4785–4801.

(295) Pan, T.; Uhlenbeck, O. C. In Vitro Selection of RNAs That Undergo Autolytic Cleavage with Lead(2+). *Biochemistry* **1992**, *31* (16), 3887–3895.

(296) Pan, T.; Dichtl, B.; Uhlenbeck, O. C. Properties of an In Vitro Selected Pb2+ Cleavage Motif.

Biochemistry **1994**, *33* (32), 9561–9565.

(297) Pan, T.; Uhlenbeck, O. C. A Small Metalloribozyme with a Two-Step Mechanism. *Nature* **1992**, *358* (6387), 560–563.

(298) Chartrand, P.; Usman, N.; Cedergren, R. Effect of Structural Modifications on the Activity of the Leadzyme †. *Biochemistry* **1997**, *36* (11), 3145–3150.

(299) Ohmichi, T. Effect of Substrate RNA Sequence on the Cleavage Reaction by a Short Ribozyme. *Nucleic Acids Res.* **1998**, *26* (24), 5655–5661.

(300) Hoogstraten, C. G.; Legault, P.; Pardi, A. NMR Solution Structure of the Lead-Dependent Ribozyme: Evidence for Dynamics in RNA Catalysis 1 1Edited by I. Tinoco. *J. Mol. Biol.* **1998**, *284* (2), 337–350.

(301) Hoogstraten, C. G.; Wank, J. R.; Pardi, A. Active Site Dynamics in the Lead-Dependent Ribozyme †. *Biochemistry* **2000**, *39* (32), 9951–9958.

(302) Legault, P.; Hoogstraten, C. G.; Metlitzky, E.; Pardi, A. Order, Dynamics and Metal-Binding in the Lead-Dependent Ribozyme 1 1Edited by I. Tinoco. *J. Mol. Biol.* **1998**, *284* (2), 325–335.

(303) Wedekind, J. E.; McKay, D. B. Crystal Structure of the Leadzyme at 1.8 Å Resolution: Metal Ion Binding and the Implications for Catalytic Mechanism and Allo Site Ion Regulation †. *Biochemistry* **2003**, *42* (32), 9554–9563.

(304) Wedekind, J. E.; McKay, D. B. Crystal Structure of a Lead-Dependent Ribozyme Revealing Metal Binding Sites Relevant to Catalysis. *Nat. Struct. Biol.* **1999**, *6* (3), 261–268.

(305) Kadakkuzha, B. M.; Zhao, L.; Xia, T. Conformational Distribution and Ultrafast Base Dynamics of Leadzyme. *Biochemistry* **2009**, *48* (18), 3807–3809.

(306) Lan, T.; Furuya, K.; Lu, Y. A Highly Selective Lead Sensor Based on a Classic Lead DNAzyme. *Chem. Commun.* **2010**, *46* (22), 3896.

(307) Cruz, R. P. .; Withers, J. B.; Li, Y. Dinucleotide Junction Cleavage Versatility of 8-17

Deoxyribozyme. *Chem. Biol.* **2004**, *11* (1), 57–67.

(308) Huang, P.-J. J.; Liu, J. Two Pb2+-Specific DNAzymes with Opposite Trends in Split-Site-Dependent Activity. *Chem. Commun.* **2014**, *50* (34), 4442.

(309) Stout, C. D.; Joyce, G. F.; Nowakowski, J.; Shim, P. J.; Prasad, G. S. Crystal Structure of an 82-Nucleotide RNA-DNA Complex Formed by the 10-23 DNA Enzyme. *Nat. Struct. Biol.* **1999**, *6* (2), 151–156.

(310) Peracchi, A.; Bonaccio, M.; Clerici, M. A Mutational Analysis of the 8-17 Deoxyribozyme Core. *J. Mol. Biol.* **2005**, *352* (4), 783–794.

(311) Schlosser, K.; Gu, J.; Sule, L.; Li, Y. Sequence-Function Relationships Provide New Insight into the Cleavage Site Selectivity of the 8-17 RNA-Cleaving Deoxyribozyme. *Nucleic Acids Res.* **2008**, *36* (5), 1472–1481.

(312) Li, Y.; Breaker, R. R.; and, Y. L.; Breaker*, R. R. Kinetics of RNA Degradation by Specific Base Catalysis of Transesterification Involving the 2‘-Hydroxyl Group. *J. Am. Chem. Soc.* **1999**, *121* (23), 5364–5372.

(313) Zuker, M. Mfold Web Server for Nucleic Acid Folding and Hybridization Prediction. *Nucleic Acids Res.* **2003**, *31* (13), 3406–3415.

(314) Wang, B.; Cao, L.; Chiuman, W.; Li, Y.; Xi, Z. Probing the Function of Nucleotides in the Catalytic Cores of the 8-17 and 10-23 DNAzymes by Abasic Nucleotide and C3 Spacer Substitutions. *Biochemistry* **2010**, *49* (35), 7553–7562.

(315) Breaker, R. R. DNA Enzymes. *Nat. Biotechnol.* **1997**, *15* (5), 427–431.

(316) Lu, Y. New Transition-Metal-Dependent DNAzymes as Efficient Endonucleases and as Selective Metal Biosensors. *Chem. - A Eur. J.* **2002**, *8* (20), 4588–4596.

(317) Schlosser, K.; Li, Y. Biologically Inspired Synthetic Enzymes Made from DNA. *Chem. Biol.* **2009**, *16* (3), 311–322.

(318) Silverman, S. K. DNA as a Versatile Chemical Component for Catalysis, Encoding, and Stereocontrol. *Angew. Chemie Int. Ed.* **2010**, *49* (40), 7180–7201.

(319) Lu, Y.; Liu, J. Smart Nanomaterials Inspired by Biology: Dynamic Assembly of Error-Free Nanomaterials in Response to Multiple Chemical and Biological Stimuli. *Acc. Chem. Res.* **2007**, *40* (5), 315–323.

(320) Silverman, S. K. Deoxyribozymes: Selection Design and Serendipity in the Development of DNA Catalysts †. *Acc. Chem. Res.* **2009**, *42* (10), 1521–1531.

(321) Liu, J.; Lu, Y. A Colorimetric Lead Biosensor Using DNAzyme-Directed Assembly of Gold Nanoparticles. *J. Am. Chem. Soc.* **2003**, *125* (22), 6642–6643.

(322) Xiao, Y.; Rowe, A. A.; Plaxco, K. W. Electrochemical Detection of Parts-Per-Billion Lead via an Electrode-Bound DNAzyme Assembly. *J. Am. Chem. Soc.* **2007**, *129* (2), 262–263.

(323) Wang, H.; Kim, Y.; Liu, H.; Zhu, Z.; Bamrungsap, S.; Tan, W. Engineering a Unimolecular DNA-Catalytic Probe for Single Lead Ion Monitoring. *J. Am. Chem. Soc.* **2009**, *131* (23), 8221–8226.

(324) Liu, J.; Lu, Y. Stimuli-Responsive Disassembly of Nanoparticle Aggregates for Light-Up Colorimetric Sensing. *J. Am. Chem. Soc.* **2005**, *127* (36), 12677–12683.

(325) Zhao, X.-H.; Kong, R.-M.; Zhang, X.-B.; Meng, H.-M.; Liu, W.-N.; Tan, W.; Shen, G.-L.; Yu, R.-Q. Graphene–DNAzyme Based Biosensor for Amplified Fluorescence "Turn-On" Detection of Pb^{2+} with a High Selectivity. *Anal. Chem.* **2011**, *83* (13), 5062–5066.

(326) Sekhon, G. S.; Sen, D. A Stereochemical Glimpse of the Active Site of the 8−17 Deoxyribozyme from Iodine-Mediated Cross-Links Formed with the Substrate's Scissile Site. *Biochemistry* **2010**, *49* (42), 9072–9077.

(327) Mazumdar, D.; Nagraj, N.; Kim, H.-K.; Meng, X.; Brown, A. K.; Sun, Q.; Li, W.; Lu, Y. Activity, Folding and Z-DNA Formation of the 8-17 DNAzyme in the Presence of Monovalent

Ions. *J. Am. Chem. Soc.* **2009**, *131* (15), 5506–5515.

(328) Peracchi, A. Preferential Activation of the 8-17 Deoxyribozyme by Ca2+ Ions - Evidence for the Identity of 8-17 with the Catalytic Domain of the MG5 Deoxyribozyme. *J. Biol. Chem.* **2000**, *275* (16), 11693–11697.

(329) Schlosser, K.; Li, Y. Tracing Sequence Diversity Change of RNA-Cleaving Deoxyribozymes under Increasing Selection Pressure during in Vitro Selection †. *Biochemistry* **2004**, *43* (30), 9695–9707.

(330) Brown, R. S.; Hingerty, B. E.; Dewan, J. C.; Klug, A. Pb(II)-Catalysed Cleavage of the Sugar–phosphate Backbone of Yeast TRNAPhe—implications for Lead Toxicity and Self-Splicing RNA. *Nature* **1983**, *303* (5917), 543–546.

(331) Da Costa, C. P.; Sigel, H. Lead(II)-Binding Properties of the 5 ’-Monophosphates of Adenosine (AMP(2-)), Inosine (IMP2-), and Guanosine (GMP(2-)) in Aqueous Solution. Evidence for Nucleobase-Lead(II) Interactions. *Inorg. Chem.* **2000**, *39* (26), 5985–5993.

(332) Fersht, A. R.; Serrano, L. Principles of Protein Stability Derived from Protein Engineering Experiments. *Curr. Opin. Struct. Biol.* **1993**, *3* (1), 75–83.

(333) Pan, T.; Uhlenbeck, O. C. A Small Metalloribozyme with a 2-Step Mechanism. *Nature* **1992**, *358* (6387), 560–563.

(334) Richens, D. T. *The Chemistry of Aqua Ions : Synthesis, Structure, and Reactivity : A Tour through the Periodic Table of the Elements*; J. Wiley, 1997.

6. Appendix A: Chapter 6 - A DNAzyme version of the leadzyme[d]

6.1 Introduction

Most RNA-cleaving ribozymes and DNAzymes require divalent metal ions for catalysis.[100,102,212,289] Among the different metal ions used for RNA cleavage, Pb^{2+} has greatly fueled the growth of this field. The interaction between Pb^{2+} and nucleic acids was observed more than 50 years back. In 1959, the hydrolysis of RNA by lead hydroxide was demonstrated.[290] A detailed investigation was published in 1968 showing that the rate of RNA depolymerization as well as its pH optimum, both varied with the Pb^{2+} concentration.[291] It first became known that Pb^{2+} can bring about site-specific cleavage of tRNA in 1973.[292] The mechanism of cleavage was proposed based on biochemical data and the crystal structure of the yeast tRNAPhe soaked in lead acetate.[293,294] Multiple variations of this well-studied yeast tRNA were used to design RNA selection libraries to isolate RNAs that undergo autolytic cleavage in the presence of Pb^{2+}.[295] Among the sequences derived from this selection, one was truncated and optimized into a minimal motif known as the 'leadzyme.' The leadzyme is a very small but interesting ribozyme with only two unpaired nucleotides 5′ rGrA 3′ in the enzyme loop and four unpaired nucleotides in the substrate strand (Figure 6.1 B). This enzyme is highly specific for lead and its reaction produces a 5′-OH end along with a 2′3′ cyclic phosphate product.[296,297] Deeper insights have been obtained about this enzyme through biochemical

[d] This chapter is the basis for a published manuscript: Saran R.; Chen Q.; Liu, J. Searching for a DNAzyme Version of the Leadzyme. *J. Mol. Evol.* **2015**, 81(5-6), 235-244.

studies,[298,299] NMR,[300–302] X-ray crystallography,[303,304] and other biophysical characterizations.[305] Parallel to the ribozyme field, Pb^{2+} has been a very important metal ion in DNAzyme research as well. The first DNAzyme, GR5 (Figure 6.1 D), was obtained as a result of a Pb^{2+}-dependent selection,[67] and it is highly specific and active with Pb^{2+}.[306] The most extensively studied 8–17 DNAzyme, initially discovered from a Mg^{2+}-dependent selection,[111] is also highly active in the presence of Pb^{2+}. A commonly used variant of the 8–17 DNAzyme is named 17E (Figure 6.1 C).[113,307]

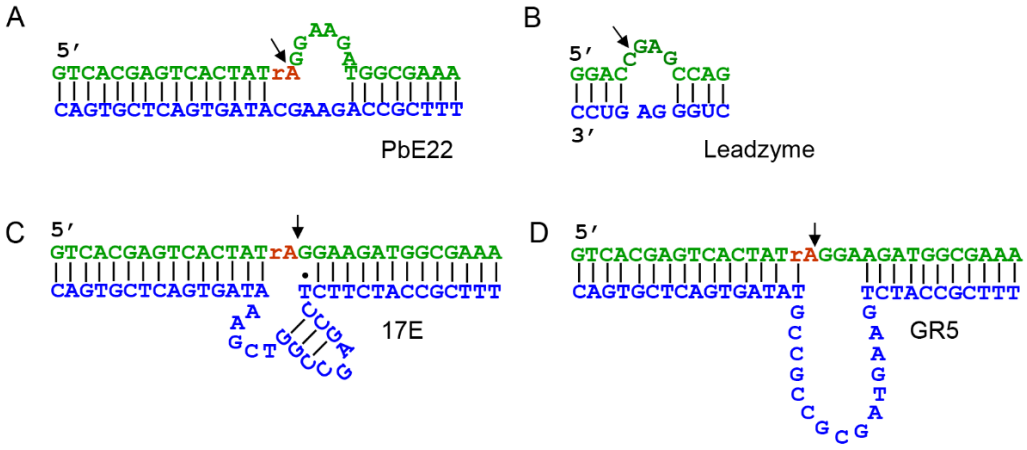

Figure 6.1 The secondary structures of the (A) PbE22, (B) leadzyme, (C) 17E, and (D) GR5 DNAzymes. The enzyme strands are in blue and substrate in green. The cleavage junction is indicated by the arrowheads.

While a few biochemical studies have been carried out on these DNAzymes, only little structure-related information is known.[229,250,308,309] These two Pb^{2+}-dependent DNAzymes (8–17 and GR5) have a similar size, containing 14 or 15 nucleotides in the enzyme loop (Figure 6.1 C and D). Since even two nucleotides can perform the catalytic function in the leadzyme, an interesting question is whether it is possible to achieve similar catalysis in a short DNAzyme.

In this work, both rational design and *in-vitro* selection were employed to search for very short DNAzymes.

6.2 Results and discussion

6.2.1 Rational design of DNAzymes

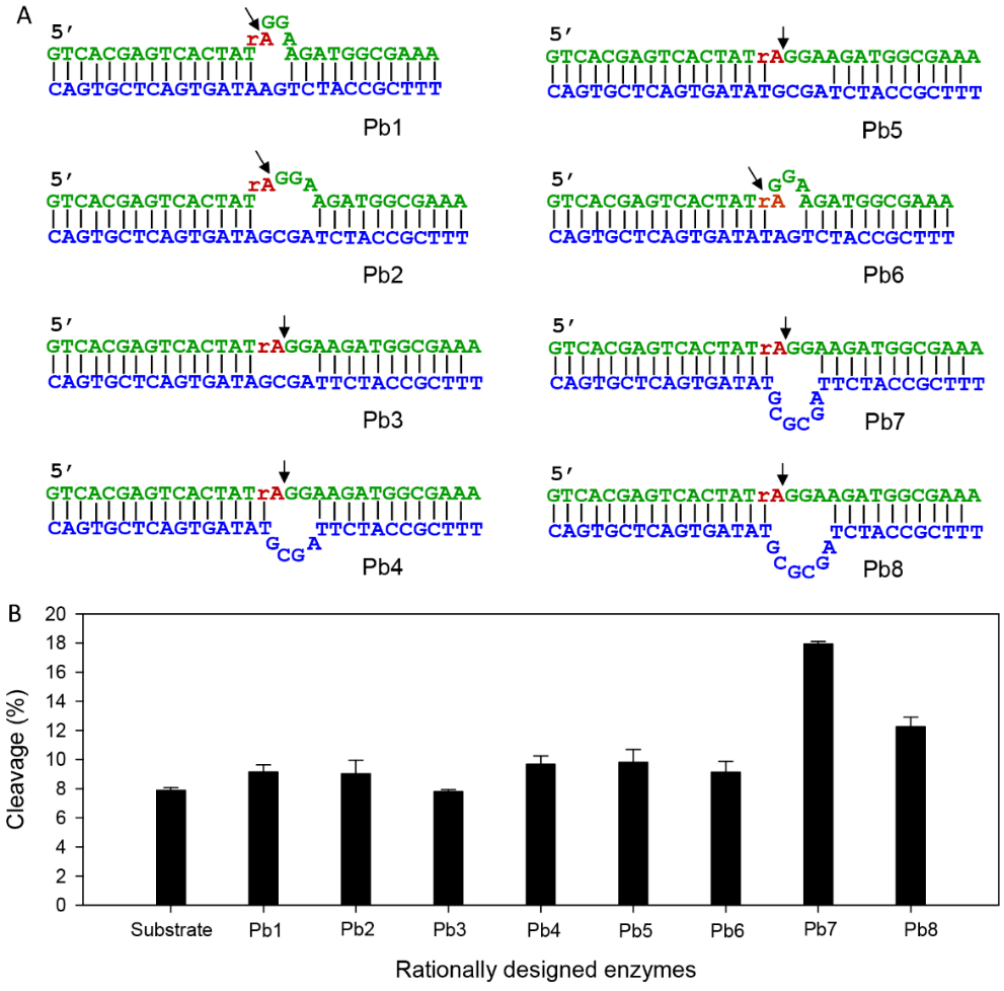

Figure 6.2 (A) The secondary structures of the eight rationally designed DNAzymes. (B) The cleavage yield of these enzymes in the presence of 100 μM Pb^{2+} at pH 7.0 for 2 h.

From the study of the 8–17 and GR5 DNAzymes, it is known that both contain a few highly conserved nucleotides which are important for catalysis.[67,230,250,310,311] In particular, the AG and CG dinucleotides in their enzyme loops have been identified to be critical. The sequence of the leadzyme also contains the unpaired AG in the enzyme loop. Based on these, a few putative DNAzyme sequences were designed which can bind to the substrate (Figure 6.2 A). However, when these sequences were assayed in the presence of 100 μM Pb^{2+} at pH 7.0 for 2 h, very low amount of cleavage was observed (Figure 6.2 B). The fastest Pb7 has a rate of only 0.05 h^{-1}, which is close to the background RNA cleavage rate by Pb^{2+} (vide infra) and is significantly slower than that of the leadzyme. Therefore, a simple combination of such nucleotides is insufficient for catalysis.

6.2.2 *In-vitro* selection

Since rational design failed to produce sufficiently active DNAzymes, *in-vitro* selection was carried out. The schematic of the protocol of *in-vitro* selection is shown in Figure 6.3 A. Since it is difficult to predict the optimal minimal length of the enzyme loop and the number of unpaired nucleotides in the substrate strand, instead of using a very short randomized region, a library containing 35 random nucleotides was employed. It can be reasoned that a larger size can offer more flexibility and sequence diversity. If shorter DNAzymes exist, they may still be reflected in the final library, by hiding redundant sequences as overhangs or hairpins. The library design is shown in Figure 6.3 B. A single RNA linkage (rA) is embedded in this DNA library to serve as the cleavage site. Since RNA is about 1-million-fold less stable compared to

DNA,[312] therefore, the cleavage is most likely to take place at the RNA position. This library was incubated with Pb^{2+} and the cleaved sequences were separated from the rest using gel electrophoresis, and amplified by two rounds of PCR to seed for the next round of selection (Figure 6.3 A). A reaction condition of 60 μM Pb^{2+} for 1 h was pursued up to the 5th round. The incubation time was reduced to 5 min in round 6, which was then subjected to sequencing. The cleavage yield at each round is shown in Figure 6.3 C.

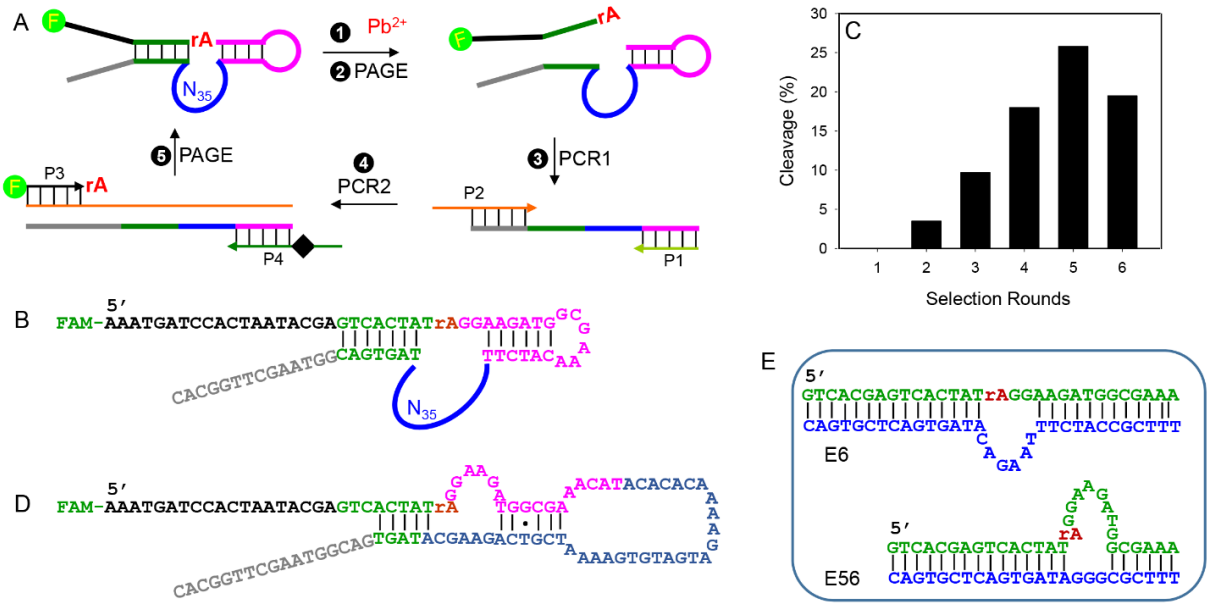

Figure 6.3 (A) Schematic of the *in-vitro* selection procedure. The library contains 35 random nucleotides (N35) and a single RNA linkage (rA) serving as the cleavage site. Sequences cleaved by Pb^{2+} are amplified by two PCR steps to seed the next round of selection. (B) The secondary structure of the library used for *in-vitro* selection. (C) Selection progress at each round. (D) The secondary structure of the original cis-cleaving enzyme (it has been engineered to the trans-cleaving PbE22 enzyme shown in Figure 6.1 A). (E) Two other examples of short DNAzyme candidates from the selection, but they are inactive.

It is interesting to note that while the first DNAzyme selection was carried out using Pb^{2+} (which resulted in GR5), it has not been used as a metal cofactor in any subsequent selections. Therefore, this work represents a second example of such an effort. The selection condition used is also quite different from the previous one. While GR5 was selected using 1 mM PbOAc in a high salt buffer (0.5 M NaCl, 0.5 M KCl, 50 mM $MgCl_2$ at pH 7),[67] this selection used only 60 μM Pb^{2+} in a low salt buffer (25 mM NaCl at pH 6.0). The selection was not pushed for very fast enzymes since the aim was to obtain shorter DNAzymes, which may not cleave very efficiently. In other words, the goal was to maximize sequence diversity in the resulting library.

6.2.3 Sequence analysis

Traditionally, at the end of *in-vitro* selection, the selected library is cloned into plasmid vectors and transformed into the bacterial cells which are further grown and disrupted for isolating the amplified plasmids. These purified plasmids are then subjected to sequencing. Although, the method is widespread in usage, it poses certain limitations upon the number of sequences and diversity of sequences that can be obtained. As a result, only a small fraction of the selected library and mostly the most abundant sequences can be obtained. This leads to loss of valuable information regarding the selection and can prove to be a great hindrance in the discovery of new enzymes. However, the technology of deep sequencing is bringing about a revolution in this area. Through this, thousands of sequences can be obtained from the selected library which can further be subjected to clustering based on their sequence similarities. This would help in

searching for very short DNAzymes, which may not be highly active and may not represent the major population in the library.

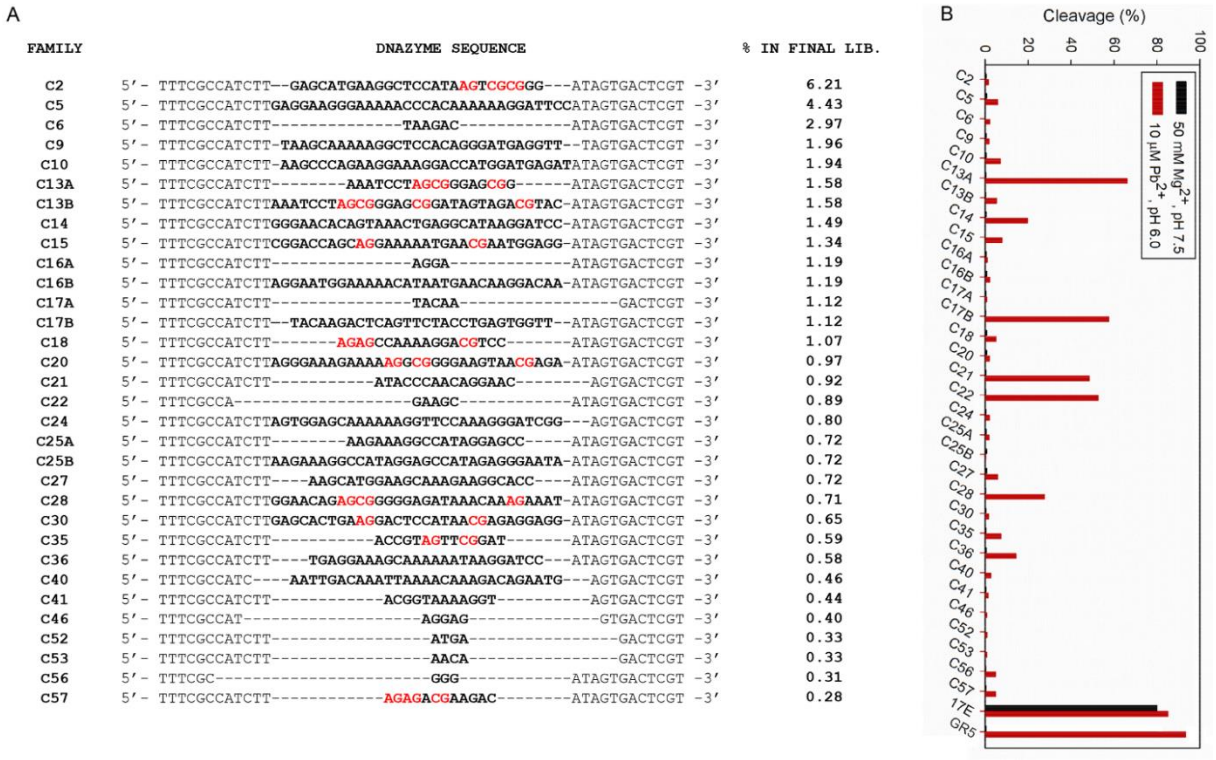

Figure 6.4 (A) Sequences of 32 putative DNAzymes tested from the selected library, and their abundance. The nucleotides that can be aligned with the conserved nucleotides in GR5 are marked in red. (B) The cleavage fraction after 1 h of reaction for the 32 trans-cleaving enzymes, tested with 10 µM Pb^{2+} (red) and 50 mM Mg^{2+} (black). The 8-17 and GR5 DNAzymes are also included for comparison.

From the sequencing results of the final library (round 6), a total of 32,144 sequences were obtained, and an exhaustive search was carried out among all possible sequences. The sequenced library was aligned into different families based on their sequence similarity, and quite high sequence diversity was observed. Even the most abundant family of DNAzyme

represents only 6.79 % of the final sequences. The sequences from the first ninety families (76.4 % of the total sequences) were individually folded using Mfold.[313] Out of these, 32 of the resulting trans-cleaving enzymes display a reasonable fold, and their trans-cleaving sequences are shown in Figure 6.4 A. These sequences represent 46.3 % of the ninety families analyzed and 35.4 % of the total sequences. Some of them have the bases 5′–AGCG–CG–3′ conserved exactly as they are in GR5, while a few have nucleotide insertions, mutations, or deletions from these conserved ones. Each of these 32 sequences were tested with 10 μM Pb^{2+} and 50 mM Mg^{2+}, one at a time. Their cleavage fraction after 1 h is plotted in Figure 6.4 B. Interestingly, like GR5, cleavage was observed only with Pb^{2+}, while unlike the 8–17 DNAzyme, none of them was active with Mg^{2+}.

6.2.4 Introduction to PbE22

Since the goal of this work is to identify very short DNAzymes, after the general understanding of the activity of all representing sequences, very short enzyme loops were focused on. Out of the many sequences, only one short enzyme (family C22 in Figure 6.4 A) was found to exhibit decent activity, achieving 50 % cleavage (Figure 6.4 B). This enzyme motif has appeared 285 times out of the 32,144 sequences. This DNAzyme its cis-cleaving form is shown in Figure 6.3 D, and the trans-cleaving construct is shown in Figure 6.1 A, which was re-named to be PbE22. PbE22 has 5 nucleotides 5′GAAGC 3′ in the catalytic loop of the enzyme and 6 unpaired nucleotides in the substrate strand 5′rAGGAAGA 3′ including the cleavage dinucleotide junction. It is interesting to note that most of these unpaired nucleotides are purines. Aside from

PbE22, two other sequences can also fold into a short enzyme loop structure (Figure 6.3 E). However, they are inactive when tested with Pb^{2+}. Therefore, PbE22 was used for subsequent studies.

6.2.5 Rate kinetics of PbE22

To characterize this new DNAzyme, biochemical studies were performed.

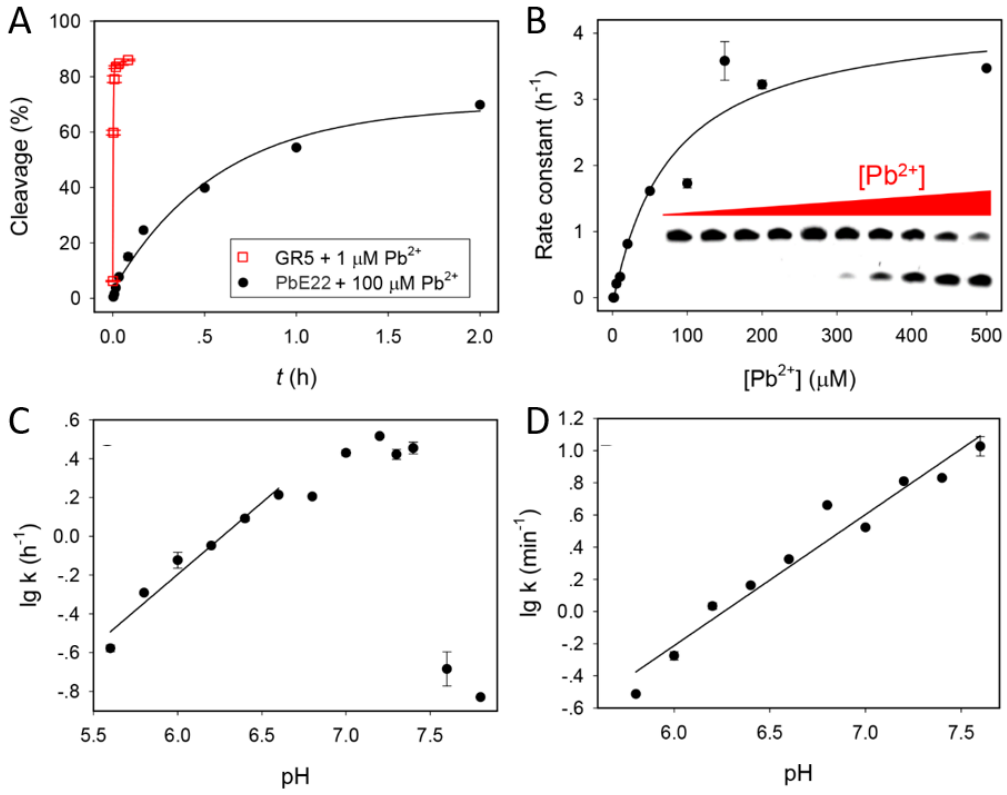

Figure 6.5 Biochemical characterization of PbE22. (A) Kinetics of PbE22 and GR5 cleavage at pH 7.0. (B) Cleavage rate constant of PbE22 as a function of $[Pb^{2+}]$ at pH 7.0. Inset = gel showing cleavage at various $[Pb^{2+}]$ after 30 min at pH 6.5. Log scale plot of the rate as a function of pH for (C) PbE22 with 20 µM Pb^{2+} and (D) GR5 with 1 µM Pb^{2+}.

First, the cleavage kinetics of PbE22 was measured in the presence of 100 μM Pb^{2+} (Figure 6.5 A, black dots). The time-dependent cleavage yield can be fitted to first-order reaction kinetics with a rate constant of 1.7 h^{-1}. Under the same condition, the free substrate was cleaved at a rate of 0.0082 h^{-1}. Therefore, the rate enhancement brought by PbE22 in the presence of 100 μM Pb^{2+} at pH 7.0 is 210-fold. For comparison, the GR5 DNAzyme (Figure 6.5 A, red dots) has a reported rate enhancement of 105,[67] while the leadzyme has a rate enhancement of 1100.[297] Therefore, PbE22 has the lowest catalytic efficiency, and GR5 has the highest. The inset of Fig. 6.5 B is a gel image showing the cleavage yield at 30 min with increasing Pb^{2+} concentrations. Indeed, more Pb^{2+} induced more cleavage, confirming that PbE22 is a Pb^{2+}-dependent DNAzyme. To quantitatively understand the effect of Pb^{2+} concentration, the enzyme kinetics was measured at various Pb^{2+} concentrations at pH 7.0 (Figure 6.5 B, black dots). An apparent dissociation constant (K_d) of 77 μM Pb^{2+} was obtained. For comparison, the leadzyme has a rate of 0.4-0.5 min^{-1} at 25 μM Pb^{2+} and pH 7.0. This is faster than PbE22 but less as compared to GR5.[296] This comparison suggests that a bigger catalytic loop might be required for optimum activity of the enzyme.

6.2.6 pH-dependency of PbE22

To further characterize this enzyme, the DNAzyme rate was studied with increasing pH at 20 μM Pb^{2+} concentration. Again it was compared to that of the GR5 at 1 μM Pb^{2+}. In case of PbE22, the log of rate increased linearly with increasing pH in the low pH region with a slope of 0.74 (Figure 6.5 C). Beyond pH 7.0, the increase in rate slowed down. The slope of GR5 was

calculated to be 0.82 and it maintained a good linearity up to pH 7.6 (Figure 6.5 D). Beyond pH 7.6, the rate was not measurable since it was too fast for manual pipetting. The reason for the narrower linear range for PbE22 might be related to the use of higher Pb^{2+} concentration (20 μM), as Pb^{2+} tends to precipitate more easily at such a high concentration. Similar to PbE22, the leadzyme also exhibits a linear increase in log (rate) with increase in pH up to 7.0 at 25 μM Pb^{2+}. Therefore, this indicates all these enzymes have a similar mechanism in terms of a single deprotonation at the rate-limiting step of this reaction, and this is often directly or indirectly linked to the deprotonation of the 2′-OH at the cleavage site.

6.2.7 Metal specificity of PbE22

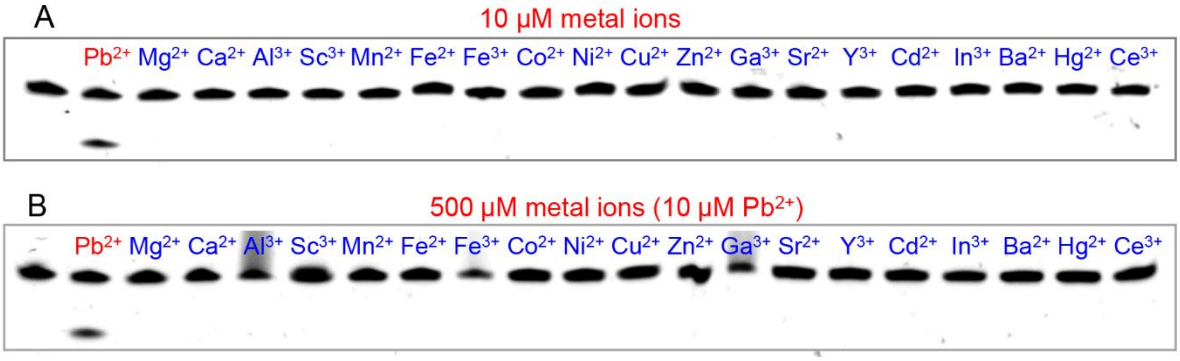

Figure 6.6 Metal specificity test of the PbE22 DNAzyme in the presence of (A) 10 μM and (B) 500 μM of all the metals compared to 10 μM of Pb^{2+} at pH 6.2.

Metal specificity tests were carried out on PbE22. First, the cleavage of the substrate was studied in the presence of an array of divalent and trivalent metal ions (10 μM each, Figure 6.6 A) and found that like GR5, PbE22 too has a high selectivity for Pb^{2+}. Furthermore, even with

500 μM of other metals still no observable activity was found (Figure 6.6 B). Therefore, PbE22 is also highly specific for Pb^{2+}. For comparison, GR5 has excellent selectivity for Pb^{2+}, and an impressive fact is that GR5 is inactive even with 50 mM Mg^{2+}. However, the 8–17 DNAzyme is quite active with such a high concentration of Mg^{2+} (1.6 min^{-1}).[111,250,314] It is worth mentioning here that up to 0.5 mM Pb^{2+} and 50 mM Mg^{2+} was tested for PbE22. Based on a rough estimation, at the same metal concentration, the rate of Pb^{2+} is 33,800-fold faster than that of Mg^{2+} for cleaving the 17E DNAzyme.[250] This difference is even larger for the GR5 DNAzyme. Since PbE22 is much slower, it would require over 1 M of Mg^{2+} to conclude that PbE22 is inactive with Mg^{2+}, if 17E is used as the standard. PbE22 was tested with 4 M Mg^{2+} and found that it has no cleavage as well (data not shown). Therefore, PbE22 is highly specific for Pb^{2+}.

6.3 Summary

Within this study, the aim was to obtain a very short RNA-cleaving DNAzyme. To achieve this goal, both rational design and *in-vitro* selection were performed. Multiple important outcomes and observations resulted from the above study. Firstly, a very short RNA-cleaving DNAzyme that uses Pb^{2+} as a cofactor named PbE22 was isolated. PbE22 contains only 5 nucleotides in its catalytic loop, and has a rate enhancement of ~200-fold which is lower as compared to that of the leadzyme or the GR5 DNAzyme. PbE22 DNAzyme gives an example for the better understanding of the effect of the size of the catalytic loop on the activity of DNAzyme. This study indicates that although site-specific and metal-specific catalysis is possible with short

loops, the presence of extra nucleotides is probably needed for optimal activity. It suggests the significance of bigger catalytic loops for better folding or scaffolding for utilizing the metal cofactor. For example, in the 8–17 DNAzyme, in addition to the four nucleotides identified to be critical for the cleavage reaction, additional nucleotides are found to have other roles to assist DNAzyme.[311,314] In PbE22, the number of nucleotides on the enzyme strand is very limited. At the same time, DNA lacks the structural versatility present in RNA due to the lack of the 2′-OH group, which may explain the faster cleavage by the leadzyme despite its even smaller size. Secondly, with the help of deep sequencing technology, a comprehensive understanding of the diversity and abundance of each sequence family was obtained, and variations within each type of family were also dug out and analyzed. As a result, multiple sequences that are active with lead are reported. Thirdly, PbE22 was demonstrated to have excellent selectivity for Pb^{2+} against 500 μM of all the divalent and trivalent metal ions tested. Also, all the catalytically active sequences obtained from the rest of the library too, were shown to be active with Pb^{2+} but not with Mg^{2+}. Fourthly, by performing pH-dependent kinetic studies, it was deduced that PbE22 undergoes a single deprotonation at the rate-limiting step, and in this respect the DNAzymes PbE22, leadzyme and GR5 share a similar cleavage mechanism. This study has provided insights into the significance of the size of the DNAzymes, Pb^{2+}-dependent activity, and metal specificity. The PbE22 DNAzyme is not a very efficient DNAzyme, but it may provide a scaffold for studying Pb^{2+} binding to DNAzyme given its much smaller size. This DNAzyme can be used for spectroscopic and structural analysis, as these experiments have been difficult to carry out with the current DNAzymes that bear relatively large catalytic loops.

6.4 Materials and methods

6.4.1 Chemicals

The DNA library for *in-vitro* selection, related primers, and fluorophore/quencher modified DNAs were purchased from Integrated DNA Technologies (IDT, Coralville, IA). The sequences of DNA used in this selection are listed in Table 6.1. The trans-cleaving enzyme strands and their mutants were from Eurofins (Huntsville, AL). Metal ions that were used for analysis include silver(I) nitrate, potassium(I) chloride, lithium(I) chloride, thallium(I) chloride, lead(II) acetate, magnesium(II) sulfate, manganese(II) chloride tetrahydrate, iron(II) chloride tetrahydrate, cobalt(II) chloride hexahydrate, copper(II) chloride dehydrate, zinc(II) chloride, calcium(II) chloride, nickel(II) chloride, strontium(II) chloride, cadmium(II) chloride, mercury(II) perchlorate, yttrium(III) chloride hexahydrate, gallium(III) chloride, cerium(III) chloride, iron(III) chloride hexahydrate. All these salts were purchased from Sigma-Aldrich except the iron was purchased from Alfa Aesar. The purity of the metals used is 99.99 %. Their solutions were made by directly dissolving their salts in water. Tris (Hydroxymethyl) aminomethane (Tris), 2-(N-morpholino) ethanesulfonic acid (MES) free acid monohydrate, 3-(*N*-morpholino) propanesulfonic acid (MOPS), 4-(2-Hydroxyethyl)piperazine-l-ethanesulfonic acid (HEPES), EDTA disodium salt dehydrate, sodium chloride, sodium bromide, sodium iodide and ammonium acetate were purchased from Mandel Scientific Inc. (Guelph, Ontario, Canada). Acrylamide/bisacrylamide 40 % solution (29:1), urea, and 10 X TBE solution were purchased from Bio Basic Inc. SsoFast EvaGreen supermix was purchased from Bio-Rad for real-time PCR analysis. T4-DNA ligase, deoxynucleotide (dNTP) solution

mix, Taq DNA polymerase with ThermoPol buffer, and low molecular weight DNA ladder were purchased from New England Biolabs. All metal ions, buffer and gel stock solutions were prepared with Milli-Q water. The pH of the buffers was measured with Denver Instrument UltraBasic pH meter.

Table 6.1 List of DNA sequences used in Appendix A (chapter 6).

DNA	Sequence (5′ – 3′)
Lib-FAM-N_{35}	CTGCAGAATTCTAATACGAGTCACTATrAGGAAGATGGCGAAACAT CTTNNNNNNNNNNNNNNNNNNNNNNNNNNNNNNNNNTAGTCG GTAAGCTTGGCAC
Lib-rA	AATACGAGTCACTATrAGGAAGAT
Splint DNA	AAGATGTTTCGCCATCTTCCTATAGTCCACCACCA
Primer P1	CTGCAGAATTCTAATACGAGTCACTATAGGAAGATGGCGAAACA
Primer P2	GTGCCAAGCTTACCG
Primer P3	FAM- AAATGATCCACTAATACGAGTCACTATrAGG
Primer P4	AACAACAACAAC-S-GTGCCAAGCTTACCG
Primer P701	CAAGCAGAAGACGGCATACGAGATTCGCCTTAGTGACTGGAGTTC AGACGTGTGCTCTTCCGATCTCTGCAGAATTCTAATACGAGTCAC
Primer P501	AATGATACGGCGACCACCGAGATCTACACTAGATCGCACACTCTTT CCCTACACGACGCTCTTCCGATCTGTGCCAAGCTTACCG
Substrate	GTCACGAGTCACTATrAGGAAGATGGCGAAA-FAM
C14	TTTCGCCATCTTGGGAACACAGTAAACTGAGGCATAAGGATCCAT AGTGACTCGT
C15	TTTCGCCATCTTCGGACCAGCAGGAAAAATGAACGAATGGAGGAT AGTGACTCGT
C16A	TTTCGCCATCTTAGGAATAGTGACTCGT

C16B	TTTCGCCATCTTAGGAATGGAAAAACATAATGAACAAGGACAAATAGTGACTCGT
C17A	TTTCGCCATCTTTACAAGACTCGT
C17B	TTTCGCCATCTTTACAAGACTCAGTTCTACCTGAGTGGTTATAGTGACTCGT
C18	TTTCGCCATCTTAGAGCCAAAAGGACGTCCATAGTGACTCGT
C20	TTTCGCCATCTTAGGGAAAGAAAAAGGCGGGGAAGTAACGAGAATAGTGACTCGT
C21	TTTCGCCATCTTATACCCAACAGGAACAGTGACTCGT
C22	TTTCGCCAGAAGCATAGTGACTCGT
C24	TTTCGCCATCTTAGTGGAGCAAAAAAGGTTCCAAAGGGATCGGAGTGACTCGT
C25A	TTTCGCCATCTTAAGAAAGGCCATAGGAGCCATAGTGACTCGT
C25B	TTTCGCCATCTTAAGAAAGGCCATAGGAGCCATAGAGGGAATAATAGTGACTCGT
C27	TTTCGCCATCTTAAGCATGGAAGCAAAGAAGGCACCATAGTGACTCGT
C28	TTTCGCCATCTTGGAACAGAGCGGGGGAGATAAACAAAGAAATATAGTGACTCGT
C30	TTTCGCCATCTTGAGCACTGAAGGACTCCATAACGAGAGGAGGATAGTGACTCGT
C35	TTTCGCCATCTTACCGTAGTTCGGATATAGTGACTCGT
C36	TTTCGCCATCTTTGAGGAAAGCAAAAAATAAGGATCCATAGTGACTCGT
C40	TTTCGCCATCAATTGACAAATTAAAACAAAGACAGAATGAGTGACTCGT
C41	TTTCGCCATCTTACGGTAAAAGGTAGTGACTCGT
C46	TTTCGCCATAGGAGGTGACTCGT
C52	TTTCGCCATCTTATGAGACTCGT

C53	TTTCGCCATCTTAACAGACTCGT
C56	TTTCGCGGGATAGTGACTCGT
C57	TTTCGCCATCTTAGAGACGAAGACATAGTGACTCGT

6.4.2 *In-vitro* selection

For this *in-vitro* selection experiment, the initial DNA library was prepared by ligating two pieces of DNA (Lib-FAM-N_{35} and Lib-rA) with a splint DNA (see Table 6.1 for complete DNA sequences). Lib-FAM DNA (200 pmol) and Lib-rA DNA (300 pmol) were mixed with splint DNA (300 pmol) first in buffer A (50 mM pH 7.5 Tris-HCl, pH 7.5, 10 mM $MgCl_2$). The three strands of DNA were annealed at 95 °C for 1 min followed by slow cooling to room temperature. The T4 ligation protocol provided by New England Biolabs was followed for the ligation reaction. The ligated DNA product was purified with 10 % denaturing polyacrylamide gel (dPAGE) at 650 V for 80 min and the DNA was extracted from the gel with buffer B (1 mM EDTA, 10 mM Tris-HCl, pH 7.0). The extracted DNA library was further concentrated via ethanol precipitation and re-suspended in 60 μL of buffer C (50 mM MES, pH 6.0, 25 mM NaCl), which was the selection buffer. This DNA was used directly as the DNA library for the first round of selection. For each of the subsequent round, the library was generated from PCR. For the *in-vitro* selection experiment, the random DNA pool was incubated with final concentration of 10 μM freshly prepared $AgNO_3$ metal ion for 60 min. After incubation, the reaction was quenched with 8 M urea and was purified in 10 % dPAGE. A fraction of the selected DNA was extracted from the gel and further purified with a Sep-Pak C18 column

(Waters). The purified selected DNA was then dried in an Eppendorf Vacufuge at 30 °C overnight. The dried DNA was re-suspended in 60 µL of 5 mM HEPES buffer (pH 7.5). A small fraction of this DNA was amplified by two rounds of PCR (PCR1 and PCR2) using thermo-cycling conditions described in section 2.4.3.

6.4.3 Deep sequencing

To prepare sample for deep sequencing, the round 6 library was subjected to PCR1 as explained above in section 2.4.3. The full-length library generated from this step was subjected to another PCR reaction so that the Illumina sequencing technology can be used. The forward primer (P701) and the reverse primer (P501), each containing a unique index sequence were used (see Table 7.1 for complete sequences). The PCR product was purified with 2 % agarose gel and extracted using a gel extraction kit (IBI Scientific). The extracted DNA was eluted in 25 µL Milli-Q water and the concentration was quantified using a NanoDrop spectrophotometer. The sequencing was performed at McMaster Genomics Facility, Mc Master University, Hamilton, Ontario, Canada.

6.4.4 Activity assays

For a typical gel-based activity assay, the DNAzyme complex were prepared by annealing the FAM-labeled substrate (10 µM) and enzyme (30 µM) in buffer 50 mM MES (pH 6.0, 25 mM NaCl) by heating at 85 °C for 1 min and then slowly cooled at room temperature until ~30 °C.

The complex was then frozen at -20 °C for at least 2 hours. To initiate the reaction at room temperature, a final of 10 - 100 μM Pb^{2+} or another metal ion (as required) was incubated with 1 μM DNAzyme complex in a total 10 μl reaction mixture in buffer 50 mM MES (pH 6.0 - 6.5) / 50 mM MOPS (pH 7.0 – 8.0) with salt concentration 25 mM NaCl, for the required time ranging from 10 s – 8 h. The samples were quenched with 8 M urea at designated time points and run in 15 % dPAGE at 120 V for 80 min. The gel images were taken with Bio-Rad ChemiDoc MP imaging system. For determining the rate of cleavage, the gel band intensities of the cleaved vs. uncleaved substrate were quantified and the data obtained were fitted (using *Sigma Plot 12.0*) according to the first-order rate equation $Y_t = Y_o + a(1-e^{-kx})$, where Y_t and Y_o are the cleavage fractions at a given reaction time '*t*' or '*0*' min, respectively, '*a*' is a constant i.e. the scaling parameter and '*k*' is the observed rate constant.

7. Appendix B: Chapter 7 - A comparison of two classic Pb^{2+}-dependent RNA-cleaving DNAzymes[e]

7.1 Introduction

DNAzymes are catalysts made of DNA. They are attractive molecules due to excellent stability, high catalytic efficiency, programmability, and ease of modification.[207,315–318] DNAzymes have found a diverse range of applications in anti-viral research,[111] nanotechnology,[319] organic synthesis,[320] and biosensor development.[275] With limited chemical functionality and a highly negatively charged backbone, DNAzymes often need to recruit metal ions for catalysis and different metal ions may prefer different DNA sequences.[102,212,289] This field has grown tremendously by studying the Pb^{2+}- specific DNAzymes. The first DNAzyme (named GR5) was selected in the presence of Pb^{2+} in 1994.[67] GR5 had not attracted much attention then, since the initial DNAzyme research was focused on RNA cleavage (e.g. anti-viral applications). GR5 cannot cleave all-RNA substrates, it only cleaves DNA/RNA chimera.[67] Three years later, the landmark paper by Santoro and Joyce reported two general-purpose RNA-cleaving DNAzymes.[111] One of them is called the 8–17 DNAzyme. A variant of it, 17E, is highly active with Pb^{2+}.[113] Since then, 17E has been coupled to many signaling mechanisms to develop biosensors.[113,321–324] The GR5 DNAzyme recently revived as a biosensor,[308,325] since the Lu group reported its exceptionally high selectivity for Pb^{2+} (much better than 17E).[306] It is also

[e] This chapter is the basis for a published manuscript: Saran R.; Liu, J. A comparison of two classic Pb^{2+}-dependent RNA-cleaving DNAzyme. *Inorg. Chem. Front.,* **2016**, 3, 493-501.

interesting to note that Pb^{2+} is active with many other DNAzymes,[100,101] especially at above neutral pH. Another intriguing observation is that 17E occurred from at least six independent selections,[111,112,118,119,307,328,329] but GR5 was reported only once.[67] GR5 and 17E form a good pair for comparison, since both have the highest activity with Pb^{2+}. Both are small DNAzymes with only ~15 nucleotides in the catalytic core and share the same substrate sequence. Extensive biochemical,[111,250,310,311,326] and spectroscopic studies have been carried out on 17E.[228,229,238,264,327] In particular, many active 17E mutants have been identified.[230,307,311] However, relatively little is known regarding GR5.[67,108,306,308] A closer examination of these two DNAzymes indicates that they contain similar conserved nucleotides. Therefore, an interesting question is whether they bear similar metal binding pockets or work with the same mechanism (e.g. they are just mutants). In this work, the aim is to answer such fundamental questions based on a side-by-side comparison of 17E and GR5, and to gain a deeper understanding of the structure-activity relationship of GR5.

7.2 Results and discussion

7.2.1 17E mutation studies

The secondary structures of the 17E and GR5 DNAzymes are shown in Figure 7.1 A and B, respectively. They share the same substrate sequence (in green). The cleavage junction is 5′rAdG 3′ (see the arrowhead). Here, rA means ribo-adenosine, which is the only RNA linkage in the substrate. Each enzyme binds the substrate via two base paired arms, and the

catalytically important nucleotides are located in the bulged loops. In the presence of Pb^{2+}, the phosphodiester bond linking, the rA·G is cleaved. With extensive biochemical studies, four highly conserved nucleotides have been identified in 17E (A6, G7, C13, and G14, highlighted in blue, Figure 7.1 A). Mutation to any of them leads to over 100-fold decrease in activity.[230,307,311]

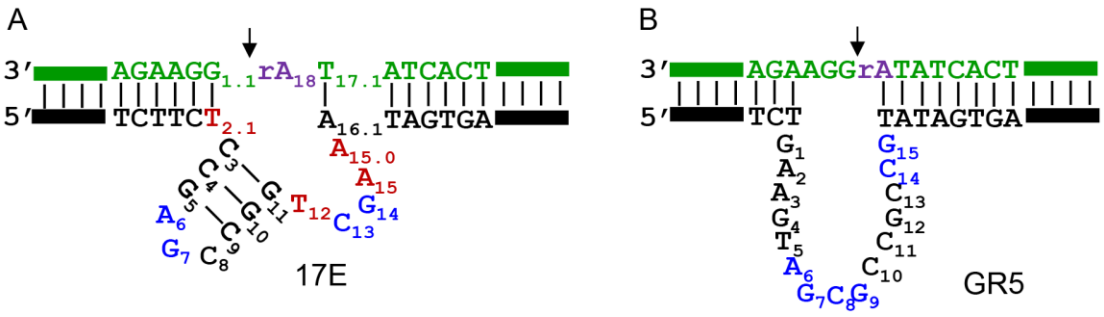

Figure 7.1 The secondary structures of (A) the 17E and (B) the GR5 DNAzymes. The top green strands are the substrates and these two DNAzymes have the same substrate sequence. The arrowheads point at the cleavage junction. The important nucleotides are numbered. The blue nucleotides are highly conserved. The four red nucleotides in 17E are important with this particular rA·G dinucleotide junction at the cleavage site to reach optimal activity.

The 17E DNAzyme has the highest activity with Pb^{2+}, but it is also active with high concentrations of many other metals such as Mg^{2+}, Ca^{2+}, Mn^{2+}, Cd^{2+} and Zn^{2+}. For 17E assays, Mg^{2+} has been the most common metal cofactor.[111,310,314] However, GR5 has no activity with 50 mM to 1 M Mg^{2+}.[108,306] For a meaningful comparison, Pb^{2+} was used as the common metal here. Pb^{2+} has a much higher apparent binding constant and can be used at much lower concentrations.[250] This would confer less perturbation to the properties of DNA. Pb^{2+} also has

a well-established nucleotide coordination chemistry,[3,330,331] making it easier to probe metal binding sites. Although very rich information is available for 17E with Mg^{2+}, it was needed to first confirm whether these can be applied to Pb^{2+}. For this purpose, a mutation study was performed with 17E in the presence of Mg^{2+} and Pb^{2+}. Each of the four highly conserved nucleotides (highlighted in blue in Figure 7.1 A) was mutated, and the cleavage rate was measured. The wild type 17E has a rate of 0.44 min^{-1} with 10 mM Mg^{2+} at pH 7.6 and a gel image is shown in the inset of Figure 7.2 A. All the mutations significantly reduced activity (Figure 7.2 A).

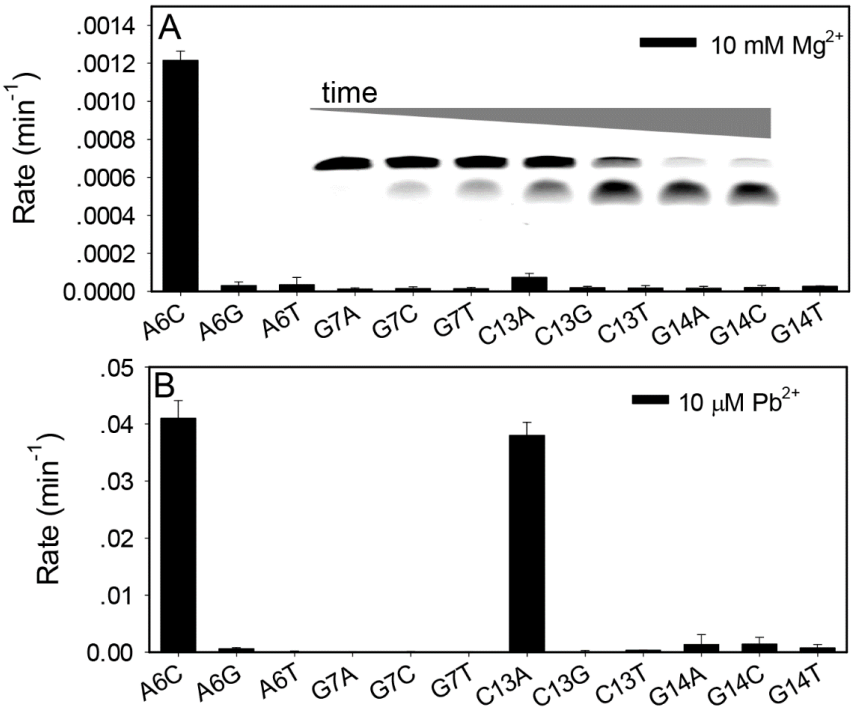

Figure 7.2 Activity of the 17E mutants in the presence of (A) 10 mM Mg^{2+} or (B) 10 μM Pb^{2+}. The buffer is 50 mM HEPES, pH 7.6 with 25 mM NaCl. The wild-type 17E activity is 0.44 min^{-1} with 10 mM Mg^{2+} and >11.9 min^{-1} with 10 μM Pb^{2+} (not shown since the scale is very different). Inset of (A): gel image of the wild-type 17E DNAzyme cleavage in 10 mM Mg^{2+}. The time points are 0, 0.25, 0.5, 1, 5, 30 and 60 min.

Even the most active A6C mutant, (e.g. the adenine at position 6 mutated to cytosine) has a rate of only 0.0012 min^{-1}, a ~370-fold drop compared to the wild type. Other mutants barely had any activity, which is consistent with the literature on Mg^{2+}.[250,307,310] The activity of the wild-type 17E is much higher with 10 μM Pb^{2+}, which is estimated to be greater than >11.9 min^{-1} at pH 7.6. Note that the rate is too fast to be accurately measured by manual pipetting. In the presence of Pb^{2+}, two mutations A6C and C13A showed moderate activity (Figure 7.2 B). Again, even for the most active mutant, the rate is still >300-fold less than the wild-type. Therefore, the nucleotides important for Mg^{2+} are also important for Pb^{2+}. It is interesting to note that the C13A mutant is relatively more active with Pb^{2+}, which hints that Pb^{2+} might have better tolerance to mutations.

7.2.2 GR5 mutation studies

After confirming the important nucleotides for Pb^{2+} in 17E, GR5 was studied next. So far, no systematic mutation studies have been carried out on GR5. From its sequence alignment,[67] six highly conserved nucleotides were identified in the original paper by Breaker and Joyce (Figure 7.1 B, in blue). These nucleotides segregate into two groups: four (A6G7C8G9) in the middle and two (C14G15) towards the end. The other nucleotides appear to be less important since their sequence and length can vary while still retaining activity.[67] Therefore, these six conserved nucleotides were focused on first. It is interesting to note that 17E has the conserved AG followed by CG. In GR5, the conserved nucleotides can be considered to be AG followed by CG and another CG. Therefore, it is possible that 17E and GR5 have similar Pb^{2+} binding pockets and even similar mechanisms. These six conserved nucleotides in GR5 were

systematically mutated (Figure 7.3 A). The wild-type GR5 has a rate greater than 10.2 min^{-1} at pH 7.6 with 10 μM Pb^{2+}. The A6C mutant retained a high activity (~2 min^{-1}), but any other mutations to A6 abolished activity. Mutations made to G7 abolished the activity as well. This trend is exactly the same as that in 17E for its A6 and G7. Therefore, these two nucleotides are likely to play the same role in these two DNAzymes. For GR5, C8 can be mutated to A or T (activity almost fully retained) but not G. Any mutations made to G9 abolished the activity. This pattern is however different from that in 17E for its C13G14. On the other hand, the activities of C14G15 mutants in GR5 are comparable with that of the C13G14 in 17E, where only the C14A mutant retained partial activity. Their relative rates are plotted (normalized to the A6C mutant of both DNAzymes) in Figure 7.3 B.

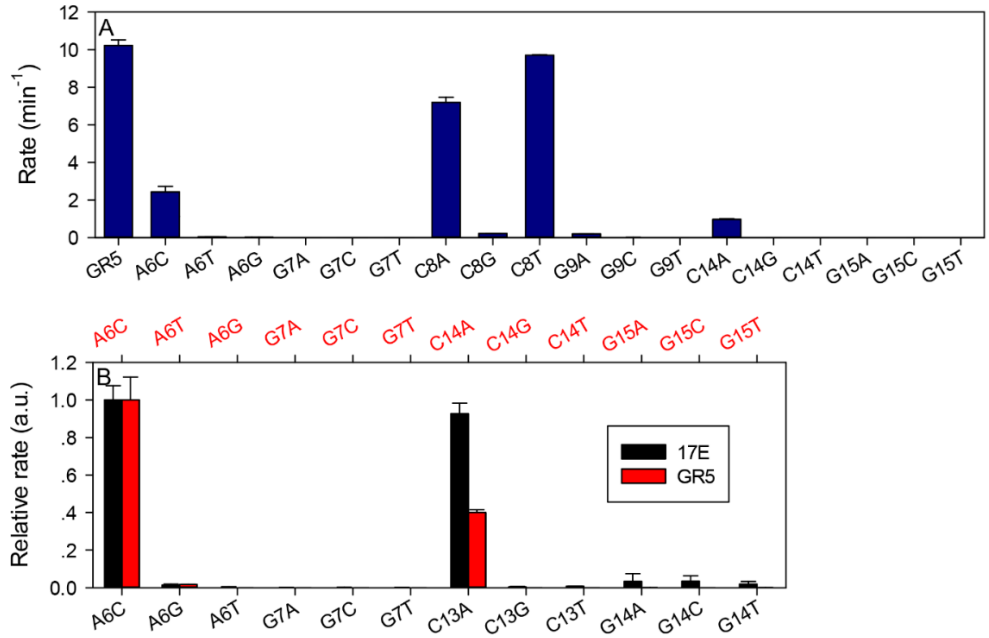

Figure 7.3 (A) Activity of GR5 wild-type and mutants. The activity buffer contained 50 mM HEPES, pH 7.6, 25 mM NaCl and 10 μM Pb^{2+}. (B) Relative activity of the 17E and GR5 mutants at pH 7.6. The rate of 17E is normalized to its A6C mutant (bottom axis) and GR5 is also normalized to its A6C mutant (top axis).

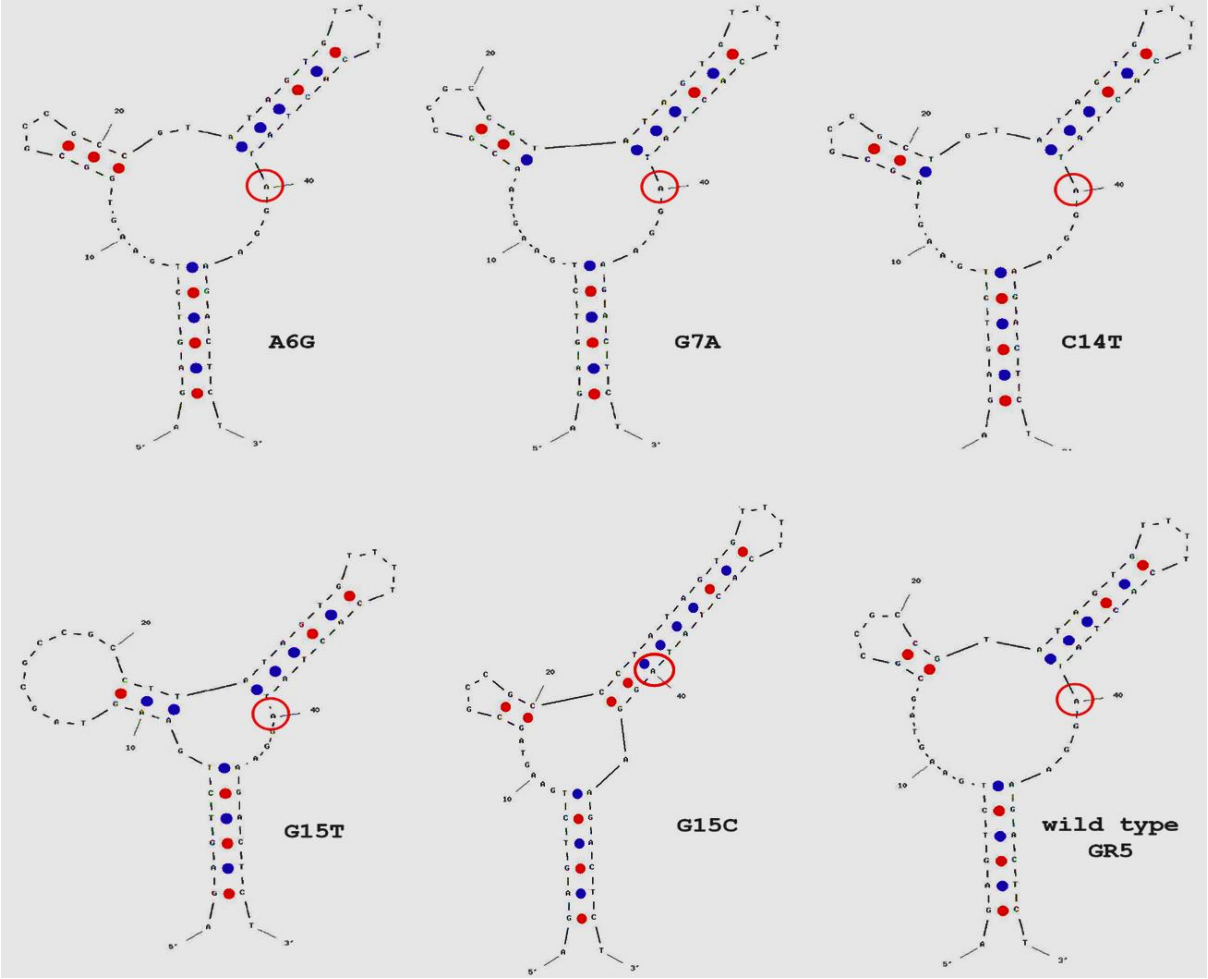

Figure 7.4 Mfold predicted secondary structures from a few GR5 mutants and the wild-type GR5. All the other mutants fold into a structure similar to that for the wild-type GR5 and are not listed here. The cleavage site adenine is marked by the red circle. The substrate and enzyme strands are linked by a TTTT loop. In the wild-type GR5 structure, two G-C base pairs are predicted in the enzyme loop. However, these nucleotides are highly conserved for catalysis and thus are unlikely to be confined in such a hairpin structure. Therefore, the simple loop structure in the original GR5 selection paper was used in this work.[67] Some mutants in this figure have three base pairs in the loop and their misfold (i.e. deviation from the simple loop structure) might also be a reason for their inhibited activity.

Using the 17E mutants as a benchmark, it can be reasoned that A6G7 and C14G15 in GR5 serve similar catalytic roles to their corresponding nucleotides in 17E. It is interesting to note that the GR5 mutants have higher activity, as the rates of the three most active GR5 mutants are greater than 1 min^{-1}, while the 17E mutants under the same conditions are less than 0.05 min^{-1}. The wild-type DNAzymes were compared at pH 5.5, and GR5 is ~4-fold more active, which partially accounts for the 20-fold difference in rate for their mutants. To test whether the mutations can change the folding of the GR5 core, all the mutants were analyzed using Mfold (Figure 7.4).[313] Under the experimental conditions used (25 mM NaCl), the GR5 DNAzyme folds into a structure with a two base-pair hairpin. However, these two base pairs involve the highly conserved C14G15, and therefore, are unlikely to be real. For this reason, the simple loop GR5 secondary structure as shown in the original paper, was followed herein.[67] According to Mfold predictions, most mutants follow the same structure as the original GR5, and the few that showed alternative folding are listed in Figure 7.4 None of these listed mutants are active. For them, misfolding cannot be ruled out as a reason for their inactivity.

7.2.3 Cleavage junction mutations

The above work focused only on the enzyme strands. Previous biochemical assays indicated that the composition of the chimeric dinucleotide junction of the substrate (e.g. rA18·G1.1) is also important.[307,311] In addition to the four highly conserved nucleotides in 17E, the ones marked in red are also conserved (T2.1, T12, A15 and A15.0) to effectively cleave the rA18·G1.1 junction (Figure 7.1 A).

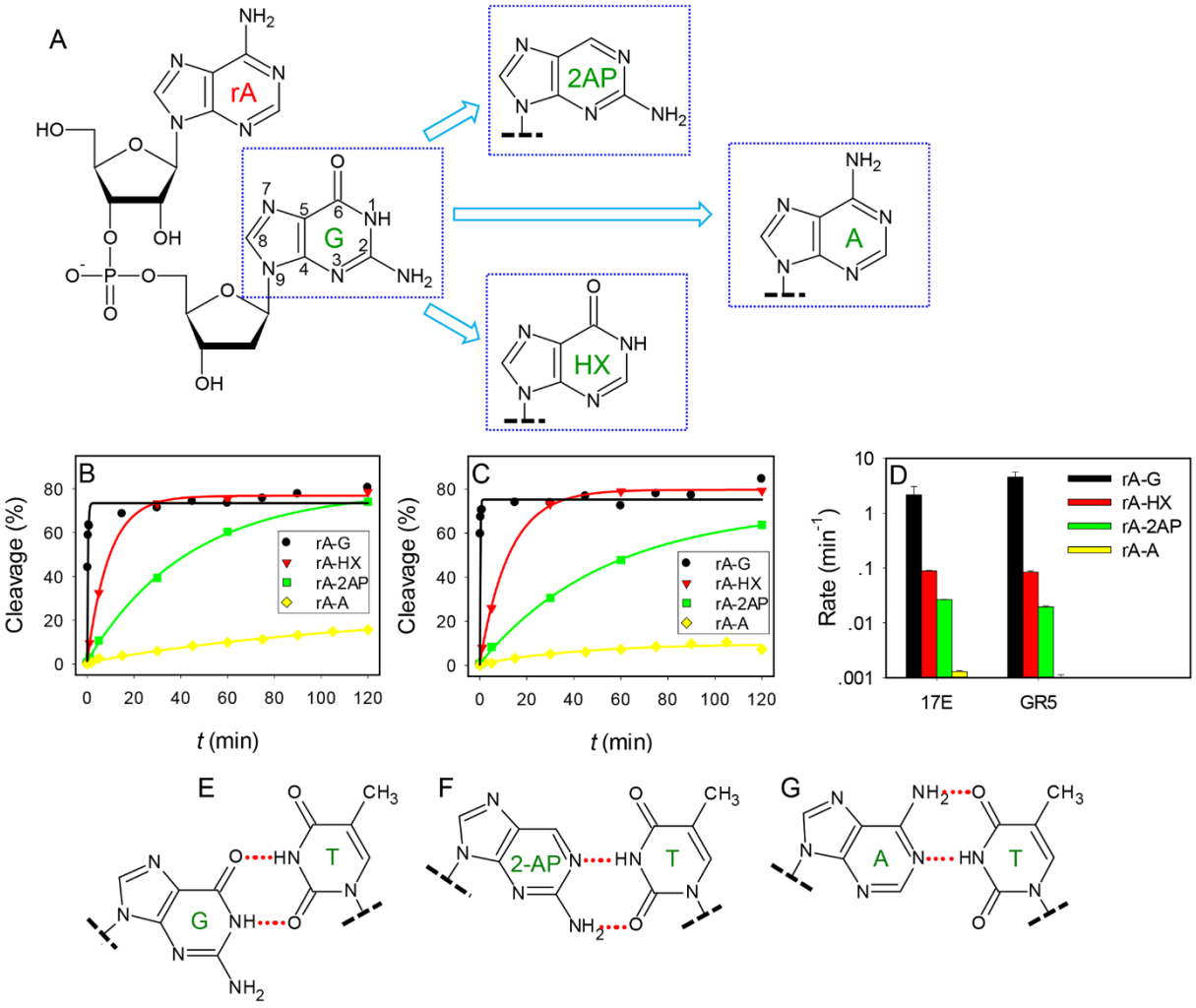

Figure 7.5 (A) Structure of the dinucleotide junction rA·G at the cleavage site, and the mutation of the G to 2AP, HX, or A. Kinetics of cleavage of the junctions at pH 6 with (B) 17E, or (C) GR5. (D) The summary of the cleavage rate. Note the y-axis is on log scale. (E) The typical wobble G·T pairing in the wild-type substrate-enzyme complex. 2AP base pairing with (F) T, and the (G) canonical Watson-Crick base A-T pairing in the mutants. The G-HX pairing is not shown since it is identical to the G·T wobble.

With other cleavage junctions, these nucleotides may need to be changed accordingly to maintain optimal activity.[311] Therefore, if the enzyme core sequence is fixed, changing the

dinucleotide junction composition may have a huge influence on enzyme activity. This might be useful for further comparing these two DNAzymes. While the structure of G and A are quite similar (both are purines), direct switching from G to A would obscure the exact chemical role of the functional groups of G (Figure 7.5 A). Therefore in this work, G was mutated to hypoxanthine (HX) and 2-aminopurine (2AP) to probe the functional groups, one at a time. HX differs from guanine by the 2-amino group, while 2AP differs from guanine by lacking the 6-keto group. The assays were carried out at pH 6.0 to obtain measurable rates for the wild-type enzymes.[308] The original rA·G junction has the highest rate for both DNAzymes (Figure 7.5 B and C, black traces). The rates of rA·HX were more than one order of magnitude slower compared to the original rA·G junction (Figure 7.5 D, red bar), and rA.2AP was even slower in both cases (Figure 7.5 D, green bar). Finally, the rates were the slowest with the rA·A junction (Figure 7.5 D, yellow bar), dropping by over 3 orders of magnitude compared to the original rA·G junction. Since all the modifications brought about the same trend in activity change, these identical patterns further suggest a similar mechanism of these two DNAzymes. Two reasons may explain the guanine mutation activity pattern: either disruption of metal binding or the enzyme structure. Pb^{2+} has well-defined coordination sites in the nucleobases. As far as guanine is concerned, the N7 and O6 positions are important for Pb^{2+} binding. Since adenine and guanine have drastically different rates (>1000-fold), this argues against the importance of the N7 position (both have the N7 position available). Since the HX mutant is only slightly more active than the 2AP mutant, it is unlikely that the O6 oxygen is involved in Pb^{2+} binding. Otherwise, a much more significant change is expected.[310,332] Therefore, this guanine should play more of a structural role. For example, it may base pair with other nucleotides to stabilize

the secondary or tertiary structure for catalysis. This guanine can formally pair with the thymine in the 17E to form a wobble pair, which has been confirmed to be crucial for cleaving the rA·G junction.[111,250,311] Other 17E mutants have been evolved to cleave other types of junctions, which lack the wobble pair.[311] Therefore, this wobble is not absolutely conserved, which also confirms its structural role. In a typical wobble pair, the O6 and N1 positions in guanine are hydrogen bonded with thymine (Figure 7.5 E). By changing the guanine to HX, the wobble formation is maintained. The drop of rate by over 10-fold suggests that the amino group might be involved in additional stabilization roles. With the 2AP junction, the same hydrogen bonding can still be formed with the wobble face of the thymine (Figure 7.5 F), but this requires slightly more structural changes explaining the drop of rates by ∼100–300 fold. On the other hand, with adenine (which confers the cumulative effect of both the HX and 2-AP mutations), the Watson–Crick face of the thymine has to be used (Figure 7.5 H), and the structure perturbation is more significant, explaining its lowest rate. It is interesting to note that GR5 has exactly the same trend as 17E for the junction mutations (Figure 7.5 D). Based on the above discussions, if the activity for different cleavage junctions is mainly related to the T2.1 in 17E, there might be a corresponding thymine in GR5. Interestingly, only one thymine, T5, resides in the GR5 enzyme loop. A careful examination of the aligned sequences resulting from the Pb^{2+} selection in the original paper, reveals that this thymine is conserved in 70 % of the sequences.[67] However, T5 in GR5 is quite far away from the cleavage junction based on the secondary structure.

7.2.4 Other GR5 mutations

To test the function of T5 in GR5, a few more mutants were studied.

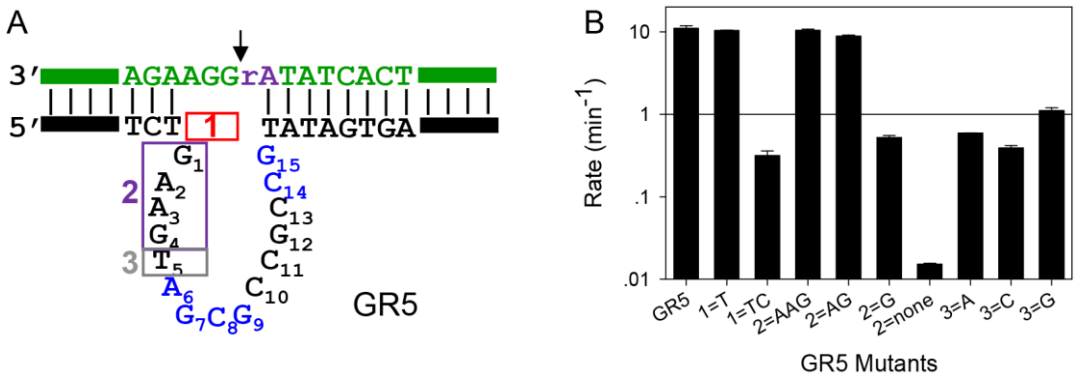

Figure 7.6 (A) Three parts (in boxes 1-3) of GR5 are further mutated. One or two nucleotides are inserted in box 1, the nucleotides in box 2 are gradually deleted and T_5 in box 3 is mutated to the other three nucleotides. (B) The rates of these mutants plotted in a log scale.

In 17E almost all the nucleotides in the substrate strand are base paired with the enzyme, while in GR5, three free nucleotides exist on the 3′ side of rA. The importance of these unpaired nucleotides in GR5 was also tested. First, they were gradually paired up by extending the enzyme. T or TC was added in the box marked 1 in Figure 7.6 A. Both the extended GR5 mutants still retained high activity (Figure 7.6 B), suggesting that the unpaired nucleotides might be useful for providing flexibility but without a specific chemical role. Then, the nucleotides before T5 (the nucleotides in box 2) were gradually deleted. These deletions did not significantly affect the activity, unless all the four nucleotides in box 2 were deleted (Figure 7.6 B). Finally, T5 in box 3 was mutated to other nucleotides and the activity was not much affected by this as well (Figure 7.6 B). These experiments suggest that T5 itself is not critically important, thus arguing against the speculation that T5 in GR5 plays a similar role to T2.1 in

17E. Therefore, some other nucleotides in GR5 might interact with the cleavage site guanine in the substrate, and this will be a topic of further studies.

7.2.5 Further discussions

GR5 and 17E are two highly efficient and widely used Pb^{2+}-dependent DNAzymes. Both have the highest activity with Pb^{2+},[67,250,306] and they share the same substrate. In this work, mutation studies on both DNAzymes were performed. The data suggests that these two Pb^{2+}-specific DNAzymes have the same catalytic mechanism in the presence of Pb^{2+}. Pb^{2+} has long been known to be highly effective in RNA hydrolysis. Using Pb^{2+} for RNA-cleaving ribozymes has been reported since early 1990s,[295–297] and the study of Pb^{2+} for RNA hydrolysis can be dated back to an even earlier time.[330 314] In the well-known leadzyme (a ribozyme), the enzyme strand contains only two unpaired nucleotides (AG) and it is quite active with Pb^{2+}.[333] Therefore, Pb^{2+} is a highly efficient metal to assist RNA cleavage. The hydrated Pb^{2+} has a pK_a value of 7.2–7.8 and its deprotonated species can interact with the 2′-OH on the rA sugar ring to assist the nucleophilic attack reaction.[3] For comparison, other metals have quite different pK_a values (8.5 for Eu^{3+}, 9.0–9.6 for Zn^{2+}, and 11.4 for Mg^{2+}).[225,334] This special property has rendered Pb^{2+} to be highly effective for RNA cleavage and the DNAzyme provides a scaffold to efficiently utilize Pb^{2+} for this purpose. This might be the reason for Breaker and Joyce to pick Pb^{2+} for their first DNAzyme selection,[67] from which GR5 was reported. Under physiological conditions, the available free Pb^{2+} concentration is close to zero and Mg^{2+} is the most important cation. To target RNA, most subsequent selections were carried out with Mg^{2+} or other

physiologically relevant metals. Under various conditions, 17E was the main outcome (e.g. with Mg^{2+},[111,119] Zn^{2+},[112] Mg^{2+}/Mn^{2+},[307] Cd^{2+},[118] or $Mg^{2+}/Mn^{2+}/Cu^{2+}$.[329]). It is easy to understand that GR5 did not appear again, since GR5 is completely inactive with these metals. Aside from the similarities between 17E and GR5, the major difference is that 17E is also active with many other metal ions, but GR5 is active only with Pb^{2+}. The recurrence of 17E in many selections indicates that only very few solutions are available for DNAzymes to catalyze RNA hydrolysis in the presence of these metals (e.g. 17E appears to be the main solution). Therefore, 17E is optimized for other metal ions. Since 17E happens to contain AG and CG conserved nucleotides, it affords high activity with Pb^{2+}. On the other hand, GR5 is optimized for Pb^{2+} and has no activity with other metals. In the Pb^{2+}-dependent *in-vitro* selection experiment described in chapter 6, many new DNAzymes were discovered.[108] The ones that are active with Pb^{2+} are inactive with Mg^{2+}. This further supports the more stringent sequence requirements for Mg^{2+}. In a sense, 17E may be considered to be a special form of GR5. More experiments are needed to test this hypothesis and to fully elucidate their relation.

7.3 Summary

GR5 and 17E are two highly efficient and widely used Pb^{2+}-dependent DNAzymes. Both have the highest activity with Pb^{2+}.[67,250,306] They share the same substrate sequence and have similar conserved nucleotides in the enzyme catalytic core. Within this study, a side-by-side comparison of these two Pb^{2+}-dependent DNAzymes was made. Mutation studies on both DNAzymes were performed. The data suggests that these two Pb^{2+}-specific DNAzymes have

the same catalytic mechanism in the presence of Pb^{2+}. By performing mutations in the enzyme core, the similar role of four highly conserved nucleotides in both enzymes was identified and it was concluded that they share the same activity pattern. By mutating guanine at the cleavage junction to adenine, HX and 2AP, it was further confirmed that these two enzymes have the same mechanism in the presence of Pb^{2+}. This guanine has been suggested to play a structural role instead of a metal binding one. In addition, Mg^{2+} and Pb^{2+} were compared for the activity of 17E as a function of enzyme mutants. This study indicates that the nucleotides important for Mg^{2+} catalysis are also important for the Pb^{2+}-dependent activity. Based on this study, the general activity of Pb^{2+} in many different DNAzymes was rationalized, a deeper understanding of the structure-activity relationship of GR5 is gained, and it was proposed that 17E may be considered to be a special form of GR5, explaining the very high activity of 17E in the presence of Pb^{2+}.

7.4 Materials and methods

7.4.1 Chemicals

The DNAs used were purchased from Integrated DNA Technologies (IDT, Coralville, IA). The sequences of DNA used in this selection are listed in Table 7.1. The trans-cleaving enzyme strands and their mutants were from Eurofins (Huntsville, AL). Metal ions that were used for analysis include lead(II) acetate, magnesium(II) sulfate. All these salts were purchased from Sigma-Aldrich. The purity of the metals used is 99.99 %. Their solutions were made by directly

dissolving their salts in Milli-Q water. Tris (Hydroxymethyl) aminomethane (Tris), 2-(N-morpholino) ethanesulfonic acid (MES) free acid monohydrate, 4-(2-Hydroxyethyl)piperazine-l-ethanesulfonic acid (HEPES), 3-(*N*-morpholino) propanesulfonic acid (MOPS), EDTA disodium salt dehydrate, sodium chloride, sodium bromide, sodium iodide and ammonium acetate were purchased from Mandel Scientific Inc. (Guelph, Ontario, Canada). Acrylamide/bisacrylamide 40 % solution (29:1), urea, and 10 X TBE solution were purchased from Bio Basic Inc. SsoFast EvaGreen supermix was purchased from Bio-Rad for real-time PCR analysis. T4-DNA ligase, deoxynucleotide (dNTP) solution mix, Taq DNA polymerase with ThermoPol buffer, and low molecular weight DNA ladder were purchased from New England Biolabs. All metal ions, buffer and gel stock solutions were prepared with Milli-Q water. The pH of the buffers was measured with Denver Instrument UltraBasic pH meter.

Table 7.1 List of DNA sequences used in Appendix B (chapter 7).

DNA	**Sequence (5′-3′)**
Substrate	
PO	GTCACGAGTCACTAT**rAG**GAAGATGGCGAAA
rAA	GTCACGAGTCACTAT**rAA**GAAGATGGCGAAA
rA2AP	GTCACGAGTCACTAT**rA2AP**GAAGATGGCGAAA
rAHX	GTCACGAGTCACTAT**rAHX**GAAGATGGCGAAA
Enzymes	
GR5	TTTCGCCATCT--**GAAGTAGCGCCGCCG**TATAGTGACTCGTGAC
A6C	TTTCGCCATCT--**GAAGTCGCGCCGCCG**TATAGTGACTCGTGAC
A6T	TTTCGCCATCT--**GAAGTTGCGCCGCCG**TATAGTGACTCGTGAC
A6G	TTTCGCCATCT--**GAAGTGGCGCCGCCG**TATAGTGACTCGTGAC

G7A	TTTCGCCATCT--**GAAGTAACGCCGCCG**TATAGTGACTCGTGAC
G7C	TTTCGCCATCT--**GAAGTACCGCCGCCG**TATAGTGACTCGTGAC
G7T	TTTCGCCATCT--**GAAGTATCGCCGCCG**TATAGTGACTCGTGAC
C8A	TTTCGCCATCT--**GAAGTAGAGCCGCCG**TATAGTGACTCGTGAC
C5G	TTTCGCCATCT--**GAAGTAGGGCCGCCG**TATAGTGACTCGTGAC
C8T	TTTCGCCATCT--**GAAGTAGTGCCGCCG**TATAGTGACTCGTGAC
G9A	TTTCGCCATCT--**GAAGTAGCACCGCCG**TATAGTGACTCGTGAC
G9C	TTTCGCCATCT--**GAAGTAGCCCCGCCG**TATAGTGACTCGTGAC
G9T	TTTCGCCATCT--**GAAGTAGCTCCGCCG**TATAGTGACTCGTGAC
C14A	TTTCGCCATCT--**GAAGTAGCGCCGCAG**TATAGTGACTCGTGAC
C14G	TTTCGCCATCT--**GAAGTAGCGCCGCGG**TATAGTGACTCGTGAC
C14T	TTTCGCCATCT--**GAAGTAGCGCCGCTG**TATAGTGACTCGTGAC
G15A	TTTCGCCATCT--**GAAGTAGCGCCGCCA**TATAGTGACTCGTGAC
G15C	TTTCGCCATCT--**GAAGTAGCGCCGCCC**TATAGTGACTCGTGAC
G15T	TTTCGCCATCT--**GAAGTAGCGCCGCCT**TATAGTGACTCGTGAC
1=T	TTTCGCCATCTT-**GAAGTAGCGCCGCCG**TATAGTGACTCGTGAC
1=TC	TTTCGCCATCTTC**GAAGTAGCGCCGCCG**TATAGTGACTCGTGAC
2=AAG	TTTCGCCATCT---**AAGTAGCGCCGCCG**TATAGTGACTCGTGAC
2=AG	TTTCGCCATCT-----**AGTAGCGCCGCCG**TATAGTGACTCGTGAC
2=G	TTTCGCCATCT-------**GTAGCGCCGCCG**TATAGTGACTCGTGAC
2=none	TTTCGCCATCT---------**TAGCGCCGCCG**TATAGTGACTCGTGAC
3=A	TTTCGCCATCT--**GAAGAAGCGCCGCCG**TATAGTGACTCGTGAC
3=C	TTTCGCCATCT--**GAAGCAGCGCCGCCG**TATAGTGACTCGTGAC
3=G	TTTCGCCATCT--**GAAGGAGCGCCGCCG**TATAGTGACTCGTGAC
17E	TTTCGCCATCTTTC**TCCGAGCCGGTCGAAA**TAGTGACTCGTGAC
A6C	TTTCGCCATCTTTC**TCCGCGCCGGTCGAAA**TAGTGACTCGTGAC
A6G	TTTCGCCATCTTTC**TCCGGGCCGGTCGAAA**TAGTGACTCGTGAC
A6T	TTTCGCCATCTTTC**TCCGTGCCGGTCGAAA**TAGTGACTCGTGAC
G7A	TTTCGCCATCTTTC**TCCGAACCGGTCGAAA**TAGTGACTCGTGAC

G7C	TTTCGCCATCTTTC**TCCGAC**C**CGGTCGAAA**TAGTGACTCGTGAC
G7T	TTTCGCCATCTTTC**TCCGAT**C**CGGTCGAAA**TAGTGACTCGTGAC
C13A	TTTCGCCATCTTTC**TCCGAGCCGGTA**G**AAA**TAGTGACTCGTGAC
C13G	TTTCGCCATCTTTC**TCCGAGCCGGTG**G**AAA**TAGTGACTCGTGAC
C13T	TTTCGCCATCTTTC**TCCGAGCCGGTT**G**AAA**TAGTGACTCGTGAC
G14A	TTTCGCCATCTTTC**TCCGAGCCGGTCA**A**AA**TAGTGACTCGTGAC
G14C	TTTCGCCATCTTTC**TCCGAGCCGGTCC**A**AA**TAGTGACTCGTGAC
G14T	TTTCGCCATCTTTC**TCCGAGCCGGTCT**A**AA**TAGTGACTCGTGAC

7.4.2 Activity assays

For a typical gel-based activity assay, the DNAzyme complex were prepared by annealing the FAM-labeled substrate (10 µM) and enzyme (30 µM) in buffer 50 mM MES (pH 6.0, 25 mM NaCl) by heating at 85 °C for 1 min and then slowly cooled at room temperature until ~30 °C. The complex was then frozen at -20 °C for at least 2 hours. To initiate the reaction at room temperature, a final of 10 µM Pb^{2+} / 10 mM Mg^{2+} or another metal ion (as required) was incubated with 10 µL of 0.7 µM DNAzyme complex in buffer 50 mM MES (pH 6.0 - 6.5) / 50 mM MOPS (pH 7.0 – 8.0) with salt concentration 25 NaCl, for the required time ranging from 10 s – 8 h. The samples were quenched with 8 M urea at designated time points and run in 15 % dPAGE at 120 V for 80 min. The gel images were taken with Bio-Rad ChemiDoc MP imaging system. For determining the rate of cleavage, the gel band intensities of the cleaved vs. uncleaved substrate were quantified and the data obtained were fitted (using *Sigma Plot 12.0*) according to the first-order rate equation $Y_t = Y_o + a(1\text{-}e^{-kx})$, where Y_t and Y_o are the cleavage

fractions at a given reaction time 't' or '0' min, respectively, 'a' is a constant i.e. the scaling parameter and 'k' is the observed rate constant.